Mechanisms underlying IL-33-driven T cell responses in alloimmunity and mucosal injury

by

Gaelen Kathryn Dwyer

BA, University of Alaska, 2012

MS, University of Alaska, 2015

Submitted to the Graduate Faculty of the

School of Medicine in partial fulfillment

of the requirements for the degree of

Doctor of Philosophy

University of Pittsburgh

2021

UNIVERSITY OF PITTSBURGH

SCHOOL OF MEDICINE

This dissertation was presented

by

Gaelen Kathryn Dwyer

It was defended on

July 20, 2021

and approved by

Angus Thomson, Distinguished Professor, Department of Surgery and Immunology

Amanda Poholek, Assistant Professor, Department of Pediatrics and Immunology

Warren Shlomchik, Professor, Department of Medicine

and Immunology

Dario Vignali, Professor and Vice Chair, Department of Immunology

Dissertation Director: Heth R. Turnquist, Associate Professor,

Department of Surgery and Immunology

Mechanisms underlying IL-33-driven T cell responses in alloimmunity and mucosal injury

Gaelen Kathryn Dwyer, PhD

University of Pittsburgh, 2021

The understanding of the IL-1 family cytokine, interleukin (IL)-33, continues to evolve with our understanding of homeostasis and immunity. In the described studies, I add new mechanistic insight into how IL-33 directs a network of regulatory T cells (Treg) and Type 1 T helper (Th1) cells in mucosal injury and alloimmunity. First, I established that IL-33 acts on Treg expressing the IL-33 receptor, Serum Stimulation-2 (ST2), to mediate the secretion of IL-13 after lung injury. By generating a mouse with Treg deficient for IL-13, I established Treg secreted IL-13, is not involved in direct T cell suppression, but is critical to control lethal inflammation and support early injury responses after lung damage. Treg IL-13 limited the presence of local myeloid populations after injury by acting on monocytes and macrophages to direct their differentiation into Arginase 1^+ macrophages that mediate tissue repair. These data identify a new regulatory mechanism involving IL-33 and Treg secretion of IL-13 in response to tissue damage that is instrumental in limiting local inflammatory responses and may shape the myeloid compartment after lung injury. Second, I revealed an unknown function for IL-33 in the activation and differentiation of alloreactive $CD4^+$ T cells after allogeneic hematopoietic cell transplantation. Specifically, I identify that IL-33 is as a stromal cell-derived damage-associated molecular pattern that is released from the recipient and functions as a costimulatory signal driving the activation and differentiation of alloreactive Th1 cells. This mechanism supports $CD4^+$ T cell differentiation into Th1 cells by augmenting TCR signaling pathways and independent of innate cell-derived IL-12. This mechanism is TCR-dependent since IL-33-stimulation of $CD4^+$ T cell is not required for

lymphopenia-induced expansion. Together the findings of my graduate studies highlight the importance of IL-33 in $CD4^+$ T cell immunobiology. These studies also support the importance of understanding pleiotropic molecules like IL-33, which is clearly an important molecule that communicates tissue conditions to a variety of immune cells across different pathologies. This knowledge will provide a foundation, allowing for the development of ways to safely and effectively modulate the $ST2^+$ immune cell network to achieved desired outcomes after injury, infection, and malignancy.

Table of Contents

List of Tables

List of Figures

Preface

I have taken a winding path to graduate school. As a young child I was fascinated with the world and exploration, which led me to sail around the world my first year after high school, explore a few of the remote corners of Alaska, study abroad in France, and fall in love with science and how living organism's function. My thirst for exploration has gotten narrower overtime. Ultimately my inherent desire for exploration led me to research, an area of constant discovery. After completing my master's degree, investigating the molecular evidence of gingival epithelial cell damage leading to oral cancer from iqmik use, an Alaska smokeless tobacco mixture, I had firmly developed a passion for research. Transitioning into my PhD work was enlightening because I was surrounded by a community of people who also shared a passion for discovery and through the skillful mentorship of many, I have finally found my space in this community where I can add to the edge or our knowledge.

There are many people to thank for supporting and guiding me along the way. My family has supported me through all my adventures and continues to support me as I reach for more. My parents, Deborah Gravel and Peter Dwyer thankfully accepted my stubborn persistence as a positive trait and have always encouraged me to achieve my goals. My husband, Ethan Story, has joyfully supported my career even when it meant disrupting his and he has always accepted change as a new opportunity to grow. My friends Maryanna Owoc, Adriana Johnson, and Laura Molina have been my day-to-day support, cheering me along as we all understood each other's journey but were removed enough to be true supports.

I want to thank my mentor Heth Turnquist, he has been a truly outstanding mentor. I appreciate his enthusiasm for research, it's contagious. I also value how Heth approaches a problem, if one arose Heth was quick to seek guidance on how to best to fix the problem from people he viewed role models and as good mentors and he encourage me to do the same. He approaches problems with an open-mind and open ears and would initiate many important discussions that changed the trajectory of his mentoring and my experience in the lab. His dedication to mentoring is remarkable, it is his top priority, and he is determined to help his mentees learn from both his successes and his mistakes. I hope that someday I can emulate his passion for teaching, mentoring and science.

I want to thank my mentors in graduate school who have been instrumental in guiding my personal growth. My committee members have offered support and constructive advice to guide my progress as a graduate student. Many thanks to Drs. Warren Shlomchik, Amanda Poholek, Angus Thomson, and Dario Vignali for the insightful scientific conversations we have had over the years. Many thanks to Drs. Jean-Philippe Girard and Anne Gonzalez de Peredo, who welcomed me into their labs in Toulouse and taught me about IL-33, proteomics and shared with me a different approach to research. I learned so many skills and gained a new perspective working with them, and I hope to apply these lessons in my future projects. Dr. Joanne Flynn has been a fabulous support and wonderful advisor through my PhD. Dr. Steinman has been instrumental in my success, often knowing what I need better than I know it myself. I have learned so much from working with Dr. Steinman and the MSTP administration to improve the MSTP and appreciate all that they have put into our program. Thank you for allowing me to make a small imprint on this program that will make a great imprint on me.

I also want to thank the Turnquist lab, past and present. Thank you for sticking together and supporting each other. I am so grateful I got the chance to work everyone in the lab. I specifically want to thank Lisa Mathews and Anna Lucas. Their support and humor in lab have been there every day and I am so much the better for it! Thank you for all that you have done over the years to make my day a little easier, for keeping a smile on my face and for the cake!

There are many more people to thank, and I am glad to have crossed paths with all of you. I am so grateful for all the help I have received along the way.

1.0 Introduction

Portions of this chapter were compiled and submitted as part of an invited review to *Annual Reviews of Immunology* in the following manuscript:

Dwyer, GK, D'cruz, L, and Turnquist, HR. Emerging Functions of IL-33 in Homeostasis and Immunity. Annu. Rev. Immunol. 2021.

1.1 IL-33 Immunobiology and Molecular Biology

1.1.1 Discovery

Despite its widespread expression in the body, interleukin (IL)-33 has always been an elusive and complicated molecule. IL-33 was first described in 2003 as an mRNA and nucleus-targeted protein abundantly expressed in endothelial cells from human lymphoid organs and designated nuclear factor from high endothelial venules (NF-HEV) by Girard and colleagues (1). Schmitz et al. subsequently identified the carboxy-terminal part of the human IL-33 protein using computational tools for GenBank searches for novel members of the IL-1 cytokine family (1, 2). The IL-33 protein had a similar three-dimensional folded structure to other IL-1 family members and thus they named this protein, IL-33, and declared it a new cytokine in the IL-1 superfamily (1, 2). Their study also provided the seminal evidence that IL-33 cytokine activity was through ligation of a previously orphan receptor in the IL-1 receptor superfamily, Serum Stimulation-2 (ST2), that induces Type 2 cytokine secretion by Type 2 T helper ((Th)2) cells, which were the

first cell pinpointed to express detectable levels of the IL-33 receptor (1, 2). The Girard group later closed the circle and confirmed that the protein they identified in 2003, NF-HEV, and IL-33 were the same protein and further characterized IL-33 as a chromatin-associated nuclear cytokine *in vivo* (3). Several past comprehensive reviews provide an excellent description of the early studies identifying and characterizing IL-33 and ST2 (4-6).

1.1.2 IL33 gene

The human *IL33* gene is located on chromosome 9 at 9p24.1, the mouse *IL33* gene orthologue is located on the same chromosome at 19qC1 (1). The only previous identified gene orthologue to human *IL33* was identified in 1999 by cloning the canine gene *DVS27* which was upregulated by vasospasm in cerebral arteries after subarachnoid hemorrhage (7). The human and mouse *IL33* gene is comprised of eight exons (4). Two promoters have been identified in humans the first promoter binds upstream of an untranslated exon (exon 1 or 1a); in both humans and mice an alternative promoter can bind to an alternative exon 1 sequence (exon 1b). The first promoter in exon 1a contains an interferon stimulated response element and several interferon gamma activation sites (8). These two promoters have been described to generate two transcripts (*Il33a* and *Il33b* mRNAs) which include unique 5'-untranslated regions but encode the same protein (8, 9).

1.1.3 Splice variants and isoforms

The single nucleotide polymorphisms (SNP) identified in human *IL33* gene are found in the promoter region and associated with increase susceptibility to asthma due to a likely increase

in promoter activity (10-13). Conversely, a rare loss-of-function mutation before exon 8 likely results in a biologically inactive truncated IL-33 protein which results in reduced numbers of eosinophils in the blood and protection against asthma similar to IL-33 deficient mice (14). In human airway epithelial cells alternative transcript splicing exists where exons 3 and 4 are deleted (**Figure 1 A**). This splicing variation confers cytoplasmic localization of a functional molecule with signaling capacity and is associated with Type 2 inflammation in patients with asthma (15). These data substantiated the contributions of IL-33 to human Type 2 responses and corroborated the contributions of IL-33 to Type 2-associated clinical immunopathologies like asthma. Importantly, they also endorse the appropriateness of transgenic rodent models where similar phenotypes have been observed in the study of IL-33-deficient mice (16), mice with cytoplasmic localized IL-33 (17), and humanized mice (18). Other splice variants have been identified but without clear physiological outcomes (19, 20).

1.1.4 Protein structure and function

The IL-33 protein is synthesized as in a full-length 270 amino acid protein that consists of two evolutionary conserved domains, a N-terminal nuclear domain (amino acids 1-65) and the C-terminal IL-1-like cytokine domain (amino acids 112-270), separated by a divergent central linker region (amino acids 65-112) (**Figure 1 A**) (3, 21). The high-resolution structure of most of the IL-1 family members, including IL-33, have been determined by X-ray crystallography or solution state nuclear magnetic resonance. IL-33 contains a conserved β-trefoil conformation and central hydrophobic core composed of 12 β-sheets, similar to the structure originally described for IL-1 (22-25). The cytokine domain is an IL-1-like structure with similar folding properties to IL-1α,

IL-1β and IL-18 (23, 24). Human IL-33 exhibits high identity with the murine form, with the central linker region providing the most divergence (5).

1.1.5 Cellular sources of IL-33

IL-33 is constitutively expressed by many types of cells and in many diverse tissues. IL-33 expression can also be induced during inflammation and injury.

1.1.5.1 Constitutive expression

In the steady-state IL-33 is constitutively expressed in the nuclei of various cell types in human and mouse tissues (26, 27). Major identified sources include endothelial cells in humans and adventitial stromal cells in mice of the vascular tree, epithelial cells in barrier tissues, fibroblast reticular cells in the lymphoid organs, and glial cells, neurons and astrocytes in the nervous system (26-33). There are species specific difference in IL-33 expression between human and mice, such as the distinct expression of IL-33 in the lung and vascular beds, which should be taken into consideration when extrapolating results from mouse models of human disease (4).

1.1.5.2 Induced expression

IL-33 is constitutively expressed by many cells during steady-state and inflammation can further induce the expression of IL-33. For example, IL-33 expression increases in the intestine of patients with graft vs. host disease (GVHD) following allogeneic hemopoietic cell transplantation (alloHCT) or in airway epithelial cells of patients with asthma or chronic obstructive pulmonary disease (COPD) (34-36). In the mouse, IL-33 expression in increased in type II pneumocytes by pathogen, allergen or an irritant (16, 37, 38). IL-33 expression can also be induced *de novo* in cells

that do not express IL-33 at the steady state following perturbation (34, 37). In addition to epithelial and endothelial cells expressing induced levels of IL-33, stromal cells that include fibroblasts, myofibroblasts and fibroblast-like cells are critical sources of IL-33 during inflammation and tissue repair (39, 40). Pro-inflammatory cytokines including IFNγ (41), Notch signaling (42), IL-4 and 13 (28), and mechanical stress (43, 44) have all been shown to facilitate IL-33 expression.

1.1.5.3 Leukocyte expression

Several studies have reported IL-33 expression in $CD45^+$ hematopoietic cells (2, 16, 45). The level of IL-33 detected in $CD45^+$ hematopoietic cells is lower than levels identified in structural cells, and it has been unclear if leukocytes were important sources of IL-33 protein *in vivo* or in humans (5, 9, 34). Recent studies by the Herbert laboratory, however, have provided compelling evidence for the importance of myeloid-derived, but not epithelial-derived, IL-33 in the generation of intestinal regulatory T cells (Treg) expressing ST2, and that regulate helminth immunity (46). They also suggest that spontaneous IL-33 release from conventional $CD103^+$ $CD11c^+$ dendritic cells (DCs) involves IL-33 generation from alternative transcripts enabling cytoplasmic localization and secretion via Perforin-2-mediated pores. Most importantly, they Fprovide data suggesting that mouse DCs and human HLA-DR^+ cells in the mucosal tissues have cytoplasmic IL-33. There have been other recent rodent studies suggesting the importance of intrinsic IL-33 activity to B cell development (47) and Treg suppressive function and stability (48). However, both studies failed to robustly establish the evidence of IL-33 protein, and instead used reporter signatures to support their conclusions. It will be exciting to watch as investigators continue to use cell specific Cre-drivers to target IL-33 and deduce if and when IL-33 is expressed during leukocyte development or how it contributes to the immune subset functions.

1.1.6 Nuclear localization, chromatin association, and gene regulation

The N-terminal domain of IL-33 contains a nuclear localization sequence (amino acids 61-78) and includes a short chromatin-binding motif (amino acids 40-58) that binds to the nucleosome in an acidic pocket formed by the histone heterodimer H2A-H2B (21). Full-length IL-33 has been convincingly determined to be uniquely localized to the nucleus (26, 27, 29, 49, 50). The conserved N-terminal nuclear domain suggests that nuclear localization is important for IL-33 function or regulation. The N-terminal domain has also been suggested to mediate gene regulation through various mechanism. The overexpression of IL-33 regulated transcription through binding to NFκB and reducing NFκB p65 binding to cognate DNA (3, 51). In contrast, ST2-independent and cell intrinsic studies of IL-33 function on gene expression were completed in transfected cell lines with IL-33 siRNA where they demonstrated IL-33 could bind to the promoter sequences of IL-13 and NFκB p65 (52-54). One study used an approach to query the global proteome of endothelial cells where endogenous IL-33 was knockdown and found only one modulated protein, IL-33, suggest intracellular IL-33 does not regulated protein expression (55). This was followed up by a study using a genome-wide analysis following the overexpression of IL-33 in epithelial cells where no transcriptional changes were observed (56). However, truncated IL-33 lacking the chromatin-binding activity increased IL-33 mobility compared to WT IL-33 following necrosis-induced release (56). In a knock-in mouse model deletion of the N-terminal nuclear domain resulted in elevated serum levels of IL-33 and ST2-dependent inflammation-induced lethality (17). These studies suggest that the predominant function of IL-33 chromatin binding in endothelial and epithelial cells is to regulate IL-33 release and the activity of the cytokine domain. Yet, analysis of murine squamous cell carcinoma cells suggested that Focal Adhesion Kinase-mediated

increases in IL-33 that regulated chemokine expression through interactions with transcriptional regulators (57) and controlling chromatin accessibility (58). Thus, there are emerging hints at nuclear IL-33 functions outside of nuclear retention, yet these may be highly situational and cell type specific.

1.1.7 Release and secretion

While IL-33 release mechanisms have been studied since its discovery, there remain important gaps in our knowledge of the mechanisms by which IL-33 leaves the nucleus and cell membrane. It is well known that IL-33 lacks a signaling sequence and therefore is not secreted from cells by the classical ER-Golgi secretory pathway. Instead, IL-33 is described as a nuclear alarmin or endogenous molecule containing a damage-associated molecular pattern (DAMP) that is released after cell damage or mechanical injury to alert the immune system of tissue damage (59). Agents causing cellular damage, necrotic cell death, or necroptosis release IL-33 in extracellular fluids (60-62). *In vivo*, IL-33 is released following viral infection induced lung damage, and into the cerebrospinal fluid 1 hour post spinal cord injury (29, 37). Released IL-33 is measured in asthma patients BAL fluids after lung challenge with plant pollens and house dust mite (63). The fungal allergen, *A. alternata* has been proposed to release IL-33 by causing cellular stress and reactive oxygen species generation, extracellular ATP secretion, and increased intracellular Ca^{2+} concentrations (**Figure 1 B**) (64-66). Unfortunately, it is difficult to exclude cell death as a mechanism since intranasal exposure of *A. alternata* is also associated with a significant reduction in IL-33^{+} cells at one hour (67). In addition, mechanical stress may contribute to IL-33 release, but further studies are needed to clarify the mechanism involved (44, 49, 68). Release mechanisms other than necrosis-induced cell death will require that nuclear IL-33 is translocated

to the cytoplasm or generated lacking they N-terminus as proposed recently (46). Momota et al. recently identified one mechanism for IL-33 release *in vitro,* which is regulated by two signals. First, IL-33 is translocated from the nucleus to the cytoplasm in a Ca^{2+} dependent manner. They also determined that nigericin, a *Streptomyces hygroscopicus*-derived potassium ionophore, which triggers gasdermin D-dependent pyroptosis mediated IL-33 release through membrane rupture (**Figure 1 B**) (69).

1.1.8 IL-33 protein regulation

IL-33 is a potent stimulus of the immune system; thus, it is highly regulated both to enhance its potency and to diminish its impact.

1.1.8.1 Positive regulation

Full length IL-33 is biologically active, but there are shorter mature (18-21 kDa) forms of the protein that lack the N-terminal domain and include the full IL-1-like cytokine domain, which are significantly more potent (70). IL-33 is processed to these "matured" forms by inflammatory serine proteases from neutrophils and mast cells (70, 71). Six distinct serine proteases have been shown to cleave IL-33 in the spacer region connecting the N-terminal and cytokine domain (**Figure 1 B**). The processing of full-length IL-33 can also occur in mice deficient in immune cell proteases, suggesting a functional role for exogenous allergen proteases and endogenous calpains (72). In mouse models of lung injury, allergen exposure, and helminth infection mature forms of IL-33 have been detected in recovered BAL fluids (66, 70, 73, 74). These findings suggest that proteolytic maturation of full-length IL-33 is an important component of IL-33 regulation and may support IL-33's diverse activities.

1.1.8.2 Negative regulation

IL-33 nuclear localization and retention is vital for immune homeostasis by controlling the release of IL-33 to limit the proinflammatory effect of IL-33 (17). In addition, IL-33 is cleaved and inactivated by caspases during apoptosis, limiting the capacity of IL-33 to trigger inflammation when cell death occurs in a controlled manner (59, 75, 76). The caspase cleavage site is in the middle of the IL-1 cytokine domain (amino acid 178 in humans) and is not found in other IL-1 super family members. Caspase-3, -7 and -1 all induce IL-33 cleavage, although caspase-1 cleavage may be mediated by caspase-7, which has the capacity to translocate to the nucleus and may be important for IL-33 inactivation in the nucleus (5, 59, 75-78). Once full length or matured IL-33 reaches the extracellular space there are several known mechanisms of IL-33 regulation, which have been identified and thoroughly reviewed (5). First, IL-33 is rapidly oxidized on critical cysteine residues in the cytokine domain, which causes the formation of two disulfide bridges and generates a biologically inactive form (73). Free IL-33 is also sequestered by the soluble decoy receptor, sST2 (**Figure 1 B**). Alternative splicing of ST2 generates sST2, which lacks the transmembrane domain and binds IL-33 in biological fluids to prevent it from triggering ST2 signaling (79, 80). Both adaptive and innate immune cells, as well as non-hematopoietic cells produce sST2 in response to proinflammatory cytokines, TLR ligands, and mechanical stress. It is elevated in the serum of patients with various inflammatory diseases and is associated with reduced IL-33-mediated immune responses (81-83).

1.1.9 IL-33 induced ST2 signaling

IL-33 signals to immune cells through the membrane bound receptor, ST2. To date, no other receptor for IL-33 or ligand for ST2 have been identified. The crystal structure of IL-33/ST2

complex identifies two binding sites in the cytokine domain of IL-33 which interact with all three Ig-like domains of ST2. Specific single-point mutations in IL-33 binding site acidic residues significantly decreased the ST2 binding affinity demonstrating that IL-33 binds to ST2 through acidic residues forming salt bridges with ST2 basic residues at each binding site (24). More detailed regarding the crystal structure of IL-33 interacting with ST2 can be found in comprehensive reviews (4-6). Binding of IL-33 allows ST2 to interact with IL-1RAcP, an IL-1 family member co-receptor (**Figure 1 B**). The IL-33 receptor complex signals through the IL-1 family common intracellular signal transducer MyD88, IRAK1 and IRAK4 kinases and TRAF6 that culminates in the activation of MAP kinases and NFκB transcription factor (2, 4, 5). These are commonly shared signaling intermediates with the IL-1R and IL-18R, and other members of the TLR/IL1R superfamily. Yet stimulation by IL-33, IL-1, IL-18, and TLR ligands can result in unique biological effects on the same cell. It is likely that the regulation expression of each of these surface receptors during development or throughout an immune response is important as suggested (4, 5, 50). Additionally, the location and timing of cytokine release is critical for the distinct immunobiology modulated by IL-33 stimulation. Also, in macrophages IL-33 ligation of ST2 induces distinct functional phenotypes relative to LPS ligation of TLR4, and IL-33 delivery with LPS regulates TLR4 signaling (84). Thus, new studies are needed to clarify how IL-33 and other TLR/IL1R ligands generate such different immune functions and how these similar, but apparently distinct, signaling pathways influence each other.

1.1.10 Regulation of ST2 signaling

Similar to the tight regulation of IL-33, ST2 expression is regulated on multiple levels. ST2 mRNA is alternative spliced to produce a decoy receptor (sST2) that lacks the transmembrane

domain, this receptor limits the amount of biologically available IL-33 and is preferentially produced by nonhematopoietic cells (4, 85, 86). The ST2 receptor is also inhibited by the ubiquitin-proteosome system which induces internalization and degradation of ST2 (87). In addition, single immunoglobulin domain IL-1 receptor-related molecule (SIGIRR) interferes with the dimerization of ST2 and IL-1RAcP (88).

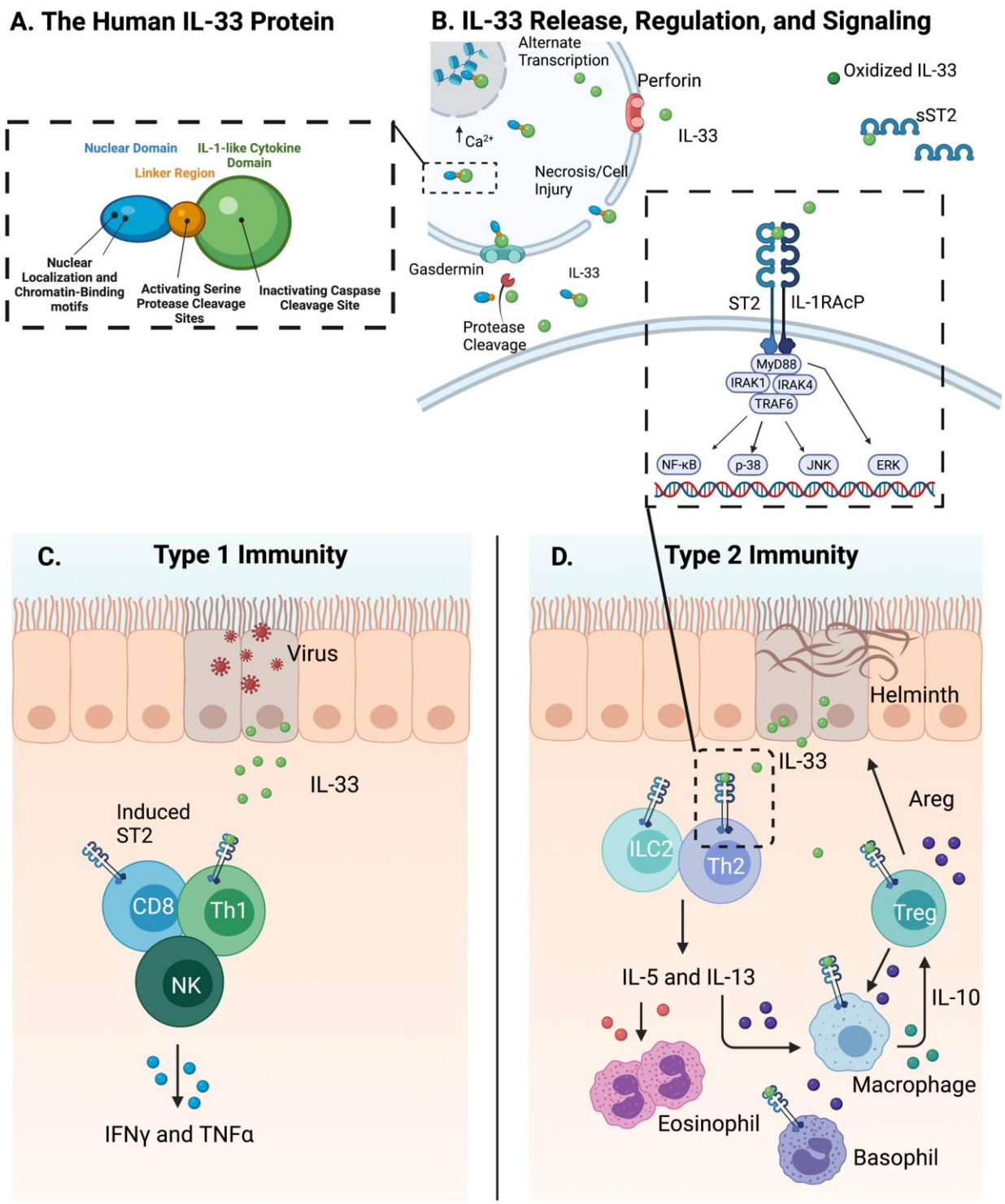

Figure 1. Structure and function of IL-33 in immunity

***A*, Full-length IL-33 is made up of two highly conserved domains, an N-terminal nuclear localization domain with chromatin binding motif (Blue) and an IL-1-like cytokine domain (green). These are separated by a**

divergent central linker region (Orange). Activating and inactivating cleavage sites are indicated. *B,* IL-33 is release from damaged or stressed cells by several potential mechanisms. 1. Necrosis or injury allows full-length IL-33 to be released from the nuclease where it is typically sequestered by the nuclear domain binding nucleosomes. 2. Full-length IL-33 can be translocated to the cytoplasm in a Ca^{2+} dependent manner and then released via gasdermin D-dependent process. 3. IL-33 lacking the nuclear domain is generated from alternative splicing transcripts enabling cytoplasmic localization and secretion via Perforin-2-mediated pores. Full-length IL-33 is functional, but cleavage by serine proteases generate mature, more active forms. IL-33 is regulated via sequestration in the nucleus, oxidation, and sequestration by sST2. Binding of ST2 and IL-1RAcP, an IL-1 family member co-receptor, by full-length or mature IL-33 leads to binding of MyD88, IRAK1 and IRAK4 kinases and TRAF6 and the activation of several MAP kinases and NFκB. *C,* Binding of IL-33 on upregulated ST2 on activated $CD8^+$ T cells and $CD4^+$ T cells, as well as NK cells, leads to augmented proliferation and increased production of pro-inflammatory cytokines. *D,* Cells mediating Type 2 immunity express ST2 and respond to IL-33 with proliferation and production of cytokines that work to support clearance of pathogens and restoration of epithelial health. IL-13 production by ILC2s, Treg, and Basophils is especially important to generate reparative and regulatory macrophages that aid repair and support local Treg. IL-5 production by ILC2s controls the accumulation and function of eosinophils that aid parasite expulsion.

1.2 IL-33 In Immunity

After the discovery of IL-33 and ST2 in the late 1990's and early 2000's, rIL-33 was administered to mice where a profound Type 2 immune response was consistently observed. Eosinophils infiltrated into tissues, goblet cell hyperplasia was observed, and elevated Type 2 cytokines, particularly IL-5 and IL-13, were measured (2, 89-91). Solid evidence for Type 2-mediated inflammation by IL-33 rapidly led to demonstrated roles for released IL-33 in parasite clearance, and Type 2-mediated pathologies, such as asthma and allergic skin disorders. In the

period since these first discoveries, the dominant immune targets of IL-33 have been shown to be adaptive and innate tissue-resident immune cells that express ST2 constitutively. Yet, many other immune, stromal, and parenchymal cells are induced to express ST2 and sST2 during activation. This leads to situations briefly outlined below where IL-33 exhibits pleotropic functions supporting IFNγ, IL-9, and IL-17-dominated immune responses as part of the host response to pathogens or immune-mediated inflammatory diseases (4, 92, 93) (**Figure 1 C and D**).

1.2.1 IL-33 and the lymphoid compartment

It was first shown that ST2 is expressed on both human and mouse Th2 cells both *in vitro* and *ex vivo* (94, 95) and these cells were the early focus of the study of ST2 immunobiology. ST2 expression on Th2 cells, which are classically described by their required transcription factor GATA3 and production of Type 2 effector cytokines, is independent of IL-4, IL-5, and IL-10, but it can be induced through IL-2-STAT5-mediated induction of GATA3 *in vitro*, but dependent on GATA3 (95-97). IL-33 stimulation of Th2 cells increases proliferation and IL-5 and IL-13 production (2). In addition to Th2 cells constitutively expressing ST2, a subset of Treg expressing ST2 have been identified. $ST2^+$ Treg are $Foxp3^+$ $GATA3^+$ and preferentially accumulate in the non-lymphoid tissues (98). $ST2^+$ Treg are especially enriched in the mucosal barrier tissues and are both thymic-derived (tTreg) and peripherally-induced Treg (pTreg) (99). IL-33 stimulation of $ST2^+$ Treg enhances their proliferation and expression of IL-13 and Amphiregulin (Areg), which support regulatory functions and directs tissue repair as described below (99-104). Furthermore, $CD4^+$ Th1 cells and Type 1 $CD8^+$ T cells express ST2 and sST2 transiently following an antigen encounter (105-107). Th1 cells upregulate ST2 in a STAT4- and Tbet-dependent manner (105). A loss of ST2 on Th1 or $CD8^+$ T cells causes in an impaired Type 1 effector function to virus (105,

106). In 2010 several groups identified a population of lineage-negative and $ST2^+$ c-Kit^+ Sca-1^+ IL-$7aR^+$ cells in the lymphoid gate that were GATA3-dependent and profound producers IL-5 and IL-13 (108-113). These novel cells making Type 2 cytokines, but lacking antigen receptors were eventually named group 2 innate lymphoid cells (ILC2s) (114). RAG2 and gamma chain-deficient (RAG/$\gamma c^{-/-}$) mice lacked ILC2s, and ILC2s transferred into RAG/$\gamma c^{-/-}$ produced Type 2 inflammation in response to helminths or IL-33 (110). These investigations led to the now appreciated role for IL-33-signaling to ILCs in immunity and immunopathology.

1.2.2 IL-33 in the myeloid compartment

Early studies of IL-33 and RAG deficient mice and suggested potent impacts of IL-33 on innate cells of the myeloid compartment (90, 115). It has emerged that both myeloid pre-cursors and unique differentiated subsets express modulated levels of ST2, which contributes to their development, differentiation, and functions. IL-33 acts directly on mast cells to promote their survival through the upregulation of BCLXL and supports their maturation and effector cytokine production including IL-13 and IL-22 (116, 117). Basophils also express low levels of ST2 and IL-33 stimulation provokes cytokine release, especially IL-4, IL-8 and IL-13 (118). This relationship is critical for basophil direction of lung development and the generation and function of alveolar macrophages (119). IL-33 also acts directly on macrophages following IL-13-mediated ST2 upregulation to support the generation of Type 2 reparative and regulatory macrophages (120, 121). IL-33 enhances the expansion, survival, and adhesiveness of human eosinophils that mediate reparative and pro-inflammatory roles throughout the body (122, 123). A mechanism where IL-33 stimulates myeloid cells to secrete IL-2, which synergizes with IL-33, potentially myeloid cell-derived IL-33, to support $ST2^+$ Treg cell expansion and functions has been established (46, 124,

125). ST2 expression on $CCR2^+$ monocytes is important to support the metabolic reprograming necessary for differentiation into reparative macrophage subsets (84). IL-33 and Hemin instructs the development of red pulp macrophages to support iron recycling and iron homeostasis (126).

1.2.3 Type 2 anti-pathogen immunity

Since the discovery of IL-33, many advancements have been made elucidating the pleiotropic roles of IL-33 in immunity. IL-33 was initially described as promoting a Type 2 immunity in infectious diseases and allergy (**Figure 1 D**) (2, 89-91). The immune response for clearance of parasitic helminth infection includes recruitment of ILC2s, M2 macrophages, mast cells, eosinophils and Th2 cells (127). Following helminth infection *Il33* mRNA levels are increased in the intestine of resistant mice, compared to susceptible mice and administration of rIL-33 conferred protection against *Trichuris muris* infection due to enhanced Type 2 cytokine expression (89). In mice infected with *Nippostrongylus brasiliensis* IL-33 levels were elevated in the peritoneal fluid shortly after infection and supported ILC2 effector cytokine secretion which supports goblet cell hyperplasia (110-112, 128). IL-33 signaling is necessary for granuloma formation, eosinophilia and Th2 effector cytokine production in the lung following a *Schistosoma mansoni* infection (129). This also translates to human disease, patients infected with *Schistosoma haematobium* had increased levels of IL-33 in their serum which correlated with increased Type 2 cytokine production and eosinophilia (130). Dahlgren and colleagues recently identified a new feedback role for IL-33 in helminth infection. They determined that a key source of IL-33 was fibroblast-like adventitial stromal cells (ASC). IL-33 and TSLP from ASCs were required for ILC2 and Th2 accumulation in the lung during helminth infection and the ILC2s promoted IL-13-mediated ASC expansion and IL-33 production (28). In response to a *Candida albicans* infection

IL-33 boosted the antifungal neutrophil response by enhancing neutrophil recruitment and phagocytic activities by enhancing peritoneal macrophages secretion of neutrophil chemotactic, CXCL1 and CXCL2, and increased the surface expression of the corresponding ligand receptor CXCR2 on neutrophils (131). Additionally, in a systemic model of *C. albicans* IL-33 treatment stimulated $CD4^+$ T cells to produce IL-13 which acted synergistically with IL-33 to promote Type 2 reparative and regulatory macrophage polarization (132).

1.2.4 Type 1 anti-pathogen immunity

IL-33 does not always have a beneficial role in all parasitic infections and its expression can increase disease burden. Visceral leishmaniasis occurs following infection with protozoans *Leishmania donovani* and *L. infantum* which target the liver, spleen, and bone marrow. The infection is best controlled in the liver by formation of granulomas mediated by a Th1 immune response. IL-33 is elevated in the serum of patients infected with *L. infantum* compared to healthy controls and IL-33 expression in the liver of a mouse model infected with *L. donovani* resulted in elevated parasitic load and hepatomegaly (133). IL-33 also promotes higher parasite burdens in the spleen, where parasite proliferation occurs, and treatments of rIL-33 reduced IFNγ and IL-12 cytokine production while promoting Type 2 cytokine production (134). In contrast, when a Type 1 anti-viral immune response dominates IL-33 is effective at promoting cell expansion and Type 1 effector cytokine production and supports an effective recall response upon reinfection (**Figure 1 C**) (106, 135-138). Leukocytes that typical respond to viral infections including, NK cells, NKT cells, Th1 cells and $CD8^+$ T cells constitutively express little to no ST2, but ST2 can be transiently induced in response to inflammatory signals such as IL-12 (107, 139, 140). Baumann and colleagues identified that Th1 cells require STAT4 and the Type 1 associated transcription factor

Tbet to induce ST2 upregulation which was necessary for an effective immune response following a LCMV infection (105). Effective anti-viral T cell response is initiated in the secondary lymphoid organs where antigen presenting cells activated T cells (141). Within the architecture of the lymphoid organs high endothelial venules and fibroblastic reticular cells (FRC) are the primary sources of IL-33 in the lymph nodes (27). FRC mediate lymph node remodeling and enlargement during a virial infection (142). Aparicio-Domingo and colleagues identify lymph node FRC as a critical source of IL-33 driving acute and chronic anti-LCMV T cell responses. Early during LCMV infection the FRC lose IL-33 protein expression which correlated with $CD8^+$ T cells ST2 expression and T cell expansion (39).

1.2.5 Immune regulation

In a fungal model using *Cryptococcus neoformans* for allergic airway inflammation IL-33 promotes detrimental immunopathology. Mice deficient in ST2 have improved survival and reduced fungal burden compared to wild-type mice due to the reduced accumulation of ILC2s and Th2s as well as reduced lung eosinophilia and Type 2 polarized macrophages (143-145). Alvarez et al. demonstrate there is a delicate balance maintained by IL-33 and IL-1 signaling supporting the regulatory immune response during a fungal infection. IL-33 stimulation supports Treg stability where as *St2*$^{-/-}$ Treg are prone to acquire RORγT and IL1R1 and lose their suppressive function becoming more inflammatory. *Il1r1*$^{-/-}$ mice infected with *C. neoformans* have a greater number of $ST2^+$ Treg, which maintain Foxp3 and resist acquiring a Th17 phenotype, resulting in reduced fungal clearance and augmenting susceptibility to fungal infection (146). Similarly, IL-33 is a negative regulator of pathogen clearing Th17 response to enteric pathogen *Citrobacter rodentium*-induced colitis by enhancing gut epithelium permeability, suppression of antimicrobial

REG3γ upregulation, increased Treg frequency and impaired Th17 differentiation (147). Several studies have shown that patients with sepsis have elevated levels of IL-33 or sST2 suggesting an association between IL-33 and bacterial infections (148-151). These have been thoroughly reviewed recently (152), but briefly, the administration of IL-33 significantly reduces mortality in the cecal ligation and puncture mouse model of sepsis and is associated with increased neutrophil infiltration into the peritoneal cavity and increased bacterial clearance compared to untreated mice (148). Survivors of sepsis can develop long-term sequalae from immune dysfunction due to an expanded Treg population. Patients who survive sepsis have increased Treg, IL-33 and IL-10 in their peripheral blood. High levels of IL-33 activate IL-4 and IL-13 producing ILC2s, which support the polarization of IL-10 secreting Type 2 macrophages that ultimately enhance Treg expansion (**Figure 1 D**) (153). IL-33 increases in cutaneous wounds challenged with *S. aureus*, which is often a common wound pathogen (154, 155). Delivery of rIL-33 increased neutrophils localization to the wound and increased antimicrobial activity of local macrophages to reduce bacterial colonization (154, 155). IL-33 increased healing, suggesting that that the functions of IL-33 in immunity and homeostasis, like the two process themselves, are tightly linked.

1.3 Mucosal Tissue Injury and Repair

1.3.1 Acute lung injury

The clinical characteristics of acute lung injury (ALI), and its most severe manifestation, acute respiratory distress syndrome (ARDS), include hypoxemic respiratory failure, pulmonary infiltrates, and normal cardiac filling pressures (156-158). Histopathological findings of ALI

include neutrophil infiltration into the alveolar space, injury to the alveolar epithelium and endothelium, hyaline membrane formation, and microvascular thrombi (156). ALI has been mechanistically challenging to define and animal models have served as the best approach for testing hypotheses formed based on human pathological and physiological findings.

In humans, ALI can result from pneumonia, sepsis, transfusions, trauma, aspiration, and reperfusion of ischemic tissues (159, 160). Mouse models attempt to replicate the pathology of ALI in humans including acute onset and bilateral alveolar injury including increased endothelial and epithelial permeability, neutrophil infiltration, with increased pro-inflammatory cytokines, exudative phase, and repair with fibrosis (161). There are many models of ALI described in the literature, such as mechanical ventilation, LPS, hyperoxia, bleomycin (bleo), oleic acid, sepsis induced by cecal ligation and puncture or acid aspiration (156). One method that is reproducible and results in acute inflammatory injury followed by fibrosis is intratracheal bleo administration (156). Aspirated bleo is typically a model for pulmonary fibrosis, but the early phase is representative of ALI pathology (162). Within 24 hours of intratracheal bleo treatment, there is well described neutrophil infiltration in the alveolar space with an adaptive immune response by day 7 post-treatment and lung fibrosis is evident after day 11 (163, 164). Bleo administration is a useful model for studying IL-33 effects in ALI, since following bleo administration IL-33 mRNA and protein level are measurably increased in lung tissue (165).

One of the most common causes of severe pneumonia and ARDS are respiratory viruses. The pathophysiology of viral induced ARDS is still incompletely understood since many respiratory viral infections are common but result in mild symptoms. In mouse models using H1N1 viral strains, viruses initially infect the respiratory epithelium and initiate tissue damage and innate

immune cell activation and recruitment, like other models of ALI and ARDS (166). Viral pneumonia resulting in ARDS are treated with supportive mechanical ventilation (166).

Very little therapeutic advancement has been made for treatment of ALI or ARDS. The primary therapy for ARDS is mechanical ventilation which still results in significant mortality from 31% -71% within 30-days of diagnosis (167-169). Therefore, there remains a significant need for further investigations into the pathophysiology of ARDS and ALI to define critical molecular therapeutic targets. Future therapeutic approach for ARDS, whether it is viral-induced or trauma-induced need to focus on targeting the host immune response and enhancing repair of tissue damage.

1.3.2 Graft vs. host disease

AlloHCT for the treatment of hematopoietic malignancies, as well as the correction of nonmalignant hematologic, autoimmune, and genetic diseases, however, creates an evolutionary novel situation where a high frequency of naïve donor T cells can respond directly to non-self, allogeneic (allo) materials (170). The resulting extensive alloreactive T cell expansion leads to an effective graft-vs.-leukemia response but also often results in GVHD. GVHD is a common, and unfortunately, life-threatening complication of alloHCT that results when alloreactive donor T cells infiltrate and destroy host tissues, particularly the gastrointestinal (GI) tract (171). GVHD is typically treated with high dose steroids, but this leads to infection complications and disease relapse (171). The risk of GVHD can be reduced by manipulating the transplant product and depleting total T cells (172), selectively removing naïve T cells (173), or the use of post-alloHCT cyclophosphamide (174). While these methods show promise, the problem of GVHD is far from eradicated after malignancy treatment (171). Likewise, these treatments do not sufficiently reduce

the risk of GVHD enough to allow for the widespread application of alloHCT for correction of genetic disorders or application in autoimmune disease or for transplant tolerance induction, where transplant products with higher T cell dose are more effective (175).

Findings from clinical studies and clinically relevant experimental alloHCT models suggest that off-target damage to recipient barrier tissues caused by pre-transplant conditioning regimens used to make space for donor stem cells and prevent their rejection by the recipient's immune system contributes to GVHD pathogenesis (171). Damage to barrier tissues, particularly of the GI tract, releases pathogen-associated molecular patterns (PAMP) from GI-associated microbes to activate local antigen presenting cells (APC). PAMP-activated APCs will cause inflammation locally but also migrate to the secondary lymphoid organ (SLO). In the SLO, they can effectively promote the proliferation and early activation of alloreactive $CD4^+$ T cell clones directly recognize polymorphic regions of fully mismatched allogeneic major histocompatibility complex (MHC) or indirectly recognize processed and presented alloantigens on matched MHC. IL-12 supports the generation of IFNγ-secreting Th1 cells, which mediates the removal of malignant cells after alloHCT (176). IFNγ is also central to GVHD pathology due to its potent cytotoxic effects on host tissues and activation of other immune effector cells (171). Yet defined APC-independent recipient-derived signals, however, must exist, as recipients with disrupted PAMP signaling pathways still develop GVHD (177).

The terminal stage of GVHD is the effector stage mediated by inflammatory cytokines and tissue infiltrating immune cell effectors (178). Recognized alloantigens are pervasive and persistent throughout the body and through the course of GVHD. The context and density by which they are presented to alloreactive T cells vary depending on the location and the cells presenting the MHC II (178-180). The process of Th1 differentiation is clearly important in GVHD pathology

and involves two phases of Tbet expression in $CD4^+$ T cell, a first phase stimulated by T cell receptor (TCR) engagement and IFNγ, and a second, IL-12-enforced phase (181). The differentiation of naïve T cells into $Tbet^+$ Th1 cells secreting IFNγ is critical for GVHD pathology, as Tbet deficient donor $CD4^+$ T cells do not cause GVHD (182). Tbet is also required for Th1 cell migration into inflamed tissues, which also controls the expression and function of CXCR3 and P-selectin (183). The suggested importance of a cytokine-mediated dialogue between APC and donor T cells for Th1 generation is leading to attempts to disrupt it with ustekinumab, an antibody that targets IL-12 and IL-23, after alloHCT for GVHD prophylaxis (184).

Prognostic and diagnostic biomarkers are important for predicting GVHD outcomes and sST2 has been repeatedly identified as a promising biomarker (185-187). IL-33 is upregulated by myeloablative total body irradiation or chemotherapy conditioning and remains elevated at least through day 14 in the small intestine epithelial cells and fibroblasts of a total MHC-mismatched lethal GVHD mouse model (36). These murine findings parallel clinical data where IL-33 is increased in colon biopsies from alloHCT patients with GVHD relative to those without GVHD (36). A lack of IL-33 in the recipient or loss of IL-33 signaling through the receptor, $St2^{-/-}$ donors cells, prevents GVHD and a diminished Type 1 immune response (36). ST2 on donor T cells is not required, however for malignancy clearance (36). Yet, the timing of immune system exposure to IL-33 after alloHCT is important to GVHD disease outcomes. Preconditioning with IL-33 increased the number of recipient-derived $ST2^+$ Treg which persisted post-alloHCT and resulted in decreased GVHD morbidity and mortality (103). Additionally, GVHD is less severe when donor $CD4^+$ T cells lack MyD88 needed for TLR, IL1R, and ST2 signaling and which favors the survival and differentiation of donor T cells into Th1, Tc1, and Th17 cells (188, 189). A lack of MyD88 signaling in donor T cells also facilitates peripheral $Foxp3^+$ Treg expansion after alloHCT to

reduce GVHD lethality (189). The study of IL-33 in alloHCT has demonstrated IL-33 pleiotropy and with provided insights into when to modulate the ST2/IL-33 axis to achieve optimal outcomes.

1.3.3 Mucosal tissue repair

Repair of the injured lung epithelium involves transition through several regulated phases involving inflammation, progenitor proliferation and differentiation, and tissue regeneration and remodeling (190). Early studies established an important role for $ST2^+$ Tregs in the resolution of epithelial injury after virally-induced lung injury due to their secretion of Areg, a bi-functional growth factor (100). Areg supports stem cell proliferation and differentiation and is secreted by ST2 Treg in response to IL-33 and independently of TCR stimulation (100). ILC2 secretion of IL-13 in response to IL-33 stimulates reparative macrophage support of lung regeneration after unilateral pneumonectomy (191). In addition to priming IL-13 secretion by ILC2 or Treg, IL-33 promotes the proliferative self-renewal and differentiation of local macrophages into reparative subsets that aide club cell regeneration and epithelial repair (192). IL-33 also expands lung ILC2s and drives their IL-9 secretion to prevent pyroptosis-mediate loss of endothelial cells (193). IL-33 is an important early signal that triggers innate repair processes, including TCR-independent secretion of IL-13 and Areg by $ST2^+$ Treg, as well as ILC2 expansion and the differentiation of reparative macrophages necessary for lung repair.

Tissue insults, inflammation and infections upregulate IL-33 in the intestines (36, 194) to support the regulation of intestinal inflammation and restore intestinal homeostasis. IL-33 expression is increased in the inflamed mucosa of patients suffering inflammatory bowel disease (IBD) and mice during experimental colitis (195). IL-13 secretion by ILC2s during helminth infections increases $IL\text{-}33^+$ in ASC (28). This appears to support a feed forward mechanism where

local IL-33 promotes goblet cell hyperplasia through IL-13 secretion by ILC2s that also directs Type 2 macrophage differentiation to mediate tissue repair and support a return to homeostasis (196). IL-33 stimulation of $ST2^+$ Treg and IL-10-producing regulatory B cells has also been implicated in the immune cell network stimulated by IL-33 to resolve GI injury and inflammation (99, 197). IL-33 also mediates repair and resolution of colitis by inducing microRNAs, particularly miR-320, to drive the proliferation of $ST2^+$ intestinal epithelial cells (IEC) (198). The IL-33 gene promoter contains a hypoxia inducible factor-1 alpha (HIF-1α) interacting element and TNF-induced HIF-1α^+ epithelial cells augmented IL-33 expression (195). These recent studies suggest that both Type 1 and Type 2 cytokine signaling can modulate IL-33 expression to support the regulation of intestinal inflammation and maintain or restore GI tract homeostasis through actions on local injured tissues as well as a local network of Treg, ILC2s, and regulatory and reparative macrophages.

1.4 Overview and Rationale for Described Experiments

A new understanding of IL-33 in the development and homeostatic functions of tissues and organ systems has been established through the recent innovative study of ST2 and IL-33 deficient mice. IL-33 is clearly a molecule that communicates tissue conditions to a variety of immune cells as they also receive other signals shaping efforts to clear pathogens or maintain or restore a functional equilibrium across organ systems. This role as a restorative and regulatory signal released during injury or cellular death is unique in the IL-1 family and there are numerous mechanistic questions that remain to be answered definitively. First, IL-33-driven $ST2^+$ Treg reparative functions appear especially potent early after injury. Yet, it remains hard to truly

separate the suppressive functions of these cells controlling early inflammation and excess damage from their repair activities. In addition to suppressing detrimental immune responses, Treg are critical for the resolution of inflammation and repair of tissue damage. It has emerged that Treg contribute to the successful resolution of epithelial injury after through the secretion of Areg (100). Areg is a bi-functional growth factor that supports stem cell proliferation and differentiation through actions on the epidermal growth factor receptor (EGFR) (199). Interestingly, it was Treg recognition of the tissue injury signal IL-33, not TCR signaling, that led to this reparative action (100). The dominant function of IL-33 acting on both innate and adaptive immune cells is to generate a Type 2 response dominated by IL-5 and IL-13. There is a close link between Type 2 cytokines and tissue repair and IL-33 has emerged as a major mediator of tissue repair and homeostasis. In the herein studies I probed this relationship and established that IL-33 acts on $ST2^{+}$ Treg to mediate secretion of IL-13 that is important for inflammation resolution and early tissue repair. In these studies, I generated transgenic mice that allowed me to test the hypothesis that IL-33-stimulation of Treg secretion of IL-13 is important to early tissue repair. By generating a mouse with Treg deficient for IL-13 ($Foxp3^{Cre}$ x *il4/il13*^{flox}), I established Treg secreted IL-13, is not involved in direct T cell suppression but is critical to control lethal inflammation and support early injury responses after chemical or viral lung injury. Treg IL-13 limited the presence of local myeloid populations after injury by acting on monocytes and macrophages to direct their differentiation in Arginase 1^{+} macrophages that mediate tissue repair.

Second, it is important to understand the how and when of IL-33 release and ST2 expression that needs to be clarified. We have previously established that IL-33 is augmented in host GI tract by conditioning and GVHD in both mice and humans. Using mouse GVHD models we have established that direct IL-33 stimulation of donor T cells is required for the potent Type

1 T cell response leading to lethal GVHD. Following alloHCT, donor T cells home to the SLO where they become activated to recipient alloantigen. Activated T cells then migrate to peripheral tissues, where tissue-derived factors are thought to provide a stimulatory network that sustains alloresponsive donor T cells to drive GVHD pathology. IL-33 is expressed both in the mucosal barrier tissues and SLO. I established that ST2-deficient T cells do not infiltrate into the tissues, which suggests a critical role for IL-33 in the SLO. In these studies, I tested the hypothesis that IL-33 is important for early donor T cell activation in the SLO prior to migrating to the target organs. My findings identify an important function for IL-33 in contributing to antigen-dependent activation and differentiation of alloreactive $CD4^+$ T cells into Th1 cells by augmenting TCR signaling pathways in the SLO. I identify IL-33 as a stromal cell-derived DAMP that is a costimulatory signal driving the activation and differentiation of alloreactive Th1 cells independently of the indirect PAMP-stimulated innate cytokine, IL-12.

2.0 IL-33-Mediated IL-13 Secretion by ST2^{+} Treg Controls Inflammation After Lung Injury

Data within this chapter were compiled and published in *JCI Insight* in 2019 in the following manuscript:

Liu, Q*, Dwyer, GK*, Zhao Y, Li H, Mathews LR, Chakka AB, Chandran, UR, Thomson, AW, Fan, M, Billiar, TR, and Turnquist, HR. IL-33-mediated IL-13 secretion by ST2^{+} Tregs controls inflammation after lung injury. JCI Insight. 2019. *These authors equal contributed to the manuscript.

2.1 Summary

Acute respiratory distress syndrome is an often-fatal disease that develops after acute lung injury and trauma. How released tissue damage signals, or alarmins, orchestrate early inflammatory events is poorly understood. Herein we reveal that IL-33, an alarmin sequestered in the lung epithelium, is required to limit inflammation after injury due to an unappreciated capacity to mediate Foxp3^{+} Treg control of local cytokines and myeloid populations. Specifically, *Il33*$^{-/-}$ mice are more susceptible to lung damage-associated morbidity and mortality that is typified by augmented levels of the proinflammatory cytokines and Ly6C^{hi} monocytes in the bronchoalveolar lavage fluid. Local delivery of IL-33 at the time of injury is protective but requires the presence of Treg cells. IL-33 stimulates both mouse and human Treg to secrete IL-13. Using *Foxp3*^{Cre} x *Il4/Il13*$^{fl/fl}$ mice, we show that Treg expression of IL-13 is required to prevent mortality after acute

lung injury by controlling local levels of G-CSF, IL-6, and MCP-1 and inhibiting accumulation of Ly6C^{hi} monocytes. Our study identifies a new regulatory mechanism involving IL-33 and Treg secretion of IL-13 in response to tissue damage that is instrumental in limiting local inflammatory responses and may shape the myeloid compartment after lung injury.

2.2 Introduction

ALI can result from direct injury caused by bacterial or viral pneumonia, aspiration, and toxin inhalation and indirect injury following sepsis, major trauma, and blood transfusion (158, 200). ALI may lead to the more severe ARDS that has a complex pathology and causes considerable morbidity and mortality (201, 202). Diffuse alveolar damage, pulmonary edema and hypoxemia due to dysregulated inflammation, reflected by increased inflammatory cytokines in the plasma or bronchoalveolar lavage fluid (BALF) and accumulation of extravascular neutrophils, are defining features of ARDS (200, 203). In addition to neutrophils, macrophages and monocytes also play a causal role in ARDS, as they initiate and perpetuate lung damage through contributing to the local inflammation that causes increased epithelial and endothelial permeability (204-206). Despite intensive basic and clinical studies over the past several decades, there remains a lack of effective treatments to prevent or resolve ARDS (200, 207-215). Thus, the risk of mortality remains high for ARDS patients (202, 216). Lung-protective mechanical ventilation and conservative fluid management reduce inflammatory cytokine levels and neutrophil numbers in the BALF of animals subjected to ALI and ALI/ARDS patients (217, 218). To date, these supportive procedures that reduce early inflammation are the only means to provide consistent improvement in patient outcome (202, 216).

The pathophysiology of ALI is commonly studied in rodent models where instillation of chemicals, such as bleo, damages the epithelial and endothelial barriers, thus increasing alveolar-capillary permeability that results in fluid and protein accumulation in the alveolus (156, 219-221). The BALF isolated in the first several days of bleo-induced ALI contains high levels of neutrophils and inflammatory cytokines, including IL-1β, IL-6, TNF and monocyte chemoattractant protein 1 (MCP-1)/CCL2 (156, 220, 222). Infiltrating inflammatory monocytes, monocyte-derived interstitial macrophages and residential alveolar macrophages (AM) are present and thought to contribute to the early inflammatory response and tissue damage after experimental ALI, including that induced by bleo (204, 223). These same cells, however, also participate in inflammation and injury resolution, as well as the development of subsequent fibrotic disease after ALI (204, 224, 225). Foxp3^{+} Treg have also been implicated in the resolution of ALI by shaping alveolar cytokines, potentially by modulating those produced by macrophages (226). Recently, Misharin et al. revealed that the primary drivers of lung fibrosis following tissue injury are monocyte-derived AM that rapidly replace depleted fetal-derived tissue-resident AM after bleo (227). Gaining an understanding of the endogenous mechanisms controlling early inflammation and shifting the local environment, including resident and infiltrating myeloid cells, away from an inflammatory state and towards one of rapid resolution and effective repair after ALI could lead to novel therapies that can prevent or rapidly resolve ALI/ARDS, as well as reduce subsequent fibrosis.

Tissue injury associated with trauma leads to the release of alarmins, or self-molecules that alert the immune system to damage (228-231). One alarmin of particular interest is IL-33, which is highly expressed in the lungs of mice and humans (4). While IL-33 supports inflammatory responses to parasites, it also drives allergic airway disease and fibrosis of the lung and other organs (4, 6, 232-234). However, Treg that express ST2, encoded by *Il1rl1*, upregulate Areg after

IL-33 stimulation and this mechanism has been implicated recently in epithelial tissue repair after viral infection of the lung (100). Related *in vitro* studies have suggested that IL-33 potentiates the suppressive capacity of Treg (98). After muscle injury, the presence of $ST2^+$ Treg has been associated with the transition of infiltrating myeloid cells from a proinflammatory subset to a reparative/regenerative subset (101). Mechanisms by which IL-33 stimulation of $ST2^+$ Treg to local control of myeloid cell function or differentiation, however, are unknown. These studies proposing the regulatory or reparative activity of IL-33 are in direct contrast to other investigations that suggest IL-33 causes functional dysregulation in Treg in the lung (235) and skin (236). This dysregulation is associated with the lost capacity to suppress (Teff) T cell proliferation and pathological induction of Type 2 cytokine production (235, 236). Accordingly, the role of IL-33 in acute organ injury is unclear and the mechanisms, especially involving Treg, by which IL-33 may shape early inflammation or contribute to injury resolution are poorly defined.

The goal of the current studies was to establish how IL-33 impacts Treg after bleo-induced ALI and to ascertain the role that this interaction plays in shaping the early inflammatory environment. In doing this, we made the unanticipated discovery that IL-33 is critical to prevent mortality after ALI by controlling the early inflammatory response after tissue injury through its actions on Treg. Mice deficient in IL-33 were found to be more susceptible to lung damage-associated lethality, which is typified by augmented levels of inflammatory cytokines and immune cell infiltration. We then established the mechanism underlying IL-33 control of the local inflammatory immune response after ALI involves the induction of the IL-13 production by $ST2^+$ Treg that served to limit local inflammatory cytokines and the presence of inflammatory myeloid cells. In total, we establish an important protective and immunoregulatory capacity of IL-13 and IL-33 after lung injury that supports resolution of the inflammation associated with ALI. Given

that inflammatory responses are considered primary drivers of ARDS, IL-13, IL-33 or IL-33-stimulated Treg secreting IL-13 may be novel therapeutic targets to further evaluate early after ALI.

2.3 Methods and Materials

2.3.1 Mouse strains

C57BL/6-*Foxp3*^{tm1Flv}/J (Foxp3-IRES-mRFP, referred to as "B6 FIR"), B6.129(Cg)*Foxp3*$^{tm3(DTR/GFP)Ayr}$/J (Foxp3-DTR-EGFP), and C.129P2(Cg)-*Il4/Il13*$^{tm1.1Lky}$/J (BALB/c *Il4/Il13*^{flox}) mice were purchased from The Jackson Laboratory. C57BL/6NTac mice were obtained from Taconic. B6 *Il33*$^{-/-}$ have been previously described (115) and were obtained from RIKEN, Japan (University of Tokyo, Tokyo, Japan). *Foxp3*-IRES-Cre mice (BALB/c *Foxp3*^{Cre}; (237)) were obtained from Dr. Dario Vignali (University of Pittsburgh). Previously described BALB/c *Il1rl1*$^{-/-}$ were obtained from Dr. Foo Yew Liew (University of Glasgow, UK) (104, 129). All mice were bred and/or maintained in a specific pathogen-free animal facility at the University of Pittsburgh.

2.3.2 Animal Treatments

For chemically-induced ALI, mice were intratracheally (i.t.) instilled with 1.0 - 1.5 IU/Kg (for mice on B6 background) or 6.0 IU/Kg (for BALB/c background) bleomycin (APP Pharmaceuticals, LLC) on day 0. Recombinant (r) mouse IL-33 (rIL-33, 1.0 μg/mouse; Biolegend)

was instilled i.t. 1 time together with bleomycin on day 0. For rIL-13 administration (1.0 μg/mouse; Biolegend), the first dose was i.t. injected together with bleomycin on day 0 and later doses rIL-13 were instilled intranasally (i.n.) on day +1, +2, and +3. For Treg depletion, *Foxp3*^{DTR} mice were treated with 15 μg/Kg diphtheria toxin (Sigma-Aldrich) on day -3, -2 and -1, and every other day starting from day 1. For virally-induced ALI, influenza A PR/8/34 H1N1 was used to inoculate mice with 100 plaque-forming unit of influenza in 50 μl of sterile PBS by oropharyngeal aspiration on day 0. Viral burden was determined by qRT-PCR on lung RNA for viral matrix as previously described (238). The weight and survival of treated animals was monitored. In survival studies, survival was defined as death or euthanasia after sustained weight loss greater than 30-35% of the starting weight.

2.3.3 Analysis of lung inflammation

On day 7 or 8, mouse lungs were lavaged with sterile PBS and BALF used for flow cytometric assessment and quantification of immune cells and assessment of total protein and IgM. In influenza studies, the middle and cranial lobes of the right lung were snap-frozen and homogenized under liquid nitrogen for RNA extraction by an RNA isolation kit (Agilent Technologies). The concentration of total protein in BALF was measured by DC Protein Assay Kit (Bio-Rad) per the manufacturer's protocol. BALF cytokine concentrations were determined by MILLIPLEX multiplex assay using Luminex (EMD Millipore) following the kit protocol and total IgM quantitated by ELISA. Collagen quantification after bleo injury was performed by hydroxyproline assay. Right lungs were removed and cut into small pieces and then digested overnight at 110°C in 20 ml/g of 6 N HCl. After neutralization with 6 N NaCl, the pH was adjusted ($6.0 < pH < 10.0$). Samples (100 μl) were mixed with 1 ml chloramine T solution (1.4% chloramine

T, 10% isopropanol, 0.5 M sodium acetate, pH 6.0) for 20 min at room temperature, followed by incubation in 1 ml Erlich's solution (14.9% p-dimethylaminobenzaldehyde, 70% isopropanol, 20% perchloric acid; Sigma-Aldrich) at 65°C for 15 min. 200 µl of each sample in a 96-well plate was measured for absorbance at 570 nm. The right lung was used consistently to allow appropriate comparisons.

2.3.4 Histopathological evaluations

For histological analyses, lungs were excised and gently inflated with 10% neutral buffered formalin and then fixed for at least 24 hours before trimming, embedding in paraffin, sectioned transversely, and adhered to glass microscope slides. Following automated hematoxylin and eosin staining, whole slide images (WSI) of each slide were captured via a Zeiss Mirax MIDI scanner utilizing a Plan-Apochromat 40x/.95N.A. objective lens, AxioCam MRm digital CCD camera (Carl Zeiss). WSI images were graded for lung pathology by a pathologist blinded to mouse genotype and/or treatment. Perivascular and peribronchial inflammation, intra-alveolar macrophages, and intra-alveolar hemorrhage were semi-quantitatively scored as follows: none: 0; minimal: 1; mild: 2; moderate: 3, and severe: 4. Fibrosis was scored according to Ashcroft et al (239). Percent area of consolidation was determined using digital slide images as follows: total area of lung consolidation/total area of lung sections. Area of consolidation were manually segmented.

2.3.5 Generation of human monocyte-derived dendritic cells (Mono-DC)

Peripheral blood mononuclear cells (PBMC) were isolated from fresh normal adult human LeukoPaks (Central Blood Bank) following density gradient centrifugation with Ficoll. $CD14^+$ monocytes were positively selected from PBMC using human $CD14^+$ monocyte isolation kits (Miltenyi Biotec). Mono-DC were generated from $CD14^+$ cells in RPMI containing human AB serum (Corning), IL-4, and GM-CSF as we have described (240). Mono-DC were harvested at day 7 and used to expand isolated human Treg.

2.3.6 Culture of human monocyte-derived dendritic cells (Mono-DC) and Treg

$CD4^+$ $CD127^{lo}$ $CD25^{hi}$ Treg were isolated through FACS-sorting with a BD FACSAria following isolation of Pan T cells by negatively selection from $CD14^-$ PBMCs using human Pan T cell isolation kit (Miltenyi Biotec). Mono-DC were suspended in OpTmizer (ThermoFisher) supplemented with 5% human AB serum, irradiated at 30 Gy and plated in 48-well plates at a ratio of 4 Treg to 1 Mono-DC. Human rIL-2 (300 U/ml; Peprotech) alone or with human rIL-33 (50 ng/ml; R&D Systems, Minneapolis, MN) were added on day 2. On day 4, half of the media was exchanged, and cytokines refreshed. On day 7, Treg were analyzed for Foxp3 and IL-13 expression by flow cytometry, suppressive capacity assessed, or transferred to new plates and further expanded in OpTmizer and cytokines until day 12.

2.3.7 Flow Cytometry

Alveolar leukocytes were obtained by centrifugation of BALF collected using methods similar to those described (241, 242). To assess interstitial leukocytes, mouse lungs were cut into small pieces and enzymatically digested using either collagenase D and DNase I (both from Sigma-Aldrich) or lung dissociation kit (Miltenyi Biotec) followed by mechanical dissociation in C tubes using a gentleMACS dissociator (Miltenyi Biotec). Single cell homogenates of splenocytes were generated for flow cytometric assessment using standard and widely published laboratory procedures. Isolated cells were incubated with anti-CD16/32 (clone 93, for FcR block) and Zombie NIR (for cell viability, both from Biolegend) before staining with the following antibodies: anti-CD45 (clone 30-F11), -CD3e (clone 145-2C11), -CD4 (clone RM4-5), -CD25 (clone PC61), -CD11b (clone M1/70), -CD11c (clone HL3), -Ly-6C (clone AL-21), -Ly-6G (clone 1A8), -Siglec-F (clone E50-2440), -I-A/I-E (clone 2G9), -CD24 (clone M1/69), -CD44 (clone IM7), -CD86 (clone GL-1), -CD103 (clone M290), -CD19 (clone 1D3), -Sca-1 (clone D7), -NK1.1 (clone PK136), -Gr1 (clone RB6-8C5), -CD127 (clone SB/199), -ICOS (clone C398.4A), -OX40 (clone OX-86), -GITR (clone DTA-1), -KLRG1 (clone 2F1, all from BD Biosciences); and anti-ST2 (clone DJ8, MD Biosciences). For ILC2 staining, lineage markers included CD3, CD4, CD8, CD19, B220, CD11b, CD11c, FcεRI, GR1, NK1.1 and TER119. For intracellular Foxp3 staining, Intracellular Fixation & Permeabilization buffer set and anti-Foxp3 (clone FJK-16s, both from eBioscience) were used per the manufacturer's instruction. Cultured Human Treg were re-stimulated for 3 h with phorbol 12- myristate-13-acetate for 3 h with GolgiPlug (BD Biosciences) and then surface stained with BD Bioscience antibodies to CD3 (clone UCHT1), CD4 (Clone RPA-TF), and then subsequently stained for intracellular IL-13 (clone JES10-5A2) and Foxp3

(clone 259D/C7). All samples were acquired with an LSRFortessa or LSRII (BD Biosciences) and data were analyzed with FlowJo (BD Biosciences).

2.3.8 RNA-Seq and bioinformatics analyses

Splenic $CD4^+$ T cells were obtained from B6 FIR mice using negative depletion with Dynabeads (Life Technologies) as we have described in detail (104). These cells were cultured for 5 days with BALB/c $CD11c^+$ bone marrow derived dendritic cells (BMDC) generated as we have described (124) in media supplemented with rIL-33 (20 ng/ml; Biolegend). Cultured cells were then stained with antibodies to CD4 and ST2, and the $CD4^+$ $Foxp3^+$ (RFP^+) $ST2^+$ population flow sorted to >95% purity using a BD FACSAria. Sorted cells were rested for 15-18 h in complete RPMI at 5% CO_2 and 37ºC, followed by a 6 hours period where they remained untreated or were stimulated with 100 ng/ml mouse rIL-33 during the culture period. Cells were collected and RNA extracted after lysing in TRIzol reagent (ThermoFisher) according to manufacturer's instructions. RNA-Seq analysis was completed by the University of Pittsburgh Health Sciences Core Research Facilities (HSCRF) shared Genomics Research Core. The RNA-sequencing data have been uploaded into Gene Expression Omnibus (GEO) and are accessible as GSE123922.

RNA-seq libraries were prepared using Ion Total RNA-Seq Kit (Life Technologies) with GeneRead rRNA Reduction kit (Qiagen). Samples were run using an Ion Torrent Proton Sequencer with PI chip and Torrent Suite software v4.2.1 (Life Technologies). The raw Ion Torrent reads were quality trimmed using cutadapt (243). These quality trimmed reads were mapped using 'Two step alignment method for Ion Proton Transcriptome data' as suggested by Life Technologies. The reads were first aligned to GRCm38 mouse Ensembl reference genome using Tophat v2.0.9 (244), then alignment for unmapped reads using bowtie v2.1.0 (245) in local mode. Cufflinks v2.2.1

(246) was used to assemble the transcripts and estimate their abundances. Cuffdiff v2.2.1 (247) was used to perform differential gene expression between the sample sets. A volcano plot using R was generated from the differential gene expression results of Cuffdiff.

2.3.9 qRT-PCR on splenic Treg for Il1rl1, Il10, and Il13 mRNA

B6 FIR mice were treated for 10 days with mrIL-33 in PBS (1 μg/mouse/day, Biolegend) or treated with PBS alone. On day 11, $CD4^+$ T cells were FACS sorted into $ST2^-$ and $ST2^+$ $Foxp3^+$ (RFP^+) populations which were used to generate total RNA that was assessed by qRT-PCR for *Il1rl1, Il10, and Il13* mRNA.

2.3.10 qRT-PCR for myeloid skewing by Treg

BALB/c $Foxp3^{Cre}$ and $Foxp3^{Cre}Il4/13^{fl/f}$ mice were treated for 10 days with 0.5 μg/mouse/day mrIL-33. On day 11, splenocytes were harvested and FACS sorted for $CD3^+$ $CD4^+$ $CD127^{lo}$ $CD25^{hi}$ $ST2^+$ and $ST2^-$ Treg cells. On the same day, splenic macrophages from $Il1rl1^{+/+}$ and $Il1rl1^{-/-}$ mice were isolated by magnetic positive selection using F4/80 beads (Miltenyi). Tregs and macrophages were co-cultured treated with either 20 ng/ml rIL-4, 200 ng/ml mouse rIL-13 (Biolegend) or 20 ng/ml mouse rIL-33 (Biolegend). After 18 hours, the cells were harvested and isolated total RNA assessed for *Arg1* and *18s* mRNA.

2.3.11 qRT-PCR methodology

Total RNA was isolated using TRIzol reagent (ThermoFisher) and Direct-zol RNA miniPrep Plus columns (Zymo Research Corporation). RNA was reverse transcribed using the iScript cDNA synthesis kit (Bio-Rad). *Il10*, *Il13*, *Arg1*, and *18s* messages were amplified with Fast SYBR Green Master Mix (Applied Biosystems) on a StepOnePlus Real-Time PCR System (Applied Biosystems). Data were analyzed using the $2^{-\Delta\Delta CT}$ method (248). Primers for *Il10*, *Il13*, and *Il1rl1* (ST2) were purchased commercially (Qiagen). Primers for *Arginase 1* (*Arg1*) were forward 5′-CAGAAGAATGGAAGAGTCAG-3′and reverse 5'-CAGATATGCAGGGAGTCACC-3'. Primers for *18s* were forward 5′-AACTTTCGATGGTAGTCGCCGT-3′ and reverse 5′-TCCTTGGATGTGGTAGCCGTTT-3′. All qRT-PCR assays were performed in triplicate and data are reflective of no less than three independent experiments.

2.3.12 Treg Suppression Assays

For mouse assays, bulk $CD4^+$ T cells were negatively selected from BALB/c *Foxp3*^{Cre} BALB/c and *Foxp3*^{Cre}*Il4/13*$^{fl/fl}$ spleens using Dynabeads and stained for FACS sorting (FACSAria; BD Biosciences) of $CD3^+$ $CD4^+$ $CD127^{lo}$ $CD25^{hi}$ Treg. Sorted Treg were tested for their ability to suppress anti-CD3/CD28 T-activator bead (5×10^4; Life Technologies)-induced, CellTrace Violet Blue (CTVB; BD Biosciences)-labeled BALB/c $CD3^+$ T cell (T effectors: Teff) proliferation at Teff/ Treg ratios of 8:1, 4:1 and 2:1. Cells were harvested on day 3 and stained intracellularly for FACS analysis. For assessment of human Treg suppressive capacity, cryopreserved Teff, ex vivo-expanded Treg, and CD40L-activated allogeneic B cells were counted before the Teff were labeled

with V450 Proliferation dye (BD Biosciences) and Treg and B cells labeled with carboxyfluorescein succinimidyl ester (BD Biosciences). Labeled cells were suspended in RPMI at 2×10^6/ml for Teff, 5×10^5/ml for Treg, and 5×10^5/ml for B cells. Treg were diluted from 1:2 to 1:128 relative to Teff, while B cell numbers were held constant. Cells were cultured for 5 days before analysis for proliferation was assessed by flow cytometry.

2.3.13 CBA Assessment of Treg cytokine secretion

B6 FIR, BALB/c *Foxp3*^{Cre}, and *Foxp3*^{Cre}*Il4/13*$^{fl/fl}$ mice were either treated for 10 days with mouse rIL-33 in PBS (1 μg/mouse/day, Biolegend) or remained PBS-treated. On day 11, $CD3^+$ $CD4^+$ $CD127^{lo}$ $CD25^{hi}$ $ST2^+$ and $ST2^-$ Treg cells were FACS sorted and plated in flat-bottom 96-well plates coated with anti-CD3 (Bio Xcell, 5μg/ml) in RPMI containing 10% FBS, 2 mM L-glutamine, 0.05 mM 2-mercaptoethanol, 1× MEM Non-Essential Amino Acids, 10 mM HEPES, 1 mM sodium pyruvate, and 100 U/ml each of penicillin and streptomycin. Anti-CD28 (BD Biosciences, 2 μg/ml) and human rIL-2 (Peprotech, 50 U/ml) were added for T cell activation. Some wells were treated with 20 ng/ml mouse rIL-33. After 3 days, the culture supernatants were harvested and analyzed by Cytometric Bead Array (CBA; BD Biosciences) per the manufacturer's instruction for mouse IL-4, IL-13, and IL-10. To measure human Treg cytokine secretion, cell-free supernatants were collected on day 7 of Mono-DC and Treg culture and analyzed for IL-10 and IL-13 by CBA. Data were collected using a BD LSRFortessa Cytometer and analyzed using FCAP Array software (BD).

2.3.14 Statistics

GraphPad Prism (GraphPad Software; San Diego, CA) was used for statistical analyses. Results are presented as means ± SD. Statistical significance was determined by unpaired 2-tailed Student's *t* test, Mann-Whitney test, 1-way ANOVA followed by Tukey-Kramer multiple comparisons test, or Log rank (Mantel-Cox) test. In all cases, a P value < 0.05 was considered statistically significant. Outliers were identified using the ROUT method and a Q value of 1%.

2.3.15 Study approval

All rodent breeding and experimental procedures were approved by and performed in accordance with the guidelines of the Institutional Animal Care and Use Committee of the University of Pittsburgh and complied with the Guide for the Care and Use of Laboratory Animals. Normal human blood products were obtained and utilized in accordance with University of Pittsburgh Institutional Review Board procedures.

2.4 Results

2.4.1 IL-33 deficiency results in an impaired ability to survive ALI induced by bleomycin

Augmenting IL-33 in IL-33 replete mice via delivery of the recombinant (r) protein or inducing over expression by adenoviral vectors has been suggested to augment the development

of fibrosis after bleo administration (165, 249). Yet the impact of endogenous IL-33 after bleo-induced ALI is poorly understood. When compared to wild-type (WT) mice after intratracheal (i.t.) bleo-induced chemical ALI, *Il33*$^{-/-}$ mice exhibited a more substantial loss of body weight (**Figure 2 A**) and the lack of IL-33 accelerated the death of *Il33*$^{-/-}$ mice (**Figure 2 B**) compared to WT. Histological examination revealed that the reduced survival of *Il33*$^{-/-}$ mice was associated with increased lung pathology and inflammation (**Figure 2 C**). Histology scored on day 7 following i.t. bleo revealed that *Il33*$^{-/-}$ mice had significant increases in perivascular and peribronchiolar inflammation (**Figure 2 C and D**). Likewise, lungs from *Il33*$^{-/-}$ mice had markedly increased levels of intra-alveolar macrophage infiltration and early fibrosis compared to WT mice (**Figure 2 C and D**). Computerized calculation of total lung consolidation suggested a more significant loss of functional lung area in *Il33*$^{-/-}$ mice (**Figure 2 D**).

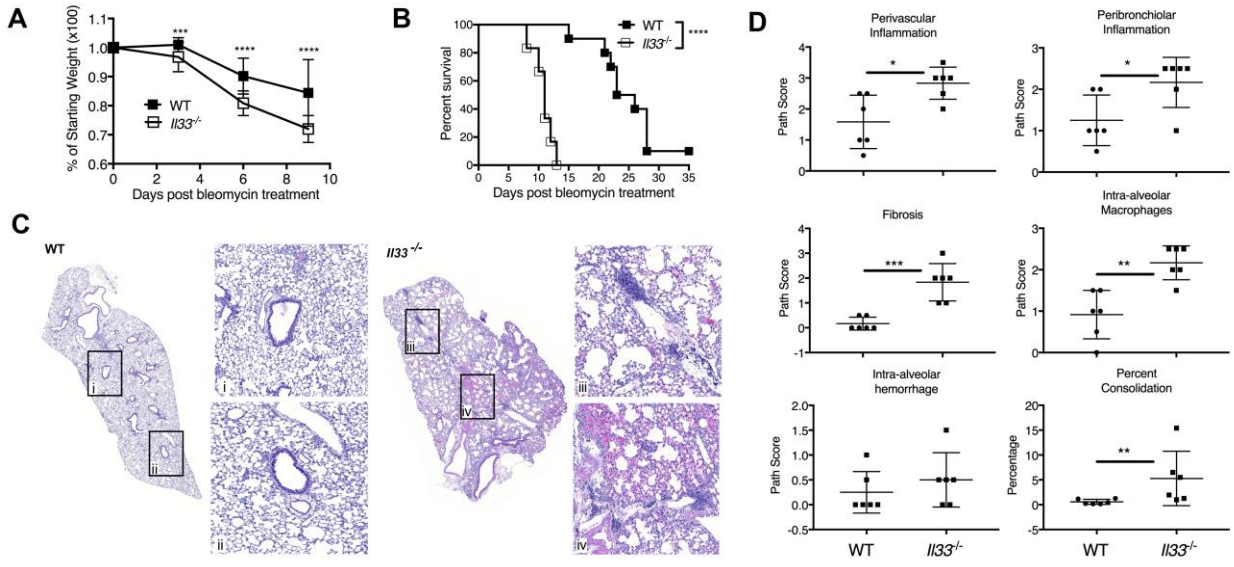

Figure 2. IL-33 deficiency increases mortality after chemically-induced ALI.

***A*, Weight loss and *B*, mortality rate of WT and Il33$^{-/-}$ B6 mice injected intratracheally (i.t.) with bleomycin (bleo, 1.5 IU/Kg). Data depicted are representative of 2 independent experiments (n = 6-10 mice per group). *C*, Representative hematoxylin and eosin (H&E) staining of lung sections from WT and *Il33*$^{-/-}$ mice at day 7 post 1.5 IU/Kg bleo i.t. delivery. *D*, Scoring of H&E stained lung sections collected at day 7 post bleo administration. Scoring for perivascular and peribronchiolar inflammation, fibrosis, intra-alveolar macrophages and hemorrhage, and consolidated parenchyma. Data depicted are from two pooled experiments and representative of 3 experiments completed (n = 6 mice per group). Data are means ± SD. *P* values are determined by log-rank test (*B*), two-tailed Student's *t*-test (*A*, *C*), or Mann-Whitney test (*C*, Percent Consolidation). **P*<0.05, ***P* <0.01, ****P* <0.001, *****P* <0.0001.**

IL-33 deficient mice also displayed a slight trend towards increased levels of total protein in BALF at days 7-8 post bleo (**Figure 3 A**). Surviving *Il33*$^{-/-}$ mice on day 13 also displayed increased levels of hydroxyproline that was consistent with the early increase in fibrosis identified by histopathology (**Figure 2 C and D; Figure 3 B**). Together, these data suggest a role for endogenous IL-33 in the protection of mice from mortality after bleo-induced ALI. Also, as the

course of the immune response to bleo injury to the lung is well-studied and described, it was apparent that IL-33-deficient mice were dying during the peak of the inflammatory immune response (250, 251).

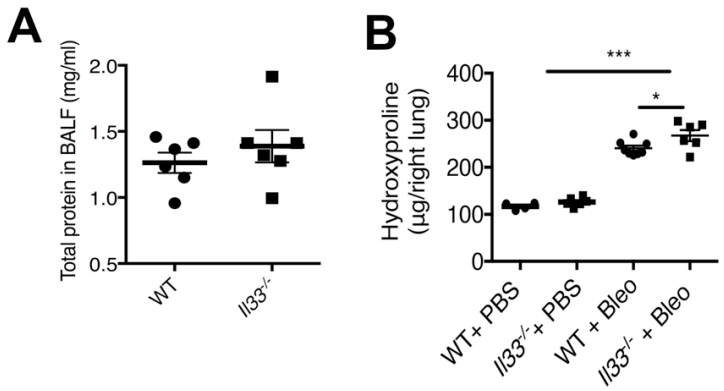

Figure 3. IL-33 reduces hydrooyproline following lung injury.

***A*, IL-33 did not significantly affect early levels of total protein in bronchoalveolar lavage fluid (BALF) at days 7-8 post i.t. bleo injection. *B*, By day 13, however, surviving bleo-treated *Il33*$^{-/-}$ mice displayed significantly increased levels of lung hydroxyproline. Data depicted are mean ± SD *P* values were determined by two-tailed Student's *t*-test. **P*<0.05, ****P*<0.001. Data depicted are from 1 experiment representative of 2 completed and n=4-8 mice per group.**

2.4.2 Evidence for increased inflammation after ALI in the absence of IL-33

We next verified that restoration of IL-33 could protect *Il33*$^{-/-}$ mice from early mortality following bleo challenge. While a onetime instillation of rIL-33 at the time of 1.5 IU/kg i.t. bleo did not rescue *Il33*$^{-/-}$ mice (data not shown), rIL-33 treatment did rescue a significant percentage of mice from mortality after 1.0 IU/kg bleo-induced lung injury (**Figure 4 A**). At this dose of bleo, *Il33*$^{-/-}$ mice again displayed an accelerated death rate relative to WT mice (**Figure 4 A**).

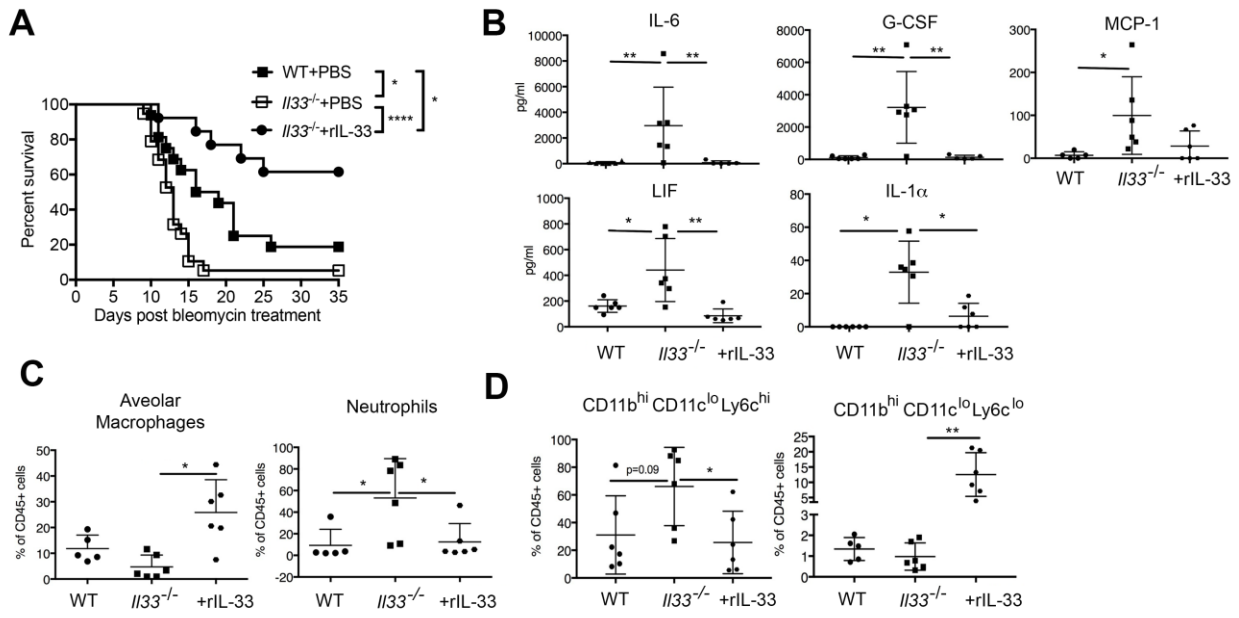

Figure 4. Local delivery of IL-33 protects *Il33*$^{-/-}$ mice from mortality after ALI and reduces the frequency of proinflammatory cytokines and myeloid cells in alveoli.

***A*, Survival of WT or *Il33*$^{-/-}$ B6 mice injected i.t. with 1.0 IU/Kg bleo alone or with 1 μg rIL-33. Data depict are from 2 pooled experiments. *B*, At days 7-8 post bleo delivery, bronchoalveolar lavage fluid (BALF) from *Il33*$^{-/-}$ mice had increased IL-6, G-CSF, LIF, IL-1α, and MCP-1 concentrations, which were significantly reduced by rIL-33 restoration. Data depicted are from 1 experiment representative of 2 and n = 5-6 mice per group. *C* and *D*, Flow cytometric assessment of BALF cells from WT and *Il33*$^{-/-}$ treated as in (A). *C*, Frequencies of alveolar macrophages (CD45^{+} CD11b^{lo} Siglec-F^{+}) and neutrophils (CD45^{+} CD11b^{hi} Siglec-F^{-} Ly6G^{hi}). *D*, Frequencies of alveolar Ly6C^{hi} inflammatory monocytes (CD45^{+} CD11b^{hi} CD11c^{lo} Ly6C^{hi}) and Ly6C^{lo} immunosuppressive and reparative monocytes (CD45^{+} CD11b^{hi} CD11c^{lo} Ly6C^{lo}). Data are representative of 2 independent experiments with 5-6 mice per group in each experiment. Data are mean ± SD. *P* values are determined by log-rank test, *A*, or 1-way ANOVA followed by Turkey multiple comparisons test, *B*-*D*. **P* < 0.05, ***P* < 0.01.**

Given the apparent failure of *Il33*$^{-/-}$ mice to control or resolve the inflammatory response after injury, we next sought to define how restoration of IL-33 altered the local immune and cytokine environment early after bleo-induced lung injury. Luminex quantification of BALF cytokines revealed that IL-33 was a negative regulator of IL-6, granulocyte colony-stimulating factor (G-CSF), MCP1/CCL2, leukemia inhibitory factor (LIF), and IL-1α in samples collected on days 7 and 8 post bleo insult (**Figure 4 B**). While detected, we did not observe significant differences between WT and *Il33*$^{-/-}$ BALF levels of Eotaxin/CCL11, IL-5, IL-9, CXCL10, CXCL1, and CXCL9 (*data not shown*). Granulocyte-macrophage colony-stimulating factor, IFNγ, IL-1β, IL-2, IL-3, IL-4, IL-7, IL-10, IL-12p40, IL-12p70, IL-13, IL-15, IL-17, and CXCL5 were not detected in the BALF at this time point (*data not shown*).

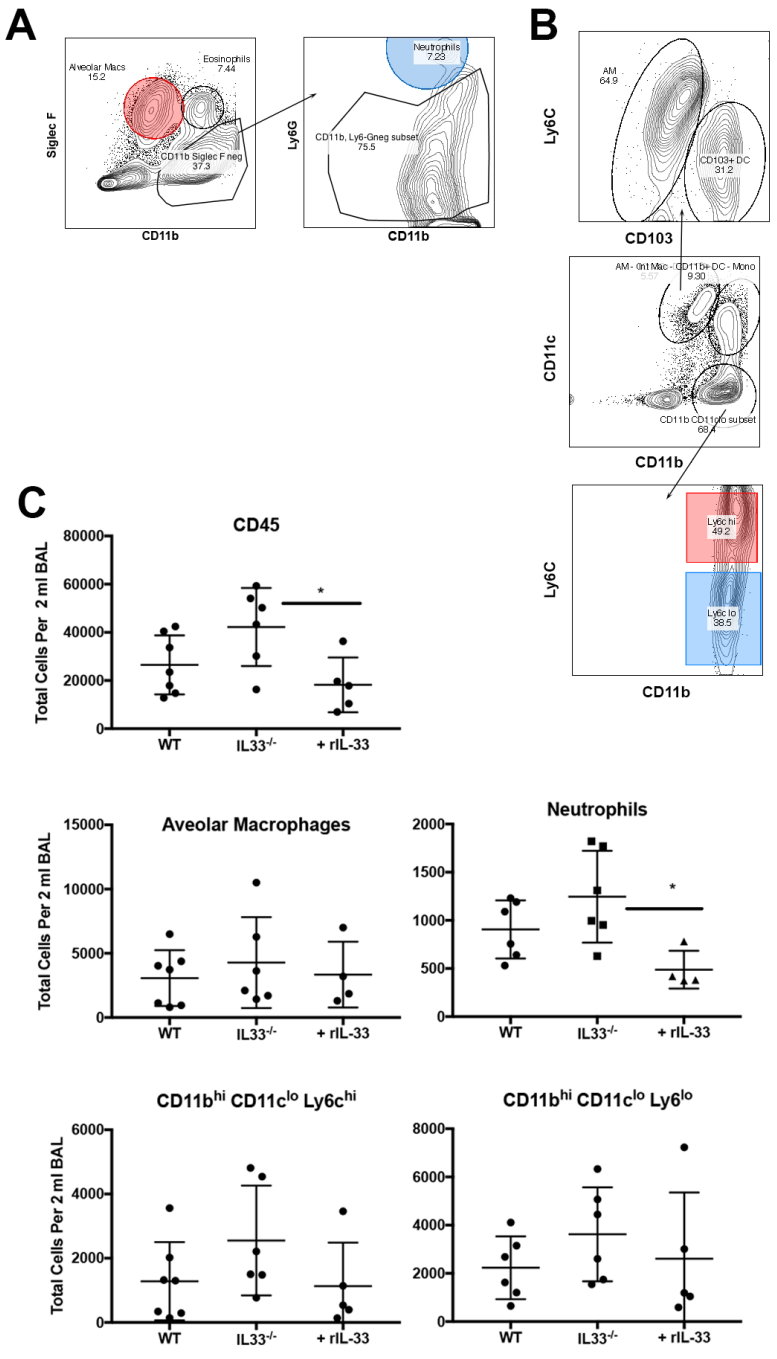

Figure 5. Administration of rIL-33 reduces total CD45$^+$ cell count and total neutrophils.

***A*, Example of gating strategy used for Figure 4 flow cytometric assessment of BALF on day 7 or 8 post i.t. bleo for alveolar macrophages (CD45$^+$ CD11b^{lo} Siglec-F$^+$), eosinophils (CD45$^+$ CD11b^{hi} Siglec-F^{hi}), and neutrophils (CD45$^+$ CD11b^{hi} Siglec-F$^-$ Ly6G^{hi}). *B*, Gating strategy used to characterize BALF on day 7 or 8 post bleo for**

alveolar macrophages (CD45$^+$ CD11b^{lo} Ly6C$^+$ CD103$^-$ Siglec-F$^+$), CD103$^+$ DC (CD11b^{lo} CD103$^+$) and monocytes (CD45$^+$ CD11b^{hi} CD11c^{lo} Ly6C^{hi} or Ly6C^{lo}). *C*, Calculated total number of indicated immune population. Data were pooled from 2 independent experiments (n = 5-6 mice per group total) and presented as means ± SD. *P* values were assessed by 1-way ANOVA. *P<0.05

When the cellular infiltrates present in the BALF of *Il33*$^{-/-}$ mice at day 7 and 8 post bleo were compared to that of WT by flow cytometry, it was found that the BALF of *Il33*$^{-/-}$ mice had significantly increased frequency of neutrophils (CD45$^+$ CD11b^{hi} Siglec-F$^-$ Ly6G^{hi}; **Figure 4 C and D and Figure 5**). Intratracheal delivery of rIL-33 to *Il33*$^{-/-}$ mice reduced the frequency and total number of neutrophils to WT levels, implicating the importance of IL-33 as a critical regulator of early neutrophil infiltration during ALI (**Figure 4 C and Figure 5 C**). While we did not see a significant difference between WT and *Il33*$^{-/-}$ mice in the anticipated loss of AM (CD45$^+$ CD11b^{lo} Siglec-F^{hi}) after bleo instillation, we did find that rIL-33 delivery limited the loss of this immune population (**Figure 4 C**). We did not find any consistent alteration in the frequency or number of eosinophils (CD45$^+$ CD11b$^+$ Ly6G^{lo} Siglec-F$^+$) between any of the groups (*data not shown*). IL-33 deficient mice did, however, display a trend towards increased frequency of Ly6C^{hi} inflammatory monocytes (CD45$^+$ CD11b^{hi} CD11c^{lo} Ly6C^{hi}) in BALF 7/8 days post bleo treatment, which was reversed by IL-33 delivery (**Figure 4 D**). An increase in Ly6C^{lo} monocytes frequency relative to that of Ly6C^{hi} monocytes in sites of injury is correlated with tissue repair and inflammation resolution (101, 225, 252). Interestingly, delivery of IL-33 at the time of bleo insult potently increased the frequency, but not total number, of Ly6C^{lo} monocytes in the BALF (**Figure 4 D and Figure 5 C**). Our data generated on day 7 and 8 after bleo injury are consistent with IL-33 acting as crucial local factor that limits and qualitatively shapes the early inflammatory response after ALI.

2.4.3 IL-33 protective function following ALI is mediated by regulatory T cells

Accumulation of Treg expressing ST2 has been implicated in muscle repair after skeletal injury and this phenomenon was differentially regulated by the availability of local IL-33 (253). Thus, we first examined whether a decrease in the baseline level of Treg, including the $ST2^+$ subset, due to a loss of IL-33 in the normal lung, could account for the observed increase in mortality of *Il33*$^{-/-}$ mice after bleo. Our analysis, however, established that the frequency of Treg in $CD45^+$ lymphocytes isolated from the lung parenchyma of normal and *Il33*$^{-/-}$ mice was not significantly different, indicating *Il33*$^{-/-}$ mice did not have a baseline deficiency in Treg (**Figure 6 A and B**). We also established that a lack of IL-33 did not significantly reduce the frequency of interstitial Treg at day 8 post bleo delivery relative to WT lungs, although delivery of rIL-33 increased the frequency of $ST2^+$ Treg in the lung (**Figure 7 A and B**). A similar phenotype was observed for type 2 innate lymphoid cells (ILC2s; $CD45^+$ $Lineage^-$ $ICOS^+$ $Sca\text{-}1^+$ cells) following bleo challenge, as the frequency of ILC2 was not reduced in *Il33*$^{-/-}$ mice after bleo-induced ALI but was increased by local rIL-33 delivery (**Figure 8**).

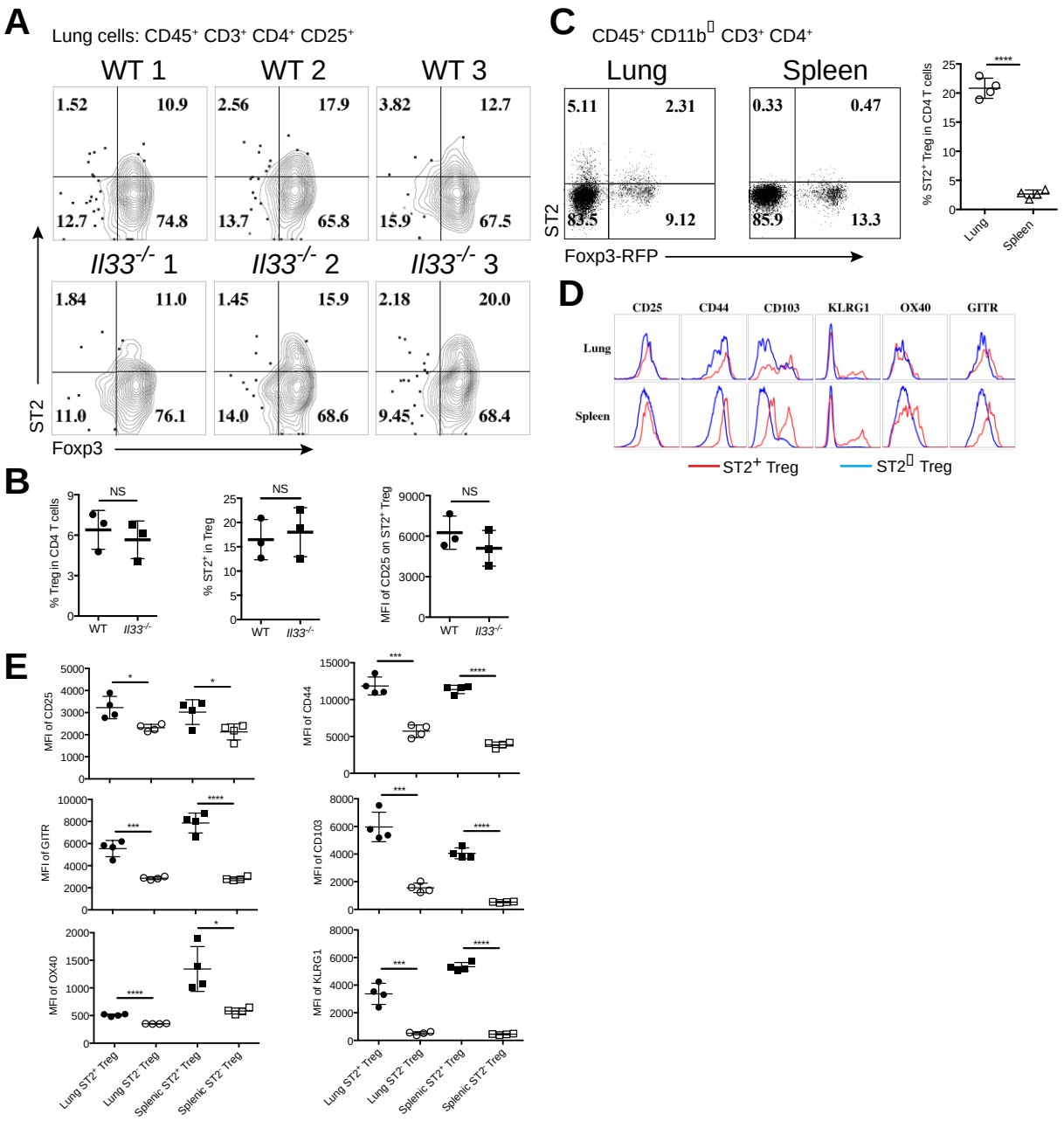

Figure 6. IL-33 deficient mice do not have defective Treg.

***A-B*, Flow cytometric assessment of CD45$^+$ CD3$^+$ CD4$^+$ CD25$^+$ cells isolated from enzymatically digested naïve WT B6 (n = 3) and B6 *Il33*$^{-/-}$ (n = 3) mouse lungs establishes that IL-33 deficiency does not result in a baseline defect in frequency of lung Treg, including the ST2$^+$ subset. Statistical significance between means ± SD were determined by unpaired, 2-tailed Student's *t*-test. *C-E*, Flow cytometric comparison of ST2$^+$ and ST2$^-$ Treg subsets from the spleen and lung regarding their expression of activation markers including CD44, CD103 and**

KLRG1, and suppressor functional molecules such as OX40 and GITR. Data are means ± SD P values were determined by two-tailed Student's *t*-test. NS, not significant. *P < 0.05, ***P < 0.001, ****P < 0.0001.

We have previously shown that rIL-33 delivery expands $ST2^+$ Treg to promote heart allograft survival (104) or prevent GVHD (103) in a Treg-dependent manner. To better define if the observed protective capacity of IL-33 after lung injury depended on Treg or ILC2, we utilized *Foxp3*^{DTR} B6 mice that permit diphtheria toxin (DT) depletion of Treg due to their *Foxp3* promoter-driven expression of the DT receptor (254). The use of this model would, however, leave ILC2s intact. Importantly, we found that rIL-33 delivery with bleo to Treg replete *Foxp3*^{DTR} B6 mice provided significant protection relative to Treg replete *Foxp3*^{DTR} B6 mice receiving bleo alone (**Figure 6C**). Thus, we demonstrated the protective capacity of local IL-33 against bleo-induced ALI in a second strain combination.

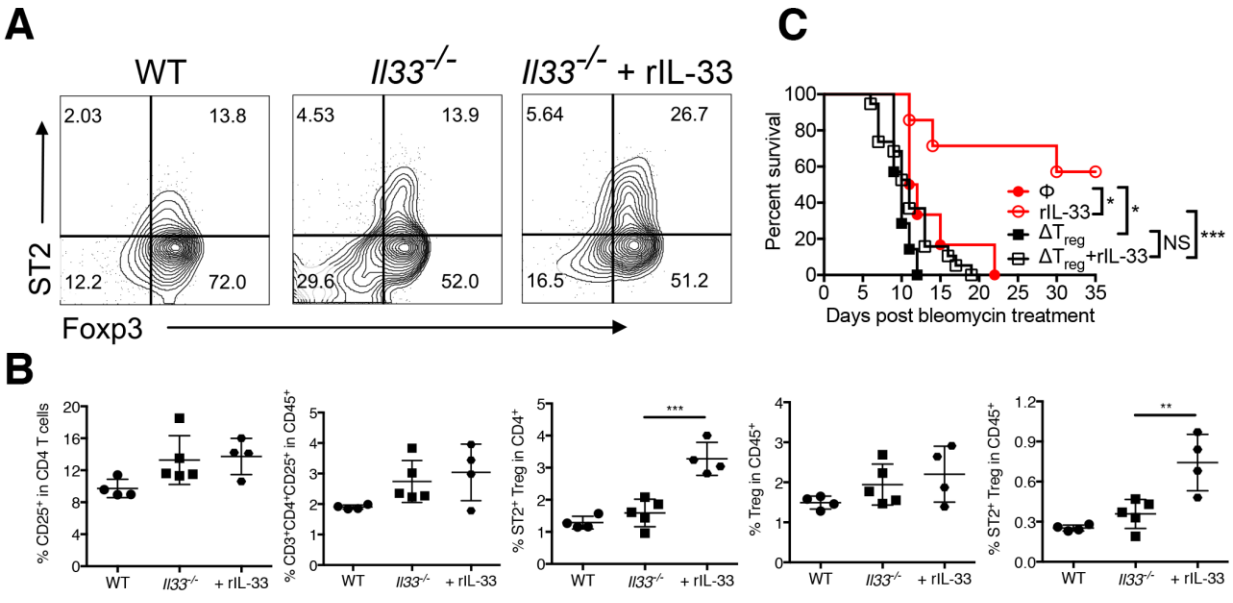

Figure 7. IL-33 increases Treg that are required for protective functions of IL-33 after ALI.

***A-B*, Flow cytometric assessment of CD45$^+$ CD3$^+$ CD4$^+$ CD25$^+$ cells isolated from enzymatically digested WT B6 and B6 *Il33*$^{-/-}$ mouse lung tissue at day 8 post bleo revealed that delivery of IL-33 increased ST2$^+$ Treg in damaged *Il33*$^{-/-}$ lung tissue. Data depicted in *B* are means ± SD and are representative of 2 independent experiments with 4-5 mice per group in each experiment. *C*, Survival of B6 *Foxp3*^{DTR} mice injected i.t. with bleo alone or with rIL-33 (1 µg i.t.) in the presence of Treg or following their deletion with diphtheria toxin (15 µg/Kg on day -3, -2 and -1, and every other day starting from day 1). Depicted data represent 1 experiment with 6-7 mice per group. *P* values are determined 1-way ANOVA followed by Turkey multiple comparisons test, *B* or log-rank test, *C*. * $P < 0.05$, ** $P < 0.01$, *** $P < 0.001$.**

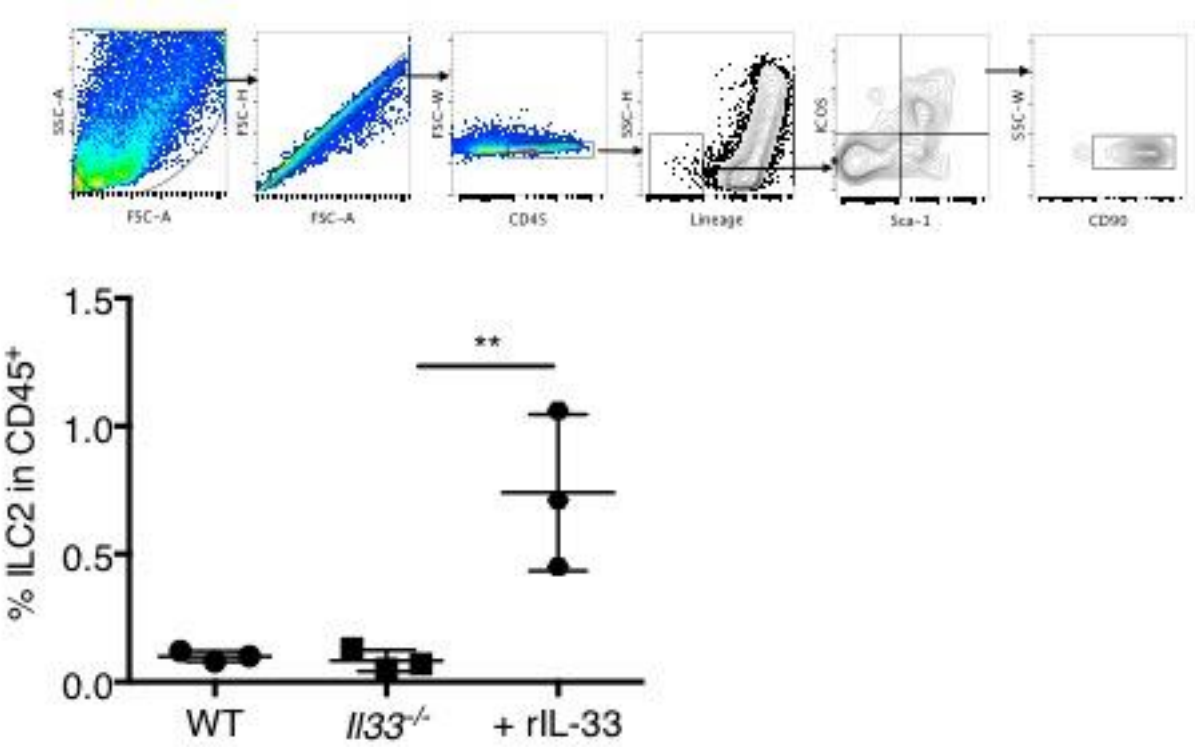

Figure 8. IL-33 deficient mice do not have reduced ILC2 post-bleo treatment.

The frequency of type 2 innate lymphoid cells (ILC2s; $CD45^+$ $Lineage^-$ $ICOS^+$ $Sca\text{-}1^+$) was not reduced in *Il33*$^{-/-}$ mice after bleo-induced ALI. *A*, Gating strategy used to assess ILC2 in WT or *Il33*$^{-/-}$ B6 mice injected i.t. with bleo (1.5 IU/Kg) alone or i.t. bleo and 1 µg recombinant IL-33 (rIL-33). *B*, Data depicted in B are means ± SD and *P* value was determined by 1-way ANOVA followed by Turkey multiple comparisons test. ** *P* < 0.01.

We also verified that there were comparable rates of DT-mediated depletion between mice treated with IL-33 and those left untreated (**Figure 9**). As expected (226), Treg-depleted mice display increased susceptibility to death after bleo compared to Treg replete mice (**Figure 7 C)**. IL-33-treated, Treg-depleted mice had a slight, but non-significant increase in survival after i.t. bleo suggesting a minimal role for ILC2 in IL-33-mediated protection early after ALI. In total, these data support the importance of IL-33 action on Treg for a protective function following ALI.

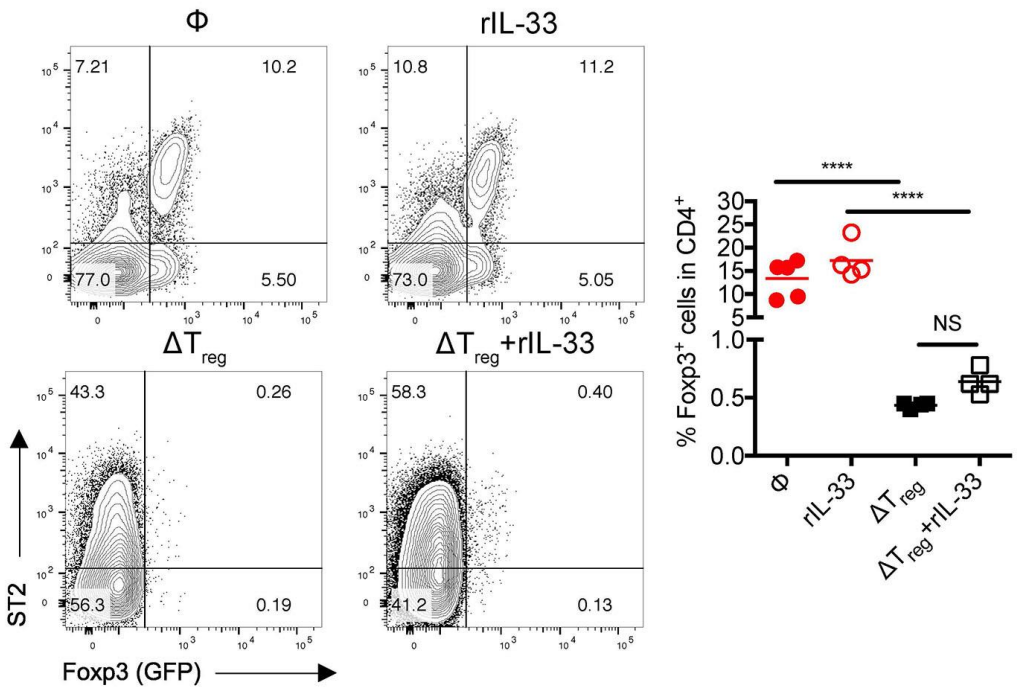

Figure 9. Comparable rates of Treg depletion.

Flow cytometric assessment of CD45$^+$ CD3$^+$ CD4$^+$ cells isolated from enzymatically digested Treg replete B6 *Foxp3^{DTR}* mice lungs at day 8 post bleo (1.0 IU/Kg i.t.) alone (ϕ) or with rIL-33 (1 µg i.t.) compared to those of B6 *Foxp3^{DTR}* mice receiving diphtheria toxin (DT) (15 µg/Kg on day -3, -2 and -1, and every other day i.p. starting from day 1) and bleo and/or rIL-33 treatment at day 0. This analysis establishes that Treg were effectively and comparably depleted by DT during bleo and rIL-33 administration. Depicted data represent 1 experiment with 4-5 mice per group. *P* values were determined 1-way ANOVA. ****$P < 0.0001$.

2.4.4 IL-33 stimulates the secretion of IL-13 by murine ST2$^+$ Treg

IL-33 can directly support the expansion of ST2$^+$ Treg via activation of the p38 pathway (103) and IL-33 support of Treg accumulation is implicated in their function in muscle repair (253) and protection against GVHD (103). We have established previously that this subset of Treg is suppressive in standard *ex vivo* Treg suppression assays (104, 124). We next used RNA-seq to

define how else IL-33 may impact Treg by assessing the expression signature of IL-33-stimulated $ST2^+$ Treg compared to that of untreated $ST2^+$ Treg (**Figure 10 A**). These data revealed that $ST2^+$ Treg stimulated with rIL-33 for 6 hours exhibited increased expression of *Il10*, as expected (255), but also exhibited increased *Il13* compared to unstimulated $ST2^+$ Treg (**Figure 10 A**). We confirmed the transcriptional upregulation of *Il10* and *Il13* in *ex vivo*-sorted $ST2^+$ and $ST2^-$ Treg from rIL-33-treated and PBS-treated mice via qPCR (**Figure 10 B**). We next utilized $Foxp3^+$ reporter mice to characterize the cytokine production induced by IL-33 in $ST2^+$ Treg relative to other $CD4^+$ T cells. As shown in **Figure 10 C**, Splenic $CD4^+$ T cells could be sorted into four populations based on their expression of CD25, Foxp3, and ST2. These populations were Th2 cells ($CD4^+$ $CD25^{hi}$ $ST2^+$ $Foxp3^-$), $CD25^{lo}$ $Foxp3^+$ T cells ($CD4^+$ $CD25^{lo}$ $ST2^-$ $Foxp3^+$), $ST2^+$ Treg ($CD4^+$ $CD25^{hi}$ $ST2^+$ $Foxp3^+$), and $ST2^-$ Treg ($CD4^+$ $CD25^{hi}$ $ST2^-$ $Foxp3^+$). As expected CD3/CD28-stimulated Th2 cells secreted significant levels of IL-10 and IL-13 (256, 257), however, the secretion of these cytokines was not modulated by IL-33, and thus IL-33-independent (**Figure 10 D and E, Columns #7 and #8**). Anti-CD3/CD28-stimulated or anti-CD3/CD28/IL-33- stimulated $ST2^-$ Treg secreted very little IL-13 (**Figure 10 E, Columns #1 and #3**). They did secrete IL-10, but the quantity was much less than that produced by the other three $CD4^+$ T cell subsets (**Figure 10 D)**. $CD4^+$ $CD25^{lo}$ $Foxp3^+$ $ST2^-$ T cells also exhibited this pattern of cytokine secretion (**Figure 10 D and E, Columns #5 and #6)**. $ST2^+$ Treg were the most abundant producers of IL-10, but this production was IL-33-independent, as it was similar between anti-CD3/CD28- and anti-CD3/CD28/IL-33-stimulated groups (**Figure 10 D, Columns #2 and #4).** IL-33 stimulation of $ST2^+$ Treg combined with anti-CD3/CD28-exposure did significantly increase their secretion of IL-13 (**Figure 10 E, Columns #2 and #4).** These data are consistent with recent findings from other groups and establish that $ST2^+$ Treg secrete both IL-10, thought to support the

suppressive capacity of Treg (98) and IL-13, which has been suggested to result in a pathophysiologic role for Treg during the development of allergic airway disease (235).

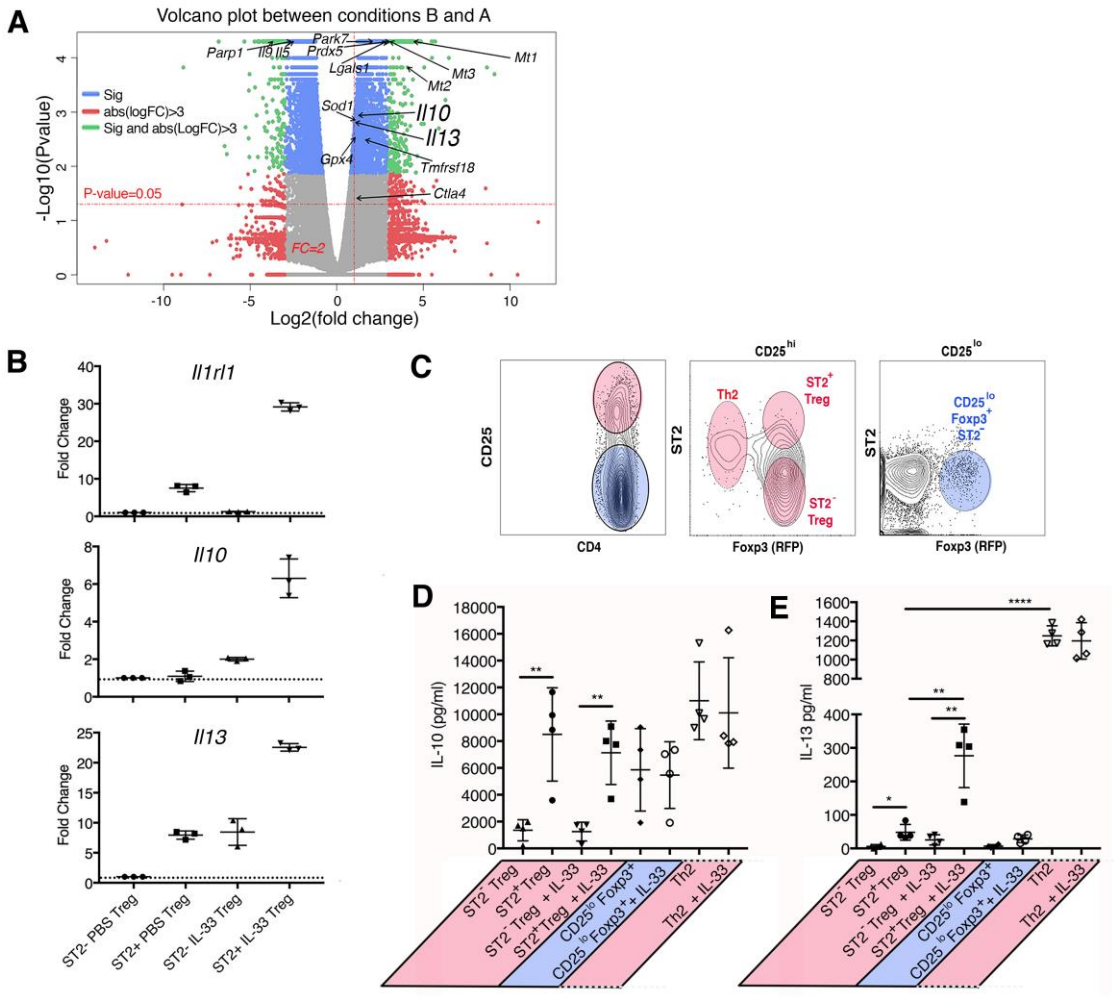

Figure 10. IL-33 stimulates the secretion of IL-13 by murine ST2$^+$ Treg.

A, **Volcano plot depicting RNA-sequencing (RNA-seq) analysis comparing ST2$^+$ Treg stimulated for 6 hours in the presence or absence of IL-33 (20 ng/ml) revealed increased message for *Il10* and *Il13* after IL-33 stimulation.** ***B,*** **qRT-PCR for *Il1rl1*, *Il10*, and *Il13* expressed by sorted CD4$^+$ Foxp3$^+$ (RFP$^+$) ST2$^-$ or ST2$^+$ cells from PBS or IL-33-treated Foxp3-IRES-mRFP reporter mice confirmed RNA-seq findings. Each column represents 3 mice. Data are from 1 experiment representative of 3 completed.** ***C-E,*** **Representative flow cytometry plot depicting the sorting strategy used for assessment of cytokine secretion by indicated CD4$^+$ T cell populations after culture with or without IL-33 (20 ng/ml). Supernatants were harvested on day 3 of culture and assessed by Cytometric Bead Array (CBA) for *D,* IL-10, and *E,* IL-13. Statistical analysis with ANOVA was used to establish significance between values indicated. **P* < 0.05, ***P* < 0.01, ****P* < 0.001, *****P* < 0.0001.**

2.4.5 rIL-33 enhances expansion of suppressive IL-13-secreting human Treg

We next determined whether rIL-33 facilitated these effects in human Treg. We have established previously that the addition of rIL-33 to cultures of mouse monocyte-derived dendritic cells (Mono-DC) and $CD4^+$ T cells was highly effective in expanding suppressive $ST2^+$ Treg (124). As such, we relied on a modification of this approach to establish if IL-33 supported the expansion of human Treg and to define whether IL-33 stimulation of human Treg altered their suppressive capacity or production of IL-10 and IL-13. When rIL-33 was added to cultures of $CD4^+$ $CD25^{hi}$ $CD127^{lo}$ Treg flow-sorted from peripheral blood mononuclear cells (PBMC) and allogeneic Mono-DC, we observed that IL-33 did indeed support the expansion of human Treg comparable to what we had observed previously in mice (**Figure 11 A and Figure 12 A**). During the 7-day culture, rIL-33-expanded Treg maintained their suppressive function (**Figure 11 B**).

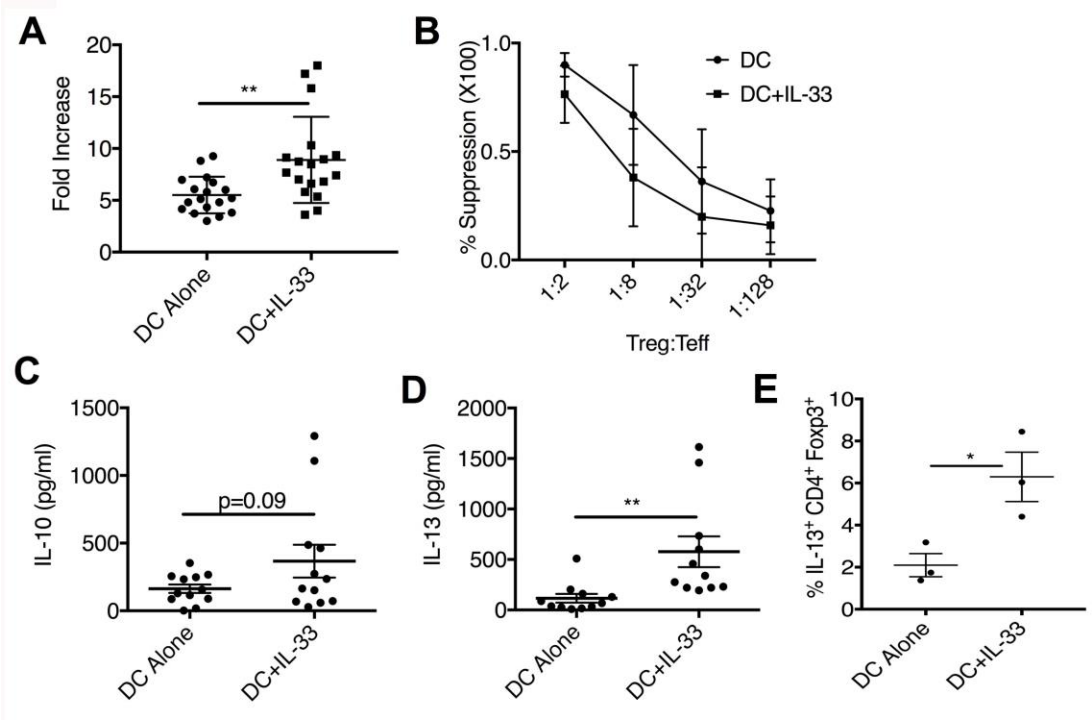

Figure 11. IL-33 expands suppressive human Treg that secrete IL-13.

A-D, **Human Treg ($CD4^+$ $CD25^{hi}$ $CD127^{lo}$) sorted from peripheral blood mononuclear cells (PBMC) were cultured with allogeneic monocyte-derived dendritic cells (Mono-DC) and recombinant human IL-2 (300 U/ml alone or with recombinant human IL-33 (50 ng/ml) added.** ***A,*** **Cells were counted on the 7^{th} day of culture and mean ± SD fold increase in Treg depicted. Data represent 8 individual experiments with 18 different Treg and Mono-DC combinations.** ***B, Ex vivo*****–expanded Treg from each culture condition were tested for their ability to suppress Teff proliferative responses to CD40L-activated allogeneic B cells. Treg suppressive function is expressed as percent suppression of T cell proliferation and the mean ± SD from 5 cultures of expanded Treg are depicted.** ***C-D,*** **Supernatants were harvested on day 7 of culture and assessed by Cytometric Bead Array (CBA) for** ***C,*** **IL-10, and** ***D,*** **IL-13. Data depicted are mean ± SD and statistical significance was determined between each condition by unpaired, 2-tailed Student's** ***t*****-test. ****P* **< 0.05, *****P* **< 0.01.** ***E,*** **Mean frequency of IL-13^+ $CD4^+$ $Foxp3^{hi}$ cells in cultures with and without IL-33 was determined by intracellular IL-13 and Foxp3 staining of one donor's Treg following 7 days of culture with Mono-DC generated from two different donors. Data depicted Treg from 3 different donors and are means ± SEM. Statistical significance was determined between each condition by unpaired, 2-tailed Student's** ***t*****-test. ****P*<0.01.**

Furthermore, while IL-33 only slightly increased the secretion of IL-10 by human Treg (**Figure 11 C**), it profoundly increased their secretion of IL-13 (**Figure 11 D**). We also verified that Treg cultured with IL-33 expressed a high level of Foxp3 (**Figure 12 B**) and established that the IL-13 production was restricted to $Foxp3^{hi}$ T cells (**Figure 11 E and Figure 12 C**). In total, our data support the capacity of IL-33 to mediate the production of IL-13 by suppressive mouse and human Treg.

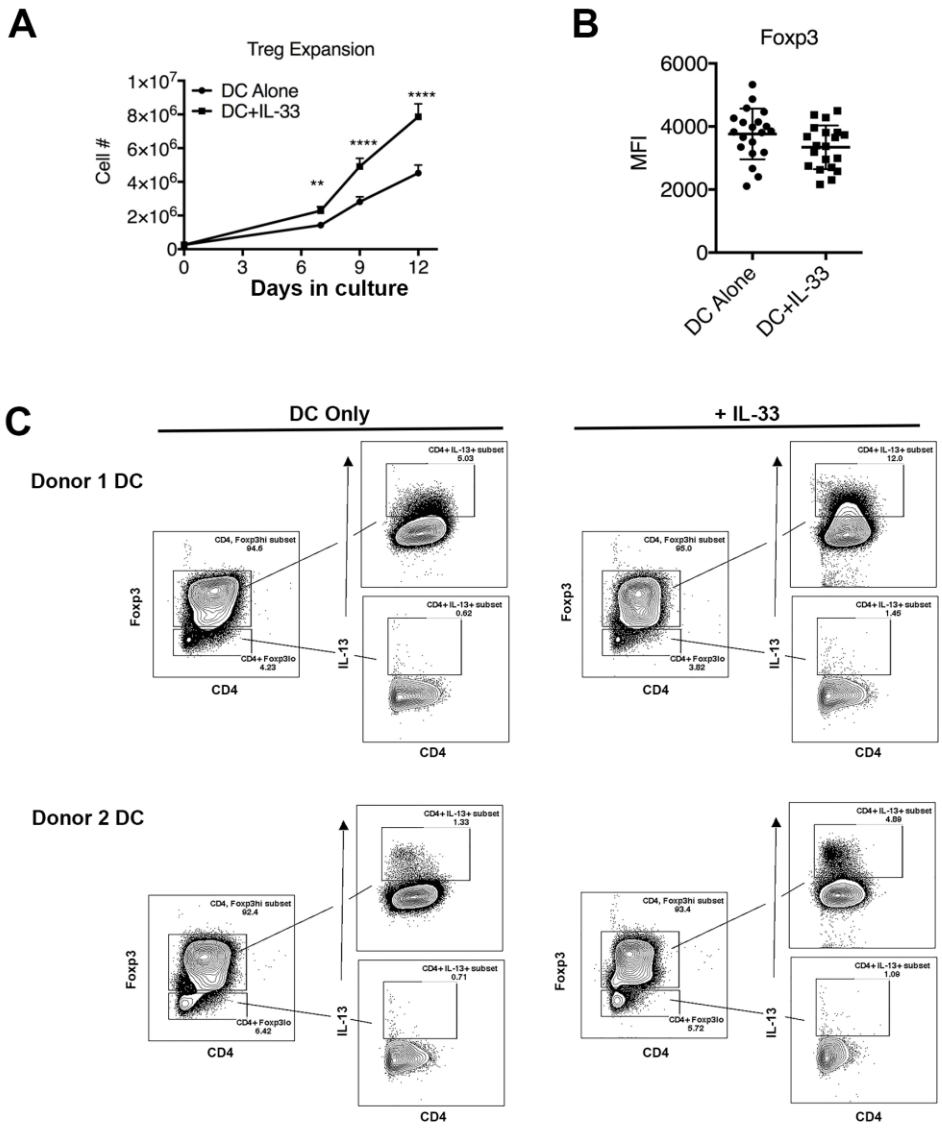

Figure 12. IL-33 treated human Treg maintain Foxp3 expression.

Human Treg ($CD4^+$ $CD25^{hi}$ $CD127^{lo}$) were sorted from peripheral blood mononuclear cells and cultured with allogeneic monocyte-derived dendritic cells (Mono-DC) and recombinant human IL-2 (300 U/ml) alone or with recombinant human IL-33 (50 ng/ml) added. *A,* Absolute count of human Treg cell numbers over the course of culture under the indicated conditions. Data depicted are means ± SD and statistical significance was determined between each condition by unpaired, 2-tailed Student's *t*-test. *****P*<0.001, *******P* **<0.0001. Data represent 8 individual experiments with 18 different Treg and Mono-DC combinations. *B,* Expression of Foxp3 in total viable cells was quantitated on the 7^{th} day of culture by flow cytometry following intracellular staining. No significant difference between the two groups was observed when the two groups were compared by an**

unpaired, 2-tailed Student's *t*-test. Lines depict mean ± SD and data are from 8 individual experiments with 20 different Treg and Mono-DC combinations. *C,* Representative intracellular IL-13 and Foxp3 staining of one Treg sample following 7 days of culture with Mono-DC generated from two different donors and stimulation of cultures with phorbol 12- myristate-13-acetate for 3 h in the presence of golgi plug.

2.4.6 Treg secretion of IL-13 is required to protect mice from mortality after ALI

To determine if IL-33-mediated local IL-13 secretion may have any protective function against ALI mortality we administered rIL-13 i.t. in conjunction with bleo challenge of *Il33*$^{-/-}$ mice and found that rIL-13 significantly improved their survival (**Figure 13 A**). When we delivered rIL-13 with IL-33 to Treg-depleted *Foxp3*^{DTR} B6, we also found that rIL-13 significantly prolonged mouse survival after bleo injury (**Figure 13 B**). These data suggest that IL-13 secreted by Treg acts as a critical factor in the protective capacity of IL-33 after ALI.

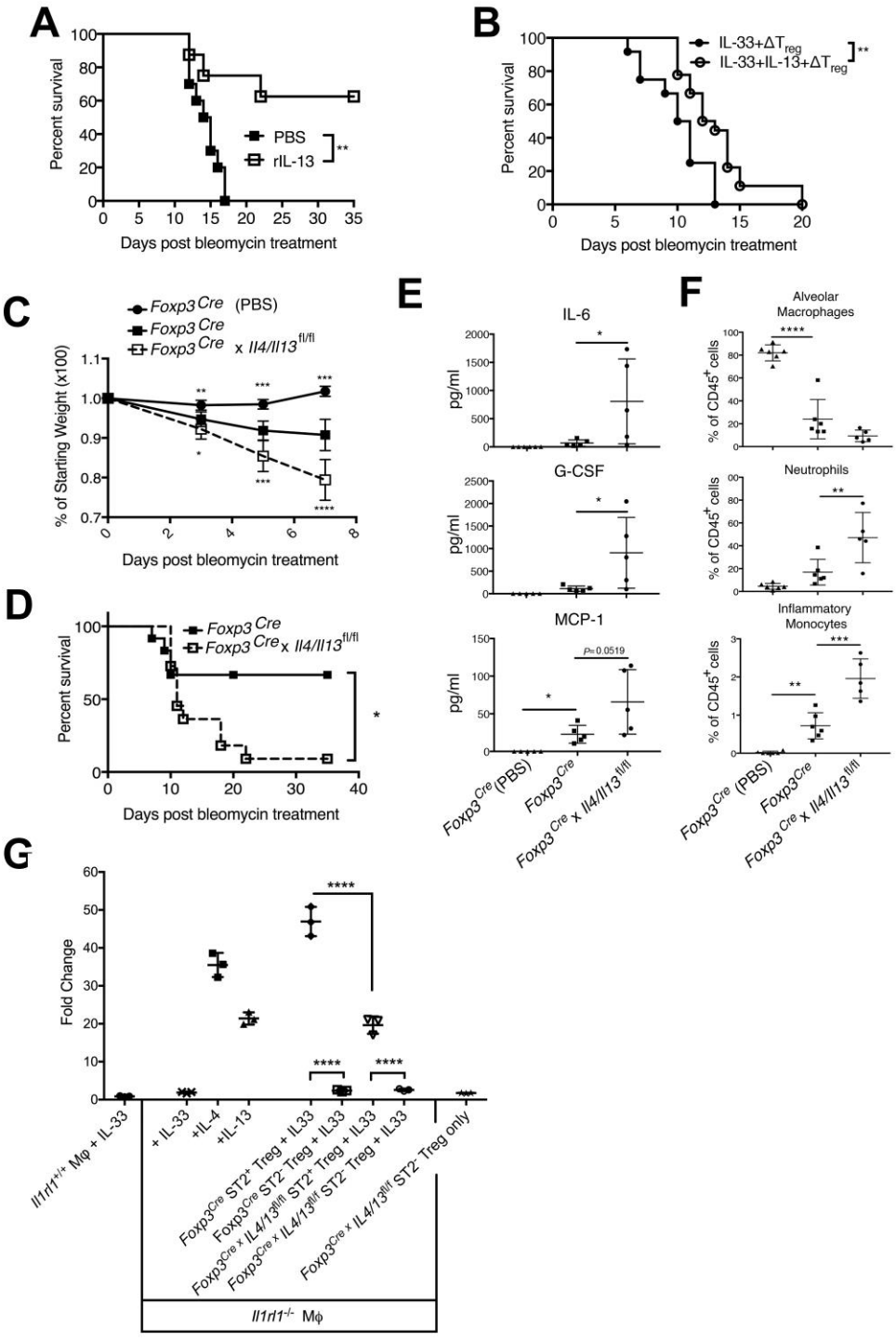

Figure 13. Treg expression of IL-13 reduces inflammatory cytokines and myeloid cell infiltration to protect against mortality after ALI.

***A*, Survival of B6 *Il33*$^{-/-}$ mice instilled i.t. with bleo (1.0 IU/Kg) and also treated with i.t. PBS (n = 10) or 1 µg recombinant (r) mouse IL-13 (n = 8). *B*, Survival of Treg-depleted mice i.t. instilled with bleo (1.0 IU/Kg) and**

1 µg rIL-33 with or without rIL-13 (1 µg). *C*, Comparisons of weight changes of BALB/c *Foxp3*^{Cre} mice (n = 7) injected i.t. with bleo (6.0 IU/Kg) with bleo-treated *Foxp3*^{Cre} x *Il4/Il13*$^{fl/fl}$ (n = 8) or PBS-treated *Foxp3*^{Cre} mice (n = 3). Data were pooled from 2 separate experiments. *D*, Survival of *Foxp3*^{Cre} (n = 12) and *Foxp3*^{Cre} x *Il4/Il13*$^{fl/fl}$ (n = 11) injected i.t. with bleo. *E*, At day 7 post bleo delivery, BALF from *Foxp3*^{Cre} x *Il4/Il13*$^{fl/fl}$ had increased IL-6, G-CSF, and MCP-1 concentrations. *F*, Flow cytometric analysis BALF cells at day 7 post bleo delivery for alveolar macrophages (CD45^{+} CD11b^{lo} Siglec-F^{+}), neutrophils (CD45^{+} CD11b^{hi} Siglec-F^{-} Ly6G^{hi}), and inflammatory monocytes (CD45^{+} CD11b^{hi} CD24^{lo} MHC-II^{lo} Ly6C^{hi}). *E-F*, Data were pooled from 2 two independent experiments (n = 5-6 mice per group total). *G*, qRT-PCR data of *Arg1* expression in cultures of F4/80-purified BALB/c splenic macrophages (*Il1rl1*$^{+/+}$ or *Il1rl1*$^{-/-}$) incubated for 18 hours under the conditions indicated. Data are from 1 experiment representative of three completed. Animal survival was compared by Kaplan-Meier analysis and the log-rank test. Data are means ± SD and *P* values were determined by two-tailed Student's *t*-test or 1-way ANOVA. **P*<0.05, ***P* <0.01, ****P* <0.001, *****P* < 0.0001.

To establish more precisely the role of Treg-secreted IL-13 in protection against ALI-induced mortality, we crossed Foxp3-IRES-Cre mice (237) to C.129P2(Cg)-*Il4*/*Il13*$^{tm1.1Lky}$/J (258) and demonstrated that sorted CD4^{+} CD25^{+} CD127^{lo} T cells from *Foxp3*^{Cre} x *Il4/Il13*$^{fl/fl}$ mice had significantly reduced IL-13 secretion relative to those from *Foxp3*^{Cre} littermates (**Figure 14 A and B**). We observed residual IL-13 in *Foxp3*^{Cre} x *Il4/Il13*$^{fl/fl}$ CD4^{+} CD25^{+} CD127^{lo} T cell cultures (**Figure 14 B**) and we ascribe this to the presence of CD25^{hi} Foxp3^{-} Th2 cells that would have contaminated these cultures due to the lack of a *Foxp3*-driven reporter in this model to assist in their removing as in **Figure 10**. While in theory, *Foxp3*^{Cre} x *Il4/Il13*$^{fl/fl}$ mice T cells would also be deficient in IL-4, we have not observed that IL-33 induces any detectable Treg production of IL-4 in response to IL-33 (**Figure 15**). Sorted *Foxp3*^{Cre} x *Il4/Il13*$^{fl/fl}$ CD4^{+} CD25^{+} CD127^{lo} cells displayed similar suppressive capacity against anti-CD3/CD28-stimulated CD4 and CD8 T cells

to IL-13-competent Treg from *Foxp3*^{Cre} mice (**Figure 14 C**). Thus, the deletion of IL-13 from Treg does not appear to alter their suppressive capacity.

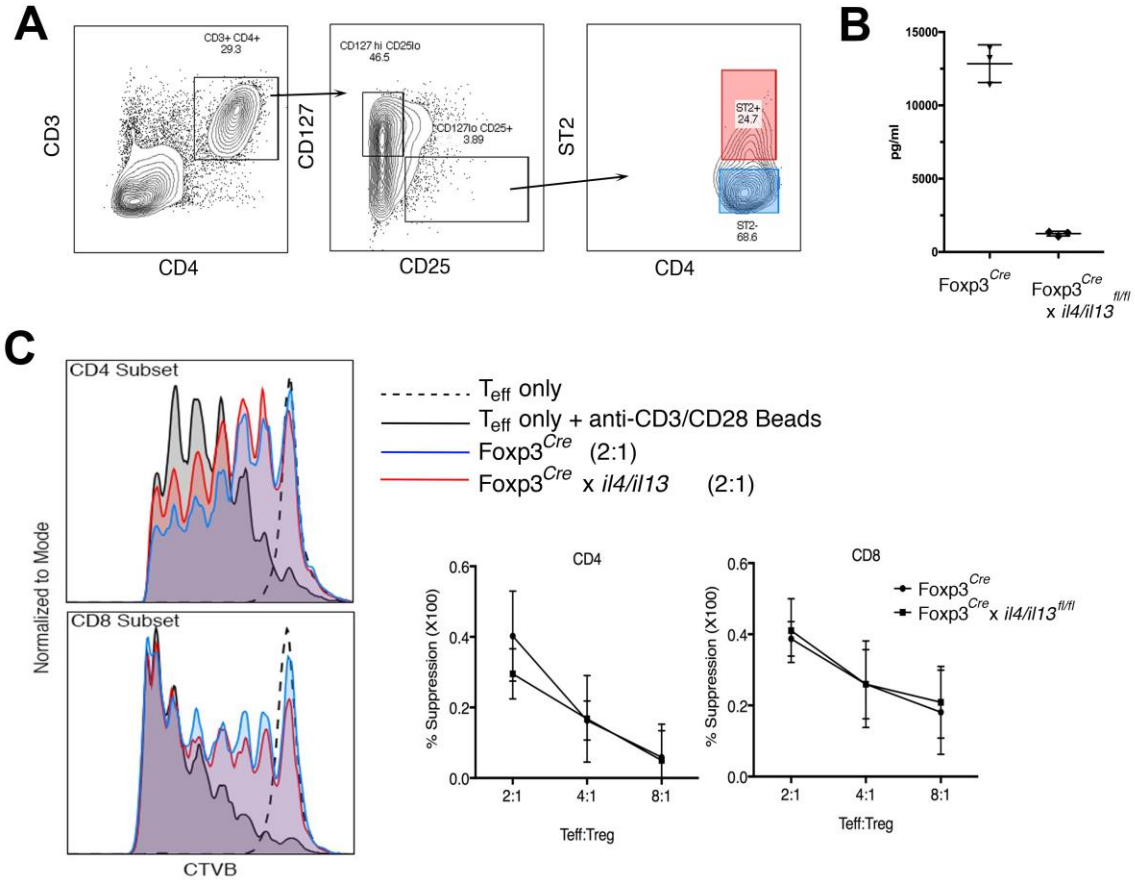

Figure 14. IL-13 secretion is reduced in Treg.

***A*, Depiction of flow sorting design used to obtain ST2^{+} Treg from BALB/c *Foxp3*^{Cre} and *Foxp3*^{Cre} x *Il4/Il13*$^{fl/fl}$ mice for functional assessment. *B*, CD3^{+} CD4^{+} CD25^{hi} CD127^{lo} ST2^{+} T cells isolated from IL-33-treated *Foxp3*^{Cre} x *Il4/Il13*$^{fl/fl}$ mice displayed reduced IL-13 secretion in response to IL-33 (20 ng/ml) compared to those isolated from IL-33-treated *Foxp3*^{Cre} controls. Data are representative of two experiments performed and depict Cytometric Bead Array (CBA) completed for IL-13 on day 3 culture supernatants. *C*, Sorted CD3^{+} CD4^{+}CD25^{hi} CD127^{lo} T cells from naïve *Foxp3*^{Cre} and *Foxp3*^{Cre} x *Il4/Il13*$^{fl/fl}$ mice displayed similar suppressive capacity. Data are representative of two experiments (n = 6 mice per group).**

When we examined how deletion of IL-13 from Treg impacted bleo-induced ALI morbidity and mortality, we found that the phenotype of *Foxp3*^{Cre} x *Il4/Il13*$^{fl/fl}$ mice was very similar to that of *Il33*$^{-/-}$ mice. *Foxp3*^{Cre} x *Il4/Il13*$^{fl/fl}$ mice had significantly increased weight loss and exhibited reduced survival following bleo-challenge compared to *Foxp3*^{Cre} controls (**Figure 13 C and D**). The dose of bleo was increased to 6.0 IU/Kg in these studies to account for the BALB/c background of the *Foxp3*^{Cre} x *Il4/Il13*$^{fl/fl}$ and *Foxp3*^{Cre} mice and the appreciated resistance of BALB/c mice to bleo (259). These data indicate that Treg are indeed an important source of protective IL-13 following chemically-induced ALI. Completing an assessment of how IL-13 production by Treg altered the local immune and cytokine environment early after bleo-induced lung injury revealed that, like the presence of IL-33, IL-13 produced by Treg was a negative regulator of IL-6, G-CSF, and MCP-1/CCL2 at day 7 post bleo insult (**Figure 13 E**). Comparison of the alveolar cellular infiltrates at day 7 post bleo between *Foxp3*^{Cre} x *Il4/Il13*$^{fl/fl}$ and *Foxp3*^{Cre} mice revealed that Treg deficiency of IL-13 did not appear to limit the decrease in frequency of AM (CD45^{+} CD11b^{lo} Siglec-F^{hi}) but did result in an increase in the frequency of neutrophils (CD45^{+} CD11b^{hi} Siglec-F^{-} Ly6G^{hi}; **Figure 13 F and Figure 16**). Likewise, at day 7 post bleo, *Foxp3*^{Cre} x *Il4/Il13*$^{fl/fl}$ mice displayed increased frequency of inflammatory monocytes (CD45^{+} CD11b^{hi} CD24^{lo} MHC-II^{lo} Ly6C^{hi}; **Figure 13 F and Figure 16).**

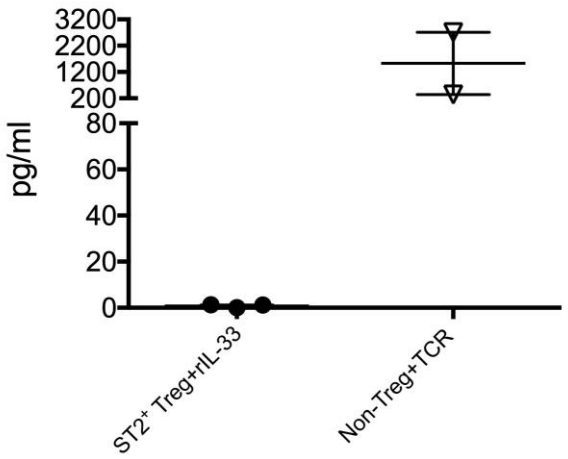

Figure 15. IL-33 stimulated Treg do not secrete IL-4

ST2$^+$ CD4$^+$ Foxp3$^+$ (RFP$^+$) were sorted from IL-33-treated Foxp3-IRES-mRFP reporter mice (n=3) and cultured with 20 ng/ml rIL-33 for 3 days. Supernatants were harvested on day 3 of culture and assessed by Cytometric Bead Array (CBA) for IL-4. Sorted CD4$^+$ Foxp3$^-$ (RFP$^-$) T cells stimulated by plate bounds anti-CD3 is provided as positive IL-4 control.

To further assess the role of IL-13 secretion by Treg in modulating local inflammation after virally-induced ALI, Foxp3^{Cre} and *Foxp3^{Cre}* x *Il4/Il13$^{fl/fl}$* mice received PR8 H1N1 influenza inoculation by oropharyngeal aspiration as we have described (238). The findings in these studies were highly reflective of those observed following bleo administration. Once again *Foxp3^{Cre}* x *Il4/Il13$^{fl/fl}$* mice displayed significantly increased weight loss compared to *Foxp3^{Cre}* controls (**Figure 17 A**), which was not due to altered viral clearance (**Figure 17 B**). Likewise, *Foxp3^{Cre}* x *Il4/Il13$^{fl/fl}$* mice also again had an increased frequency of inflammatory monocytes at day 7 post infection (**Figure 17 D**). In total our data generated using this novel mutant Treg mouse in two distinct models of ALI support a critical role for IL-13 secreted by Treg for regulation of the early inflammatory response, especially the accumulation of neutrophils and inflammatory monocytes after lung injury.

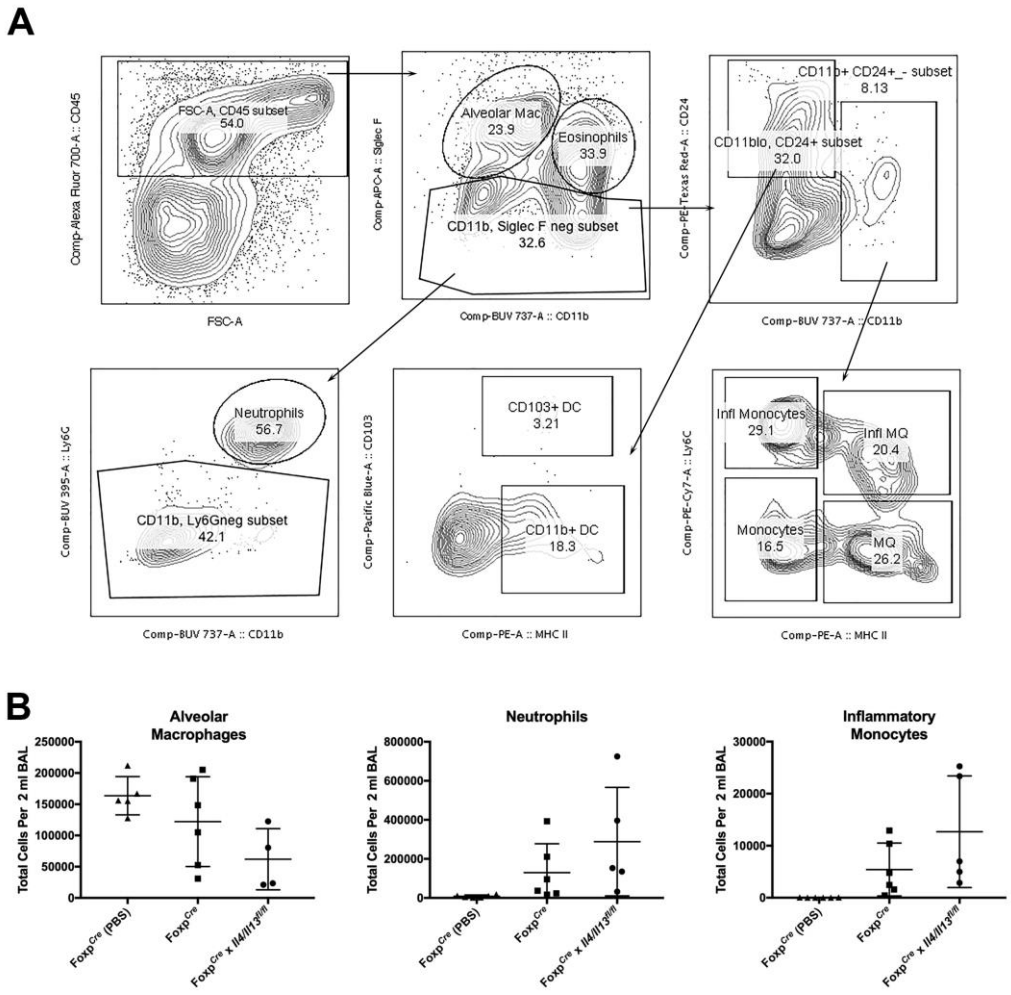

Figure 16. Treg-mediated IL-13 increases local neutrophils and monocytes.

A, **Gating strategy for Figure 13 flow cytometric assessment of bronchoalveolar lavage fluid (BALF) cells on day 7 post bleomycin for alveolar macrophages (CD45$^+$ CD11b^{lo} Siglec-F$^+$), eosinophils (CD45$^+$ CD11b^{hi} Siglec-F^{hi}), neutrophils (CD45$^+$ CD11b^{hi} Siglec-F$^-$ Ly6G^{hi}), CD103$^+$ DC (CD11b^{lo} CD103$^+$ MHC-II$^+$), CD11b$^+$ DC (CD11b^{lo} CD103$^-$ MHC-II$^+$), macrophages (CD45$^+$ CD11b^{hi} CD24l^o MHC-II$^+$ Ly6C^{hi} or Ly6C^{lo}) and monocytes (CD45$^+$ CD11b^{hi} CD24^{lo} MHC-II^{lo} Ly6C^{hi} or Ly6C^{lo}).** ***B,*** **Calculated total number of indicated immune population. Data were pooled from 2 two independent experiments (n = 5-6 mice per group total) and presented as means ± SD.** ***P*** **values were assessed by 1-way ANOVA.**

Arginase 1 (*Arg1*) is commonly expressed by immunoregulatory or reparative myeloid cells (260-262). Interestingly, we could show that while rIL-33 alone did not induce *Arg1* expression in either *Il1rl1*$^{-/-}$ or *Il1rl1*$^{+/+}$ splenic macrophages *ex vivo (***Figure 13 G, Columns #1 and #2***)*, IL-33-stimulated ST2^{+} Treg did effectively induce Arg1 in *Il1rl1*$^{-/-}$ splenic macrophages (**Figure 13 G, Column #5**). These data suggest that ST2^{+} Treg can be stimulated by IL-33 to support the differentiation of myeloid cells towards that of those with reparative or regulatory functions, such as myeloid-derived suppressor cells (MDSC) or reparative macrophages (260-262). This capacity was reduced significantly when IL-13 was deleted from Foxp3-expressing cells (**Figure 13 G, Column #7**). These data suggest that IL-33-mediated Treg secretion of IL-13, while not important for suppressive function, may act as a potent modulator of infiltrating myeloid cells after tissue injury.

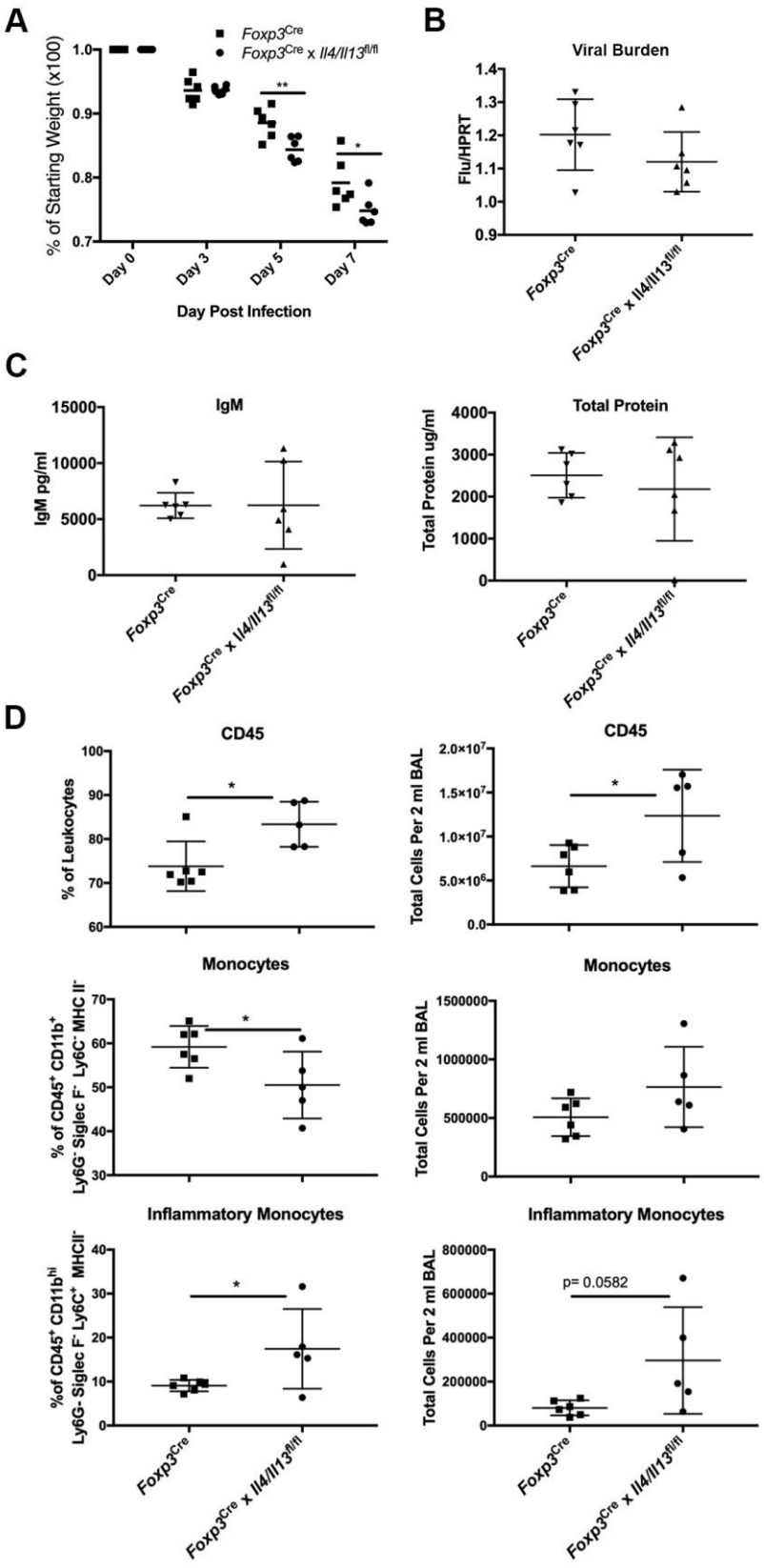

Figure 17. IL-13 secretion by Treg in modulating local inflammation after virally-induced ALI.

***A,* Weight loss for BALB/c *Foxp3*^{Cre} and *Foxp3*^{Cre} x *Il4/Il13*$^{fl/fl}$ mice inoculate with 100 plaque-forming units of influenza. *B,* Viral burden measured by relative expression of influenza mRNA in the right lung on day 7 following influenza inoculation. *C,* Total IgM and protein were measured in the BALF on day 7 post-influenza infection. *D,* Cell counts and frequency assessed by flow cytometric of BALF at day 7 post influenza delivery for leukocytes (CD45^{+}), monocytes (CD45^{+} CD11b^{hi} CD24^{lo} MHCII^{lo}), and inflammatory monocytes (CD45^{+} CD11b^{hi} CD24^{lo} MHCII^{lo} Ly6c^{hi}). *A-D,* Data depicted are from 1 experiment (n=5-6 mice per group total). Statistical differences were determined by two-tailed Student's t-test relative to Foxp3^{Cre}. **P*<0.05, ***P*<0.01.**

2.5 Discussion

We have made several novel and impactful findings in the current studies. First, by demonstrating the sensitivity of IL-33 deficient mice to bleo-induced ALI and the reversibility of this phenotype by complementation with rIL-33, we have established that IL-33 is a crucial local factor necessary to limit the early inflammatory response after chemically-induced ALI. Second, we found that Treg are the cellular mediator of the protective capacity of IL-33 after ALI. Third, we identified that IL-33-stimulated IL-13 production by Treg is critical for controlling inflammation after chemically- and virally-induced ALI and can shape macrophage activation *ex vivo*.

Our observations may seem counterintuitive given the compelling evidence for a pathological role for IL-13 in tissue fibrosis and asthma development (263-266). Yet, IL-13 has also become known for regenerative and reparative functions, due in large part to its capacity to activate tissue-repair macrophages (260, 267-269). Recently, it was demonstrated that ILC2-produced IL-13 promotes lung regeneration after pneumonectomy by stimulating macrophage support of Type 2 alveolar epithelial stem cell proliferation (191). GVHD studies demonstrate

potent protective capacities of ILC2-secreted IL-13, which diminished Th1 and Th17 responses, generated MDSC, aided gastrointestinal homeostasis, and promoted animal survival (270). IL-13 administration to GM-CSF and G-CSF-driven bone marrow cultures generates $Arg1^+$ MDSC able to limit GVHD lethality through immune regulation (271). Our current study establishes that in the absence of IL-13-expression by Treg, ALI results in increased lethality associated with augmented frequency of phenotypic inflammatory monocytes. We also find that IL-33-stimulated Treg secreting IL-13 directly induces *Arg1* gene expression in splenic macrophages. These data are similar to recent *ex vivo* studies demonstrating that Treg-produced IL-13 stimulates IL-10 production in interacting macrophages to support macrophage efferocytosis of apoptotic cells (272). Together, our studies define an important role for IL-33-stimulation of Treg secretion of IL-13 for control of the myeloid response and inflammation after injury.

Peripheral tissues, including the lung, have higher frequencies of $ST2^+$ Treg relative to the SLO (**Figure 6 C)** and (101, 255, 273). Yet, due to the greater overall immune cell number of the spleen, the incidence of $ST2^+$ Treg in the spleen is comparatively quite high relative to the lung. Importantly, unlike macrophages, there is no existing evidence suggesting that Treg within peripheral tissues are embryonically distinct from those of SLO (274, 275). Therefore, we chose to compare splenic $ST2^+$ vs. $ST2^-$ Treg in the mechanistic and characterization studies requiring high cell numbers. Consistent with our previous findings (124) and those of others (99, 255), $ST2^+$ Treg from both lymphoid and non-lymphoid tissues showed higher expression of activation markers including, CD44, CD103 and killer cell lectin-like receptor subfamily G member 1 (KLRG1), and suppressor functional molecules such as OX40 and glucocorticoid-induced TNFR-related protein (GITR), compared with $ST2^-$ Treg (**Figure 6 D**). These data suggest that $ST2^+$ Treg are a comparable population, regardless if they are isolated from SLO or non-lymphoid peripheral

tissue. A recent comparison of the DNA-methylome and transcriptome of $ST2^+$ and $ST2^-$ Treg from non-lymphoid peripheral tissue and SLO support the conclusion that $ST2^+$ Treg in the spleen have transcriptomic and epigenomic patterns highly comparable to peripheral tissue $ST2^+$ Treg and splenic $ST2^+$ Treg represent a recirculating fraction of tissue-resident Treg (255). For these reasons we are confident in extrapolating findings based on the mechanistic study of splenic Treg to tissue Treg in the lung.

While our *ex vivo* data using splenic macrophages suggests that Treg-produced IL-13 can act directly on infiltrating myeloid cells to induce gene expression representative of reparative or regulatory myeloid activity, lung epithelial cells can also express IL-13 receptors (IL-13R) (276), and both myeloid and epithelial cells can release IL-6, MCP-1/CCL2, G-CSF (277-279), which we found increased in the BALF in the absence of IL-33 or Treg IL-13. By using WT or *Il13ra1*$^{-/-}$ bone marrow chimeric mice, Karo-Atar et al suggested that IL-13R in both hematopoietic and structural cells (epithelial cells and fibroblasts) played a role in tissue repair after bleo-induced lung injury (280). These findings are consistent with ours in their support for a critical role of IL-13 signaling in protection after ALI. However, the chimeric animal models used by Karo-Atar were unable to delineate the cell type that was instrumental in IL-13-mediated protection after injury, as they resulted in both hematopoietic and non-hematopoietic cell engraftment. A prior study has also demonstrated that rIL-4 administration after LPS-induced ALI resulted in increased survival and improved lung function (281). In this journal article the authors demonstrated that this effect was due to an IL-4-mediated, STAT6-dependent reprogramming of macrophages towards anti-inflammatory subsets and did not require Treg. While we do not find that IL-33 induces IL-4 production by Treg (**Figure 15**), our current findings are compatible with this study, as IL-13 produced by Treg would activate this same STAT6-dependent pathway in local myeloid

cells and stromal cells. Furthermore, several reports have suggested an important reparative relationship between IL-33 and Treg production of Areg after injury of the lung, muscle, and brain (100, 101, 282). In the current study we have now identified a new mechanism by which IL-33-stimualted Treg support inflammation resolution through secretion of IL-13. Moving forward it will be important to answer if IL-33-stimulated Treg expression of IL-13 supports resolution of early inflammation by targeting resident alveolar macrophages and infiltrating myeloid cells, altering stromal cell cytokine and chemokine expression, or both. Likewise, establishing how Treg use secretion of reparative molecules such as Areg, myeloid-shaping factors like IL-13 and IL-10, and T cell suppressive functions to control inflammation and resolve wounds is important basic knowledge and broadly impactful. This knowledge may allow development of therapies designed to augment required Treg functions or lead to novel cell therapies utilizing Treg generated specifically to perform repair, suppress myeloid cell inflammation, or control T effectors.

After alveolar barrier disruption, dysregulated inflammation and immune cell activity can lead to increased ALI pathology and ARDS (158, 200). Failure to rapidly resolve inflammation and associated tissue injury, support alveolar progenitor cell renewal, and direct appropriate regeneration of the alveolar epithelium can also lead to pulmonary fibrosis (283). IL-33 is constitutively expressed, but sequestered, in the lung epithelium and Type 2 alveolar cells (AEC2) of both mice and human (27, 34, 37, 284). Upon its release due to local injury or following systemic trauma, IL-33 appears to play a complex, yet integral role in shaping early inflammation, resolution of inflammation and injury, as well as fibrotic disease development in the lung. Numerous immune cells express ST2 constitutively or can be induced to express it (4). We have recently established that IL-33 is detectable in the serum of rodents and patients 6 to 12 hours after blunt trauma, and targeted $ST2^+$ ILC2 and cause early lung injury mediated by ILC2-secreted IL-5 and $CXCR2^+$ lung

neutrophils (83). Yet, these current studies would suggest that early inflammatory functions of IL-33 may rapidly give way to IL-33-triggered protective mechanisms involving Treg. Our data demonstrating a protective role for IL-13 is similar to the recent observation that IL-5 produced by $ICOS^+$ ILC2 can support survival after bleo-induced ALI (285). Yet, it is easy to envision how sustained or repeated release of IL-33, even if targeting $ST2^+$ Treg to secrete IL-13 or ILC2 release of IL-5, could eventually transition to a detrimental role and support fibrotic disease or general inflammatory processes (17, 165).

Furthermore, we found that both IL-33 and IL-13-secretion by Treg modulated IL-6, G-CSF, and MCP-1/CCL2 after bleo-induced ALI. This is consistent with prior studies where $CD4^+$ $CD25^+$ T cells were demonstrated to suppress IL-6 and MCP-1/CCL2 after LPS-mediated ALI (226). While it is tempting to conclude that a reduction of these effector molecules underlies the observed decrease in mortality after ALI, like IL-33 and IL-13, these molecules possess a pleotropic nature during ALI. IL-6 is a mediator of acute phase inflammation and orchestrates the immune responses leading to fibrosis after bleo insult (286, 287), but IL-6 is also important for supporting alveolar progenitor renewal (288, 289). Blocking G-CSF signaling reduces inflammation and MCP-1/CCL2 levels (290). Monocyte recruitment to the inflamed lung is dependent on CCR2 and serves to accelerate and augment neutrophil accumulation (291, 292). Intra-peritoneal bleo delivery to *Ccl2*$^{-/-}$ mice fails to instigate the typical monocytic lung inflammation or cause significant lung fibrosis (293). Sustained expression of MCP-1/CCL2 is associated with increased recruited macrophage in ARDS patients and worse prognosis (204, 294). Thus, the local regulation of MCP-1/CCL2 by $ST2^+$ Treg stimulated with released IL-33 could be an important mechanism to control pathology early after ALI. However, mice with lung-specific over expression of MCP-1/CCL2, however, display resistance to bleo-induced lung injury (241).

This was due to an increased ability of MCP-1/CCL2 overexpressing mice to recruit a monocyte/macrophage subpopulation that mediates clearance of apoptotic neutrophils. As such, these mice could better complete a critical step in the initiation of inflammation resolution after ALI (200). The complexity of the cytokine and immune cell networks that control an inter-related inflammatory and resolution/repair response are quite evident. It is safe to conclude that IL-33 is as an important tissue-derived signaling molecule that is active in both the inflammatory and resolution/repair phases after tissue injury. Our current studies place IL-33 upstream of a potent Treg response that dampens early inflammatory responses after injury and is required to survive an insult to the lung epithelium. It will now be important to use techniques such as bioinformatics and math modeling of the immune cell/cytokine interactions (83) to establish how these pleotropic cytokines, chemokines, and alarmins interact with a changing collection of localized immune cells at each step after injury, inflammation, resolution, and remodeling. Such studies will provide a framework to develop precision medicine approaches where biologicals targeting specific cells or cytokines/chemokines are delivered after first determining what cytokine/immune networks are dominant. This approach would allow care providers to orchestrate the appropriate immunological or physiological outcome.

Patients that develop ARDS have long suffered significant morbidity and mortality (157). A recent study involving intensive care units (ICU) from 50 countries demonstrated that 10.4% of ICU patients and 23.4% of mechanically ventilated patients suffered ARDS, of which mortality ranged from 34.9 - 46.1% (202). Despite intensive basic and clinical research, there are few effective targeted ARDS therapies apart from mechanical ventilation (206, 216). Consequently, there remains a need for understanding the pathophysiology underlying ARDS and ALI to identify molecular targets for the development of effective therapies. In the current studies, we identify

endogenous IL-33 and Treg-secreted IL-13 as critical molecules that are essential to control the early inflammatory response after during ALI. Our mechanistic studies reveal that the effect of IL-33 and IL-13 in limiting local inflammatory responses may be mediated, at least partially, by shaping the myeloid compartment after lung injury. Our findings provide a novel pathway to develop immunotherapies that could improve clinical outcome of ALI/ARDS. Remarkably, we showed a potent effect of one-dose of exogenous rIL-33 or rIL-13 in decreasing lethality after bleo-induced ALI. This is very clinically relevant and exploration of IL-33/Treg pathway in clinical ALI and ARDS warrants further exploration.

3.0 IL-33 Acts as a Novel Costimulatory Agent to Generate Alloreactive Type 1 T Helper Cells

Data within this chapter were compiled, submitted and under revision for *J Clin Invest* in 2021 in the following manuscript:

Dwyer, GK, Mathews, LR, Lucas, A, Gonzalez de Peredo, A, Blazar, BR, Girard, JP, Shlomchik, W, Poholek, A, Turnquist, HR. IL-33 acts as a novel costimulatory agent to generate alloreactive Type 1 T helper cells. J Clin Invest. 2021

3.1 Summary

APC integrate signals emanating from local pathology and program appropriate T cell responses. In alloHCT, recipient conditioning releases DAMPs that generate pro-inflammatory APC that secrete IL-12, which is a driver of donor Th1 responses causing GVHD. Nevertheless, other mechanisms exist to initiate alloreactive T cells responses, as recipients with disrupted DAMP signaling or lacking IL-12 develop GVHD. We establish that early tissue damage signals are perceived directly by donor $CD4^+$ T cells and promote IL-12-independent T cell expansion and differentiation. Specifically, the stromal cell-derived DAMP, IL-33, is induced by recipient irradiation and is critical for the initial activation, proliferation, and differentiation of alloreactive Th1 cells. IL-33-stimulation of $CD4^+$ T cell is not required for lymphopenia-induced expansion, however. IL-33 promoted IL-12-independent expression of Tbet and generation of Th1 cells that infiltrate GVHD target tissues. Mechanistically, IL-33 augments $CD4^+$ T cell TCR-associated

signaling pathways in response to alloantigen to enhance Th1 cell activation while inhibiting the expression of regulatory molecules like IL-10 and Foxp3. These data establish an unappreciated role for IL-33 as a costimulatory signal for donor Th1 generation after alloHCT.

3.2 Introduction

AlloHCT is a curative therapy for high-risk hematopoietic malignancies and is also used to correct life-threatening lymphohematopoietic disorders. AlloHCT has also shown promise as a method to induce tolerance to solid organ transplants. Transplant products include donor T cells to support engraftment, post-transplant immunity, and mediate the removal of malignant cells. Unfortunately, donor T cell responses to polymorphic host MHC molecules and minor histocompatibility (miH) antigens often lead to GVHD. Despite evolving prophylaxis strategies (172-174), acute GVHD remains a common life-threatening complication that typically arises by 3-12 weeks post-alloHCT when alloreactive donor T cells infiltrate and destroy host tissues, particularly the skin, liver, and GI tract (295). GVHD causes significant morbidity and mortality in the treatment of malignancy (295). The risk of GVHD is also a barrier to develop alloHCT for correction of genetic disorders or to induce tolerance to solid organ transplants (296, 297). Targetable mechanisms to prevent or limit GVHD are of considerable interest.

Alloreactive Th1 and Type 1 $CD8^+$ T cells (Tc1) producing IFNγ and TNFα, as well as lytic and apoptosis-inducing proteins cause GVHD-target tissue damage (298-300). Thus, methods to limit their generation or functional impact after alloHCT are being explored (301, 302). In general, it is thought that Type 1 responses are generated when materials containing PAMP or DAMP are recognized by Pattern Recognition Receptors (PRR) on APC. These stimuli upregulate

MHC and costimulatory molecules, but also dictate APC cytokine production to direct the differentiation of interacting T cells into the subsets necessary for effective anti-pathogen response (303-305). For example, microbial PAMP recognition by PRRs, particularly the Toll-like receptors (TLR), initiates APC secretion of IL-12 that activates STAT4 signaling to generate pathogen clearing Th1 and Tc1 cells (302). Yet, alloHCT involves a distinct immunobiology relative to anti-pathogen response, as it creates conditions where a high frequency of donor T cells can respond with varied TCR affinity directly or indirectly to pervasive and persistent alloantigens. Furthermore, recipient-conditioning with radiation or chemotherapeutic agents to make space for donor cells and prevent their rejection causes lymphodepletion, leading to cytokine-driven homeostatic expansion of donor T cells (306). In addition, myeloablative recipient-conditioning causes recipient tissue injury that introduces PAMPs from intestinal microbiota after barrier tissue breakdown and causes ample release of typically sequestered self-derived DAMPs (307). While PAMP activation of recipient APC has emerged as an important contributor to GVHD pathology, recipients with disrupted PAMP signaling pathways, or lacking recipient APC-expressed costimulatory molecules and IL-12, can still develop GVHD (177). Additionally, GVHD is less severe when donor $CD4^+$ T cells lack MyD88 signaling, which favors the survival and differentiation of Th1, Tc1, and Th17 cells (188, 189). These data suggest that APC-independent, recipient-derived signals exist and are of significant importance due to their ability to stimulate donor T cells directly and mediate GVHD.

IL-33 is sequestered in the nucleus of cells expressing it, which include epithelial cells and mesenchymal cells of barrier tissues, endothelial cells of blood vessels, and FRC in the SLO (4). Consistent with described DAMP functions for IL-33, it is inactivated by caspase cleavage before apoptotic cell death, but full-length IL-33 is biologically active when released from necrotic cells

(4). In the current studies, we have used transgenic mice allowing precise targeting of donor T cell IL-33 signaling or recipient expression of IL-33 in multiple alloHCT models of $CD4^+$ T cell-mediated GVHD to make novel observations into how stromal cell-derived, DAMP-mediated stimulation of donor T cells is critical to pathologic alloimmune responses after alloHCT. Specifically, we identified a unique role for IL-33 in the SLO where it contributes to the initial activation and proliferation of alloreactive $CD4^+$ T cells. This early IL-33 signaling to donor $CD4^+$ T cells acts independently of IL-12 to promote $Tbet^+$ Th1 differentiation and effector functions. This activity was due to IL-33 acting as a novel costimulatory signal that augments early TCR signaling pathways in donor alloreactive $CD4^+$ T cells responding to alloantigen. Our findings identify IL-33 as a highly desirable therapeutic target at the time of alloHCT to prevent acute GVHD.

3.3 Methods and Materials

3.3.1 Mice

C57BL/6 (B6; H2-K^b), Bm12, BALB/c (H2-K^d), B6 $CD45.1^+$, B6 $CD90.1^+$, B6 Nur77-GFP, B6 *R26-cre^{ERT2}* mice were purchased from The Jackson Laboratory (Bar Harbor, ME). The *Il33$^{-/-}$* mice were from S. Nakae (University of Tokyo, Tokyo, Japan) (115). *CD4-cre x R26-LSL-YFP* mice (C57BL/6; *CD4^{Cre}* were from Dr. Dario Vignali (University of Pittsburgh). Bm12 *Il33$^{-/-}$* mice were generated by backcrossing Bm12 mice 6 times onto the *Il33$^{-/-}$* background at the University of Pittsburgh. *St2$^{-/-}$* mice were originally generated on a BALB/c background (129) and backcrossed 10 times onto the B6 before use. The B6 *St2$^{fl/fl}$* mice were provided by

Giorgio Trinchieri (National Cancer Institute, Bethesda, Maryland) and crossed to *CD4*^{Cre} to generate *CD4*^{Cre} x *St2*$^{fl/fl}$ mice and crossed to B6 *R26-cre*^{ERT2} to generate B6 *R26-cre*^{ERT2} x *St2*$^{fl/fl}$. All mice used were 6-10 weeks-old at the time of initiation of experimental procedures. All mice were bred and/or maintained in a specific pathogen-free animal facility at the University of Pittsburgh. All breeding and experimental procedures were approved by and performed in accordance with the guidelines of the Institutional Animal Care and Use Committee of the University of Pittsburgh and complied with the *Guide for the Care and Use of Laboratory Animals*.

3.3.2 AlloHCT and GVHD

Female recipient mice were exposed to lethal TBI (B6: 1100 cGy; BALB/c: 800 cGy; BM12: 900 cGy over two doses separated by 3 hours) d-1 prior to alloHCT. On d0, B6 and BALB/c recipient mice were given 1x10^7 T cell-depleted (TCD) allogeneic bone marrow (BM) cells alone or with 2x10^6 CD3-purified splenic allogeneic T cells, Bm12 recipient mice were given 1x10^7 T cell-depleted (TCD) allogeneic bone marrow (BM) cells alone or with 1x10^5 CD4-purified splenic allogeneic T cells by IV injection. Mouse survival and weights were recorded, and clinical score assessment was performed as described (36, 103).

3.3.3 Animal Treatments

BALB/c mice were treated with PBS or 0.5 μg recombinant mouse IL-33 (BioLegend; San Diego, CA) by i.p. injection every day (d) for 5d. The first dose was on day 3 – post alloHCT through day 7. For anti-IL-12p40 treatments mice were treated with 500 μg/mouse/d or IgG as control starting on day -1, the same day as the TBI and every three days after (d2, 5 and 8 for

survival studies and d2 and 5 for mechanism studies). The weight and survival of treated animals was monitored. In survival studies, survival was defined as death or euthanasia after sustained weight loss greater than 30-35% of the starting weight.

3.3.4 Isolation of lamina propria lymphocytes (LPLs), splenocytes, and lymph node cells

LPLs were isolated from the small intestines using the MACS Mouse Lamina Propria Dissociation Kit (Miltenyi Biotec) according to the manufacturer's instructions as described (103). Following LPL isolation, T cells were enriched using a debris removal kit (Miltenyi Biotec) and density gradient centrifugation before staining and flow cytometric analysis. Single cell homogenates of splenocytes and mesenteric lymph nodes were generated for flow cytometric assessment by mechanical isolation. The single cell suspensions were filtered before staining.

3.3.5 Flow cytometry

For lymphocyte cell analysis, cells were stained using the following antibodies: BD Bioscience: CD45.1 (A20), CD4 (RM4-5), CD44 (IM7), Tbet (O4-46), GATA3 (L50-823), Rorγt (Q31-378), Foxp3 (MF23), ST2 (U29-93), CD90.1 (OX-7), H2-K^d (SF1-1.1.1), BioLegend: CD25 (PC61), Ki67 (16A8), GFP (FM264G), CXCR3 (CXCR3-173), CD62L (MEL-14), CD69 (H1.2F3), CD8 (53-6.7), CD3ε (17A2), CD45.2 (104). Flow cytometry data were acquired using an LSR Fortessa (BD Biosciences) or Aurora (Cytek Biosciences) and analyzed using FlowJo (Tree Star, Ashland, OR). Intracellular staining was carried out using Foxp3/Transcription Factor staining buffer set (eBioscience; San Diego, CA). All fluorochrome-conjugated antibodies were

purchased from BioLegend or BD Biosciences. Live/dead exclusion was completed using E506 Viability Dye (Invitrogen).

3.3.6 Phosphoflow

$CD3^+$ T cells from $CD45.2^+$ *CD4-Cre x R26-LSL-YFP x* $St2^{fl/fl}$ B6 ($1x10^6$) and $St2^{+/+}$ $CD45.1^+$ B6 ($1x10^6$) mice were labeled with CTV and adoptively transferred with $1x10^7$ WT B6 TCD-BM into lethally irradiated BALB/c recipients. On d1 single cell suspensions of splenocytes were prepared For surface and intracellular staining, cells were fixed and permeabilized in saponin-based Perm/Wash buffer (Cat#: 554732, BD Biosciences) supplemented with 1.5% paraformaldehyde (PFA) and blocked with Fc receptor antibody (CD16/32, 93; BioLegend) prior to staining with surface antibodies (listed above) and fluorochrome-conjugated phospho-antibodies: phospho-p38 MAPK (Thr180/Tyr182; A16016A; BioLegend), phospho-S6 (S235/236, A17020B; BioLegend), or phospho-Erk1/2 (T202/Y204, 4B11B69; BioLegend).

3.3.7 RNA-Seq and bioinformatics analyses

B6 $CD45.1^+$ ($ST2^{WT}$) and B6 $CD45.2^+$ *CD4-Cre x R26-LSL-YFP x* $St2^{fl/fl}$ ($ST2^{fl/fl}$) donor splenic $CD4^+$ T cells were enriched from $CD90.1^+$ B6 or H2-K^d BALB/c recipient mice (*n*=4 per group) using negative depletion with Dynabeads (Life Technologies). The cells were stained for CD3, CD4, CD90.1, H2-K^d CD45.1, CD45.2 and sorted for $ST2^{WT}$ and $ST2^{fl/fl}$ $CD4^+$ populations on a FACSAria II, directly into SmartSeq low-input RNA kit lysis buffer. Libraries were prepared using Nextera XT DNA library prep kits, and RNA sequencing was performed on Illumina NextSeq500 by the Health Sciences Sequencing Core at University of Pittsburgh. Raw sequencing

data was processed using CLC Genomics Workbench 20.0.3 (QIAGEN Inc., https://digitalinsights.qiagen.com) for quality control and aligned to the *Mus musculus* genome version GRCm38.p6. Reads assigned to each gene underwent TMM normalization and differential expression analysis was performed using *edgeR* within CLC Genomics to compare $ST2^{WT}$ versus $ST2^{fl/fl}$ donor T cells. The top differentially expressed genes were filtered by adjusted p-value $q<0.05$ and fold-change greater than 1.5 for subsequent downstream pathway analysis. Relative expression shown in heatmaps was calculated as the fragments per kilobase exon per million mapped reads value for each sample divided by mean expression of that gene in all samples per each experiment. GSEA from the Broad Institute (http://www.broad.mit.edu/gsea) was used to calculate enrichment of genes in each set.

Table 1. Gene signatures used in RNAseq analysis

Gene signatures	Genes included in signature
Anergy and tolerance	Cd70, Ifng, Tnfrsf8, Lgals3, Gzmb, Tbx21, Cdk4, Jun, Cd40lg, Il2rb, Cdk2, Icos, Ptger2, Il6, Il2ra, Itga1, Lat, Tnfsf14, Itch, Gata3, Il4, Cd27, Ccr4, Tnfrsf14, Dgka, Ing4, Pdcd1, Nfatc2, Tgfb1, Tnfrsf4, Mef2a, Stat3, Jak1, Tnfrsf9, Lta, Nfatc1, Cd28, Fas, Nfkb1, Tnfsf10, Jak3, Nfatc3, Stat6, Tnfsf8, Tnfrsf18, Notch1, Icam1, Dgkz, Ctla4, Foxp1, Tnfrsf10b, Prf1, Irf4, Csf2, Cblb, Fasl, Fos, Rnf128, Il2, Egr2, Foxp3, Eomes, Il7r, Il10ra, Sell, Csf1, Il10, Ccl3
T helper cell differentiation	Ifng, Tmed1, Tbx21, Socs1, Irf8, Pou2f2, Icos, Il1rl1, Il2ra, Nfatc2ip, Perp, Havcr2, Gata3, Stat4, Il4, Myb, Ccr4, Il1r2, Il18r1, Hopx, Tlr6, Rel, Nfatc2, Runx3, Irf1, Id2, Zeb1, Rora, Chd7, Zbtb7b, Tgif1, Jak1, Tnfrsf9, Nfatc1, Il18rap, Gfi1, Tnf, Nr4a1, Tnfsf11, Stat6, Maf, Stat1, Il12rb2, Socs5, Il21, Irf4, Cebpb, Runx1, Csf2, Ikzf2, Rorc, Il4ra, Il18, Pparg, Lrrc32, Fasl, Il2, Trp53inp1, Foxp3, Il1r1, Ccr3, Nr4a3, Ccl5, Ndufb7, Ndufa2, Ndufv3, Cox6b1, Ndufa3

Table 1 continued

Mitochondrial energy	Atp6v1c2, Cyc1, Ppa1, Ndufv1, Uqcrc1, Lhpp, Atp5b, Cox11, Ppa2, Ndufab1, Atp5a1, Ndufc1, Sdhd, Sdhc, Uqcrfs1, Cox5a, Ndufs7, Ndufs1, Ndufc2, Atp5g1, Atp5d, Ndufb6, Ndufb8, Ndufa10, Atp5f1, Ndufa5, Atp5c1, Atp5g3, Ndufv2, Cox7a2, Ndufb2, Ndufs2, Ndufs3, Ndufs8, Sdhb, Ndufb9, Atp5g2, Ndufb10, Ndufa8, Ndufb5, Atp5o, Atp6v1g3, Uqcrc2, Ndufa4, Atp5j, Ndufb4, Uqcr11, Ndufs5, Cox6a1, Uqcrq, Ndufs6, Atp5j2, Cox8a, Ndufa11, Bcs1l, Cox5b, Ndufs4, Sdha, Cox7b, Ndufb3, Cox4i1, Cox6c, Ndufa6, Ndufb7, Ndufa2, Ndufv3, Cox6b1, Ndufa3
Myc targets	Shmt1, Pold2, Mthfd1, Apex1, Cdc25a, Srm, Gnl3, Tpi1, Eno1, Pa2g4, Phb, Hk2, Tyms, Ccnb1, Cct5, Nolc1, Eif4a1, Psmg1, Snrpb, Ppat, Msh2, Myc, Mat2a, Cad, Cdk4, Fasn, Paics, Nap1l1, Nbn, Chek1, Ncl, Ctsc, Dkc1, Nme1, Trp53, Pcna, Csde1, E2f1, Ilk, Npm1, Ddx39b, Eif4e, Ybx3, Lta4h, Exosc8, Hnrnpa1, Odc1, Ube2c, Hnrnpa2b1, Top1, Max, Cks2, Rpl13, Srsf1, Cstb, Bcat1, Ddx10, Pten, Rpl5, Cbx3, Maz, Rpl27a, Itgb1, Rps5, Rpl19, Rpl23, Atf4, Pias2

3.3.8 In vitro Th1 skewing and ELISA assay

For *in vitro* experiments $CD4^+$ T cells were enriched from $St2^{+/+}$ B6 mice using negative depletion with Dynabeads (Life Technologies). 3 hours prior to plating the T cells the plates were incubated with anti-CD3 (5μg/ml) and anti-CD28 (5μg/ml). T cells were Th1 skewed with rIL-12, rIL-2 and anti-IL-4 for 4 days, followed by a 3hr rest and 24hr rIL-33 (1ng/ml) stimulation (or no stim) with or without p38 inhibitions. The p38 MAPK inhibitor SB203580 (Tocris/Bio-Techne; Minneapolis, MN) was added at 5 μM final concentration. At the end of culture supernatant were harvested for analysis by ELISA. Supernatants were frozen at time of collection and stored at –80°C until use. Samples were batch thawed and diluted at no less than 1:10. Samples were run in triplicate and levels of IFNγ were measured per manufacturer specification. The assay limit of detection was 15.6 pg/mL.

3.3.9 Protein isolation and analysis

$CD4^+$ T cells were enriched from $St2^{+/+}$ B6 mice using negative depletion with a Naïve $CD4^+$ T cell isolation kit (Miltenyi) and were stimulated *in vitro* with anti-CD3/CD28 plate-bound antibodies with or without rIL-33 (5ng/ml) co-stimulation. T cells were lysed through heating in strong sodium deoxycholate detergent buffer as described (308). Following sonication to homogenize samples and shear the DNA, the crude protein extracts were enzymatically digested with Lys-C and trypsin, followed by peptide micro-purification on styrene divinylbenzene-reversed phase sulfonate StageTips to remove detergent and salts. Eluted peptides were analyzed using an UltiMate 3000 RSLC nanoflow chromatography system (Thermo Fisher Scientific) coupled to a Q-Exactive HFX mass spectrometer (Thermo Scientific), by separation of the peptides

using a 120min gradient of acetonitrile-containing mobile phase, on a 50 cm analytical C-18 column, in-house packed with 2µm porous silica beads. Online mass spectrometry analysis was performed in data-dependent acquisition mode. Raw MS files were processed with MaxQuant for protein identification through database search, and protein relative quantification by analysis of peptides MS signal intensity.

3.3.10 Immunofluorescent histology

Optimal cutting temperature compound–embedded (Thermo Fisher Scientific) frozen mouse spleens were sectioned (6 µm), placed on glass slides, and stained for H2-K^d (eBioscience, 34-1-2S) and IL-33 (R&D Systems, AF3626), and then fluorochrome-conjugated and species-specific secondary antibodies as described (103). Primary antibodies were followed by secondary antibodies conjugated to Alexa Fluor 555 (Donkey anti-Goat IgG, Invitrogen, A21432), and Alexa Fluor 647-conjugated Streptavidin (Jackson ImmunoResearch Labs, Inc., 016-60-084). Nuclei were stained with 4′,6-diamidino-2-phenylindole (DAPI; Sigma). Sections were visualized following whole slide image capture using a Zeiss Axio Scan.Z1 scanner, on the 40x objective, utilizing a 16-bit color sCMOS camera (Hamamatsu Photonics), and HXP-120V metal halide excitation source or monochrome camera, and appropriate filters. Images were acquired and processed using ZEN Blue 3.1 software and analyzed with Image J (Fuji). All czi file from ZEN Blue 3.1 were exported from ZEN Blue 3.1 as tiffs.

3.3.11 Statistics

Statistical details of each experiment can be found in the respective figure legends. Data are presented as mean±standard deviation (sd). *n* refers to biological replicates. $P<0.05$ was considered statistically significant. GraphPad PRISM 9.0c software was used for statistical analyses. Littermate controls were used throughout the study. Data significance was analyzed using a two-tailed unpaired Student's t test or Mann-Whitney test in cases where two groups were being compared. In cases where more than two groups were being compared, one-way or two-way ANOVA were used with Sidak's test to correct for multiple comparisons.

3.4 Results

3.4.1 IL-33 functions independent of IL-12 to drive Th1 differentiation and lethal GVHD

Th1 cells are distinguished by their expression of Tbet, which binds to and activates the gene for IFNγ (181, 309, 310). Tbet also controls the expression and function of CXCR3 and P-selectin that facilitate Th1 cell migration into inflamed tissues (183). The process of Th1 differentiation involves two phases of Tbet expression, a first phase stimulated by TCR engagement and IFNγ, and a second, IL-12-enforced phase (181). IL-12 is a contributor to GVHD and targeting IL-12p40 alleviates GVHD lethality (302, 311, 312). *In vitro*, IL-12 promotes Tbet-dependent expression of ST2 (313), and augments T cell IFNγ production (36, 107). We have also established that *St2*$^{-/-}$ T cells display significantly less IFNγ expression at d10 post alloHCT in fully MHC mismatched recipients (129 to BALB/c; BALB/c to B6) (36). This reduced IFNγ expression

was associated with decreased GVHD mortality and was consistent with IFNγ contributing to GVHD lethality (299, 311). To test if IL-12 contributed to IL-33-mediated activation and differentiation of donor $CD4^+$ T cells after alloHCT in a B6 to BALB/c model, we neutralized IL-12 via anti-IL-12p40 antibodies alone or with IL-33 treatment (**Figure 18 A**). While we confirmed our earlier finding (36) that treatment with rIL-33 post-alloHCT accelerates early death from GVHD (**Figure 18 B**), we revealed that targeting IL-12p40 after alloHCT did not provide any protection against IL-33-driven GVHD lethality (**Figure 18 B**) or morbidity (**Figure 18 C**). Anti-IL-12p40 delivery alone delayed death, thus confirming effective therapeutic IL-12 blockade. IL-12-independent promotion of GVHD by IL-33 was further verified using *Il12rb2*$^{-/-}$ donor T cells, which again suggested no role for IL-12 in IL-33-augmented GVHD lethality (**Figure 18 D**) or clinical scores (**Figure 18 E**). These data suggest that the mechanism by which IL-33 drives donor T cell pathology in GVHD is independent of IL-12.

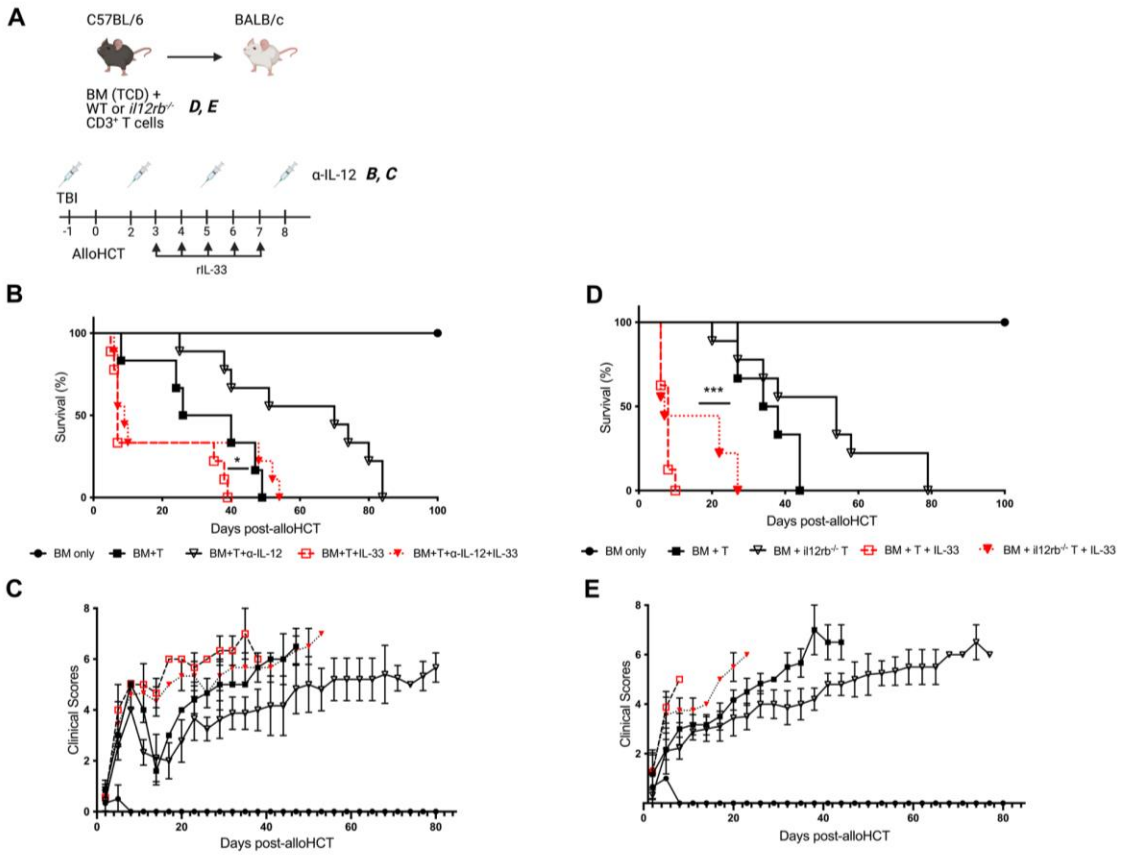

Figure 18. Administration of IL-33 post-alloHCT increases the severity of GVHD independent of IL-12. ***A-E,*** **On day (d)-1 pre-transplant, BALB/c recipient mice received lethal TBI (8Gy) and cohorts received a first dose of anti-IL-12p40 (500 µg/mouse/d) or IgG as control, and this treatment was repeated every three days (d2, 5 and 8 post-alloHCT). On d0, BALB/c recipient mice received 1x10^{7} WT C57BL/6 (B6) T cell depleted bone marrow (TCD-BM) alone or with 2x10^{6} B6 CD3^{+} T cells (*B*) or 2x10^{6} *il12rb2*$^{-/-}$ B6 CD3^{+} T cells (*C*) by IV injection. Cohorts were treated with rIL-33 (from d+3 to +7 after HCT; 0.5 µg/mouse/d) or phosphate-buffered saline (PBS) as control.** ***A,*** **Schematic of B6 to BALB/c GVHD model as it relates to antibody (IgG or anti-IL-12p40) (*B,C*) donor T cells (*D,E*) and rIL-33 treatments (*B-E*).** ***B,*** **Survival graph depicting the influence of rIL-33 with anti-IL-12p40-treated group or** ***D,*** **on *il12rb2*$^{-/-}$ CD3^{+} T cells.** ***C,*** **Clinical scores depicting influence of rIL-33 with anti-IL-12p40-treated group or** ***E,*** **on *il12rb2*$^{-/-}$ CD3^{+} T cells. Data in *B,D* Kaplan-Meier survival curve, *C* and *E* clinical scores, *n*=6-9/group. *, P<0.05, ***, P<0.001.**

To further define the impact of neutralizing IL-12 on IL-33-mediated early donor $CD4^+$ T cell activation and differentiation, we performed alloHCT experiments where donor B6 *St2*$^{-/-}$ and *St2*$^{+/+}$ T cells were adoptively transferred into distinct (**Figure 19 A-F**) or the same (**Figure 20 A-E**) BALB/c recipients with IL-12p40 blockade. Unlike *in vitro* studies where IL-12 increased T cell ST2 expression (36, 107), neutralization of IL-12p40 did not significantly modulate the frequency of donor $ST2^+$ $CD4^+$ cells at day 7 post-alloHCT (**Figure 19 B and C**). IL-33 stimulation of donor $CD4^+$ T cell was crucial for the expansion of donor $CD4^+$ T cells in the absence of IL-12p40 stimulation given that $CD4^+$ T cells were decreased significantly when they lacked the IL-33 receptor, ST2, regardless of whether anti-IL-12p40 or IgG was delivered (**Figure 19 D**). These differences were not due to differences in alloimmune-mediated inflammation between recipients of *St2*$^{-/-}$ or *St2*$^{+/+}$ T cells. Since, when *St2*$^{-/-}$ T cells were co-transferred with *St2*$^{+/+}$ T cells into the same recipient (**Figure 20 A**), donor $CD4^+$ T cells lacking the ST2 receptor failed to expand at the same rate as wild type (WT) cells (**Figure 20 B and C**).

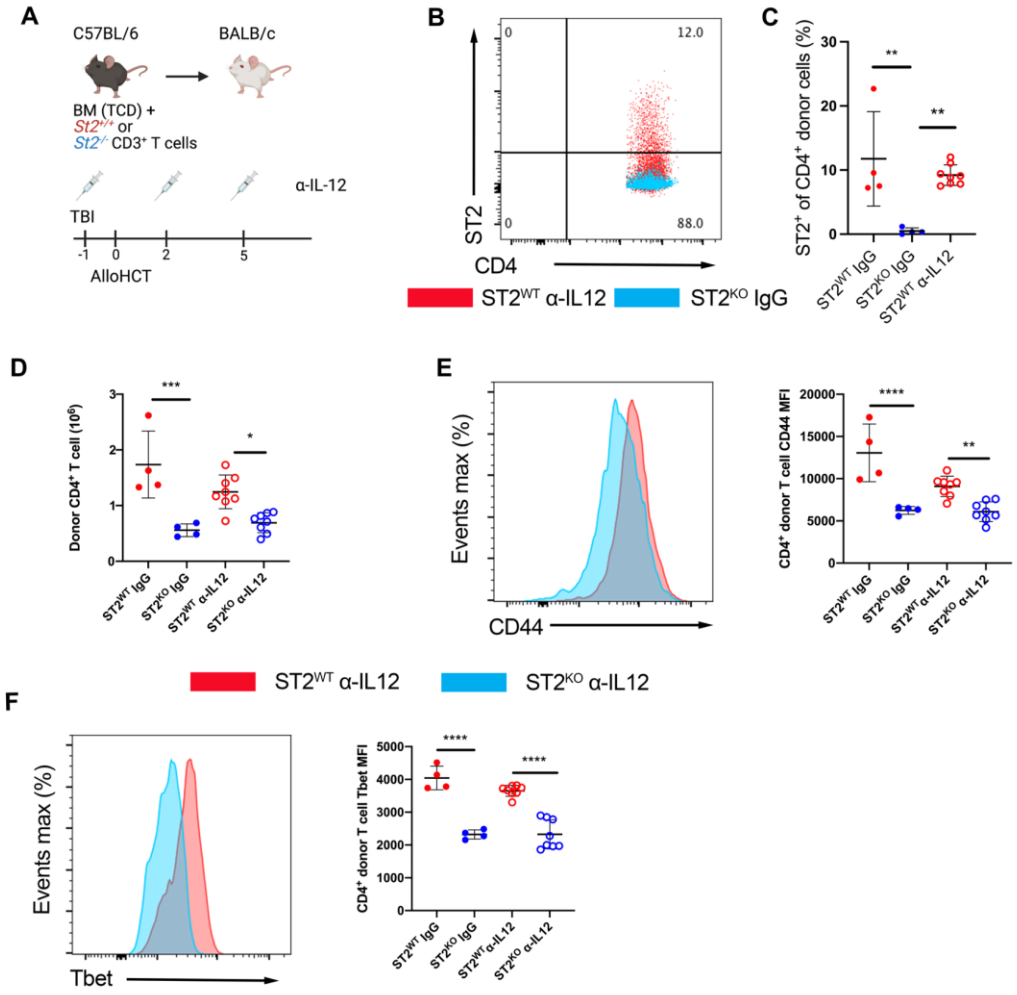

Figure 19. IL-33 stimulation post-alloHCT expands *St2*$^{+/+}$ CD4^{+} donor T cells independent of IL-12.

***A-F*, On d-1 BALB/c recipient mice received anti-IL-12p40 or IgG as control (as described in Fig. 1) and received lethal TBI. On d0, mice received 1x10^{7} B6 TCD-BM with 2x10^{6} CD90.2^{+} B6 *St2*$^{-/-}$ (ST2^{KO}) or CD90.1^{+} *St2*$^{+/+}$ (ST2^{WT}) CD3^{+} T cells. Total splenocytes were assessed at d7 by flow cytometry. *A*, Schematic of B6 to BALB/c GVHD model as it relates to antibody (IgG or anti-IL-12p40) treatments. *B*, Representative flow plots of ST2 expression on donor CD4^{+}CD90.1^{+}H2-K^{d-} ST2^{WT} (red) and CD4^{+}CD90.1^{-}H2-K^{d-} ST2^{KO} (blue) cells from isolated from the spleen of the recipient at day +7. *C*, Frequency of ST2^{+} donor CD90.1^{-} ST2^{KO} and CD90.1^{+} ST2^{WT} CD4^{+} T cells. *D*, Donor CD90.1^{-} ST2^{KO} and CD90.1^{+} ST2^{WT} CD4^{+} T cells counts in recipients that received anti-IL-12p40 or IgG. *E*, Representative histogram of CD44 expression on CD90.1^{-} ST2^{KO} (blue) and CD90.1^{+} ST2^{WT} (red) CD4^{+} T cells and quantification of CD44 MFI *F*, Representative histogram of Tbet expression on CD90.1^{-} ST2^{KO} (blue) and CD90.1^{+} ST2^{WT} (red) CD4^{+} T cells and quantification of Tbet MFI.**

Data in *B-F* indicate mean+/-SD, *n*=4-8/group. *, P<0.05, **, P<0.01, ***, P<0.001, ****, P<0.0001, one-way ANOVA (*C-F*).

Anti-IL-12 neutralization was not as impactful as the lack of IL-33 stimulation on donor $CD4^+$ T cell activation or Th1 differentiation based on CD44 (**Figure 19 E**) and Tbet expression (**Figure 19 F**) at day 7 post-alloHCT. $St2^{+/+}$ T cells exhibited significantly higher MFI for CD44 and Tbet than *$St2^{-/-}$ T cells*, regardless of IL-12p40 blockade. These findings were recapitulated when $St2^{-/-}$ and $St2^{+/+}$ T cells were adoptively transferred into the same recipient (**Figure 20 D and E**). These data support that ST2 signaling is critical for early T cell activation, expansion, and differentiation through a mechanism independent of IL-12.

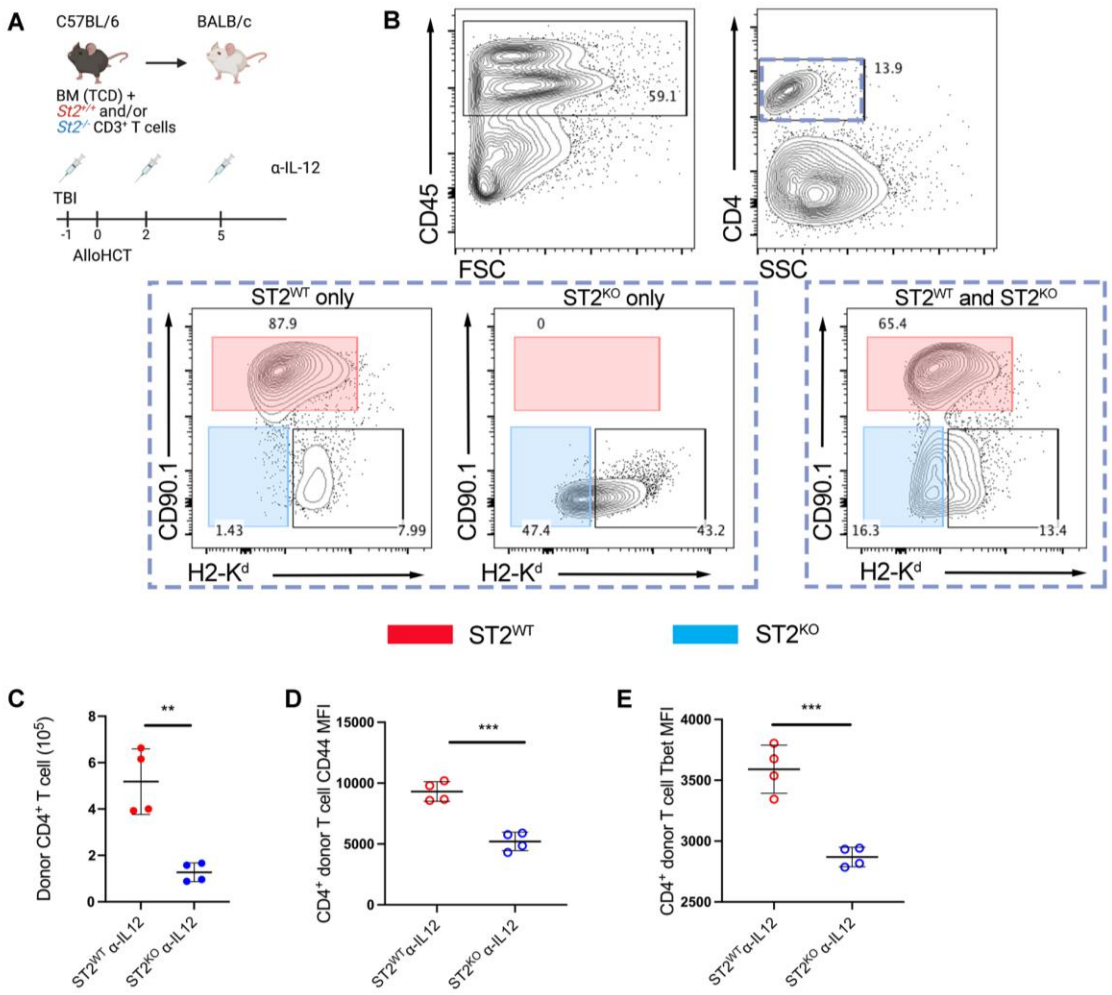

Figure 20. *St2*$^{-/-}$ donor CD4^{+} T cells fail to expand at the same rates as *St2*$^{+/+}$ donor CD4^{+} T cells in response to alloantigen in the absence of IL-12 signaling.

A-C, **On d-1 BALB/c recipient mice received anti-IL-12p40 or IgG as control and received lethal TBI. On d0, mice received 1x10^{7} B6 TCD-BM with a combination of CD90.1^{-}*St2*$^{-/-}$ (ST2^{KO}) (1x10^{6}) and CD90.1^{+}*St2*$^{+/+}$ (ST2^{WT}) (1x10^{6}) CD3^{+} T cells. Donor CD4^{+} T cells from the same spleen were compared at d7 by flow cytometry.** ***A,*** **Schematic of B6 to BALB/c GVHD model as it relates to antibody (IgG or anti-IL-12p40) treatments.** ***B,*** **Representative flow plot gating to identify CD4^{+}CD90.1^{+}H2-K^{d-} ST2^{WT} (red) and CD4^{+}CD90.1^{-}H2-K^{d-} ST2^{KO} (blue) donor CD4^{+} T cells in the same spleen (co-transfer) or separate spleens.** ***C,*** **Co-transferred donor CD4^{+}CD90.1^{+} ST2^{WT} and CD4^{+}CD90.1^{-}H2-K^{d-} ST2^{KO} cell counts in recipients that received anti-IL-12p40.** ***D,*** **MFI of CD44 on co-transferred donor ST2^{WT} and ST2^{KO} CD4^{+} T cells from the same recipient spleen.** ***E,*** **MFI**

of Tbet on co-transferred donor ST2^{WT} and ST2^{KO} CD4^{+} T cells from the same recipient spleen. Data in *B-E* indicate mean+/-SD, *n*=4/group. *, P<0.05, **, P<0.01, ***, P<0.001, Student's *t* test (*C-E*).

3.4.2 AlloHCT conditioning upregulates IL-33 protein expression in the T cell zones of the spleen

We previously reported that IL-33 is upregulated in the small intestine following TBI and during GVHD (36). We observed a similar upregulation of IL-33 in the SLO (**Figure 21 A-D**). IL-33 expression is increased 5-6-fold by day 3 post-alloHCT in the spleen of lethally irradiated B6 *Il33*$^{+/+}$ recipients compared to *Il33*$^{-/-}$ recipients (**Figure 21 B and C**). IL-33 was primarily expressed in the T cell zone of the spleen, which is where CD4^{+} donor T cells home at day 3 (314). Consistent with a role for IL-33 in CD4^{+} T cells expansion, we also observed a reduction in the frequency of donor H2-K^{d+} T cells in *Il33*$^{-/-}$ recipients compared to *Il33*$^{+/+}$ recipient spleens (**Figure 21 B and D**). Thus, IL-33 is upregulated following alloHCT conditioning in the SLO in areas of high donor T cell trafficking.

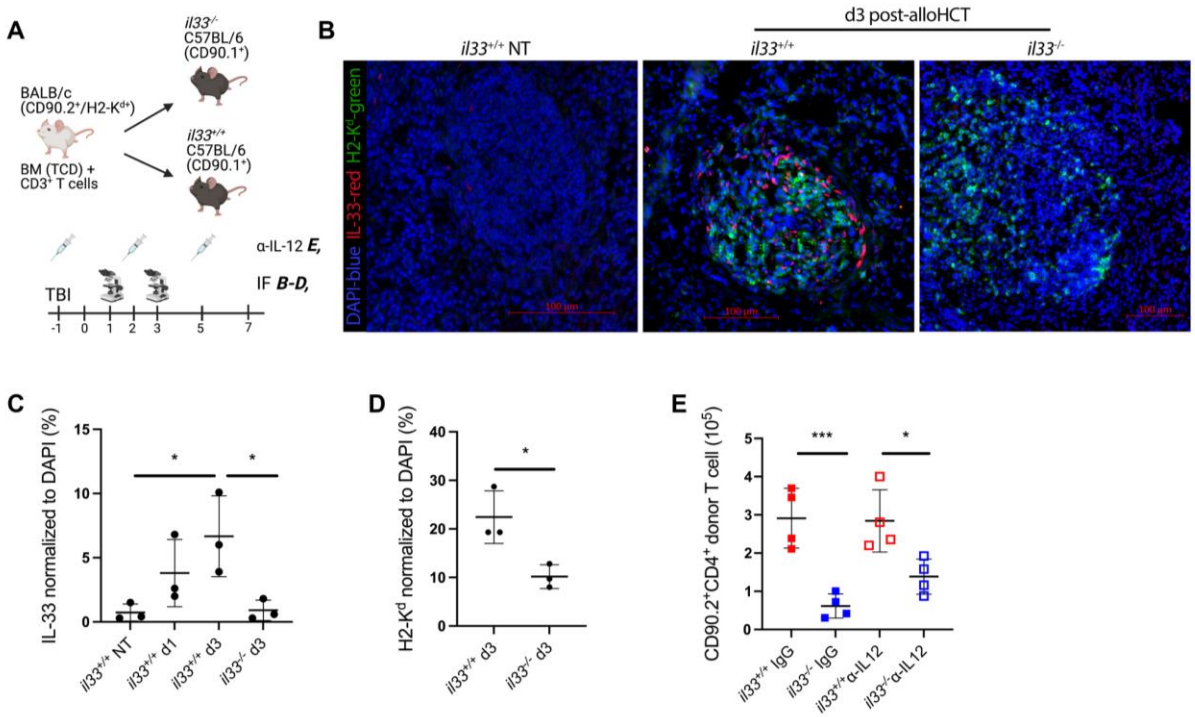

Figure 21. AlloHCT conditioning increases recipient IL-33 expression in the spleen and is necessary for donor T cell expansion independent of IL-12.

A-E, **On d-1 CD90.1$^+$ *Il33*$^{-/-}$ or CD90.1$^+$ *Il33*$^{+/+}$ B6 recipient mice received lethal TBI (11Gy), and some cohorts received anti-IL-12p40 or IgG as control (as described in Fig. 1). On d0, mice received 1x10^7 H2-K^{d+}CD90.2$^+$ BALB/c TCD-BM with 2x10^6 H2-K^{d+}CD90.2$^+$ BALB/c CD3$^+$ T cells. Donor H2-K^{d+} splenocytes were assessed at d1 and 3 by immunofluorescence microscopy and at d7 by flow cytometry. *A*, Schematic of BALB/c to B6 GVHD model as it relates to immunofluorescence imaging (*B-D*) and antibody (IgG or anti-IL-12p40) treatments (*E*). *B,* Representative image taken from complete spleen cross-section from each cohort on d3. *C,* Frequency of IL-33$^+$ cells in the recipient and naïve spleens, one complete scanned cross-section of the spleen was analyzed per mouse. *D,* Frequency of H2-K^{d+} donor T cells in the recipient spleens at d3, analyzed from one complete scanned cross-section per mouse. *E,* Donor CD90.2$^+$CD4$^+$ cell counts from the spleen on d7.**

We next utilized B6 CD90.1$^+$ *Il33*$^{+/+}$ and *Il33*$^{-/-}$ mice to assess the impact of neutralizing IL-12 in the absence of recipient IL-33 on WT donor T cell expansion. In this fully MHC-mismatched model where CD90.1$^+$ *Il33*$^{+/+}$ and *Il33*$^{-/-}$ recipients received WT CD90.2$^+$ BALB/c

donor BM and T cells (**Figure 21 A**), we observed that donor BALB/c (CD90.2$^+$) CD4$^+$ T cells isolated from the spleen of *Il33*$^{-/-}$ recipients did not expand at the same rate as donor CD4$^+$ T cells isolated from *Il33*$^{+/+}$ recipients on day 7 post-alloHCT (**Figure 21 E**). This decreased expansion was independent of IL-12 blockade since donor CD90.2$^+$ CD4$^+$ T cells isolated from CD90.1$^+$ *Il33*$^{+/+}$ recipients that received IgG had similar expansion to T cells isolated from recipients that received IL-12 blockade (**Figure 21 E**). These findings support the overall concept that a dominant role of recipient IL-33 after alloHCT is to directly promote CD4$^+$ T cell proliferation, independent of IL-12 signaling. These data also point to a novel relationship where CD4$^+$ T cells, not APC, sense and respond to stimulatory DAMP signals released from non-hematopoietic recipient cells.

3.4.3 IL-33 stimulation augments early T cell expansion following an alloantigen encounter

The ST2/IL-33 axis is broadly implicated in organ and tissue homeostasis as well as diverse immune cell development and functions (302, 311, 312, 315, 316). To rule out any indirect defects due to the global lack of IL-33 or ST2, we generated B6 CD45.2$^+$ *CD4-Cre x ROSA(R)26-LoxP-Stop-LoxP (LSL)-YFP x St2*$^{fl/fl}$. Using these mice as a source of donor T cells also allowed us better focus on YFP$^+$ ST2$^-$ CD4$^+$ T cell in CD4-driven GVHD models (317). We first sought to answer if IL-33 was acting directly on donor CD4$^+$ T cells early during activation in the SLO to cause the striking decrease in cell numbers of *St2*$^{-/-}$ donor CD4$^+$ T cells (**Figures 19 D and 20 C**) and decreased CD4$^+$ T cell numbers in *Il33*$^{-/-}$ recipients (**Figure 21 E**) on day 7 post-alloHCT. In these studies, donor CD3$^+$ T cells from CD45.2$^+$ *CD4-Cre x R26-LSL-YFP x St2*$^{fl/fl}$ (ST2$^{fl/fl}$) and CD45.1$^+$ *St2*$^{+/+}$ (ST2^{WT}) mice were labeled with CellTrace Violet (CTV) and co-transferred into the same lethally irradiated BALB/c (allogeneic; allo) or B6 (syngeneic; syn) recipients (**Figure 22 A**). CD4$^+$ T cells were harvested from the spleen on days 1, 2, 3, 5, and 7 to determine the effect of

IL-33 stimulation on $CD4^+$ T cell early expansion after alloHCT (**Figure 22 A**). $ST2^{fl/fl}$ $CD4^+$ T cells were identified as YFP^+ subset to ensure they had expressed the Cre recombinase (**Figures 22 D and G, and 23 A**) and the absence of ST2 on YFP^+ cells was verified (**Figures 22 B and C, and 23 A**). ST2 was upregulated on donor $ST2^{WT}$ $CD4^+$ T cells from both allo and syn recipients (data not shown), but more rapidly and strongly in allo recipients (**Figure 22 B**). This is similar to $CD4^+$ T cell upregulation of ST2 early after viral antigen exposure in response to an LCMV infection (105).

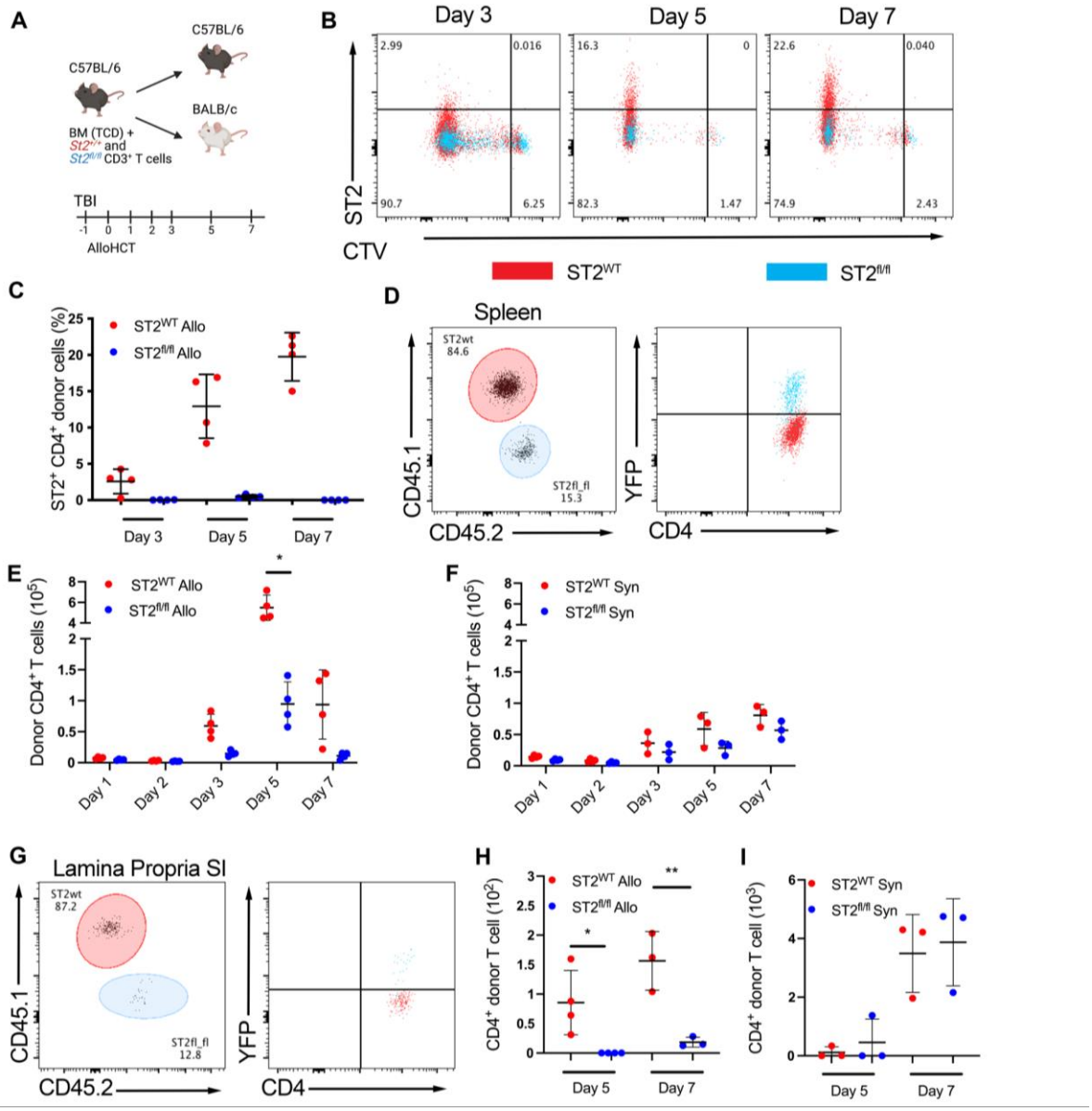

Figure 22. Early donor CD4$^+$ T cell proliferation is dependent on IL-33.

***A-H*, BALB/c (allogeneic; allo) and B6 (syngeneic; syn) recipient mice received lethal TBI (8Gy or 11Gy, respectively) on d-1. On d0 the BALB/c and B6 recipient mice received 1x10^7 WT B6 TCD-BM with 1x10^6 CD3$^+$ T cells from CD45.2$^+$ *CD4-Cre x R26-LSL-YFP x St2$^{fl/fl}$* (ST2$^{fl/fl}$) and 1x10^6 CD3$^+$ T cells from *St2$^{+/+}$* CD45.1$^+$ (ST2^{WT}) B6 mice. T cells were labeled with CTV prior to adoptive transfer. T cells were harvested from the spleen on d1, 2, 3, 5 and 7 post-alloHCT and from the small intestine lamina propria on d5 and 7 and assessed by flow cytometry. *A*, Schematic of mechanistic examination of the impact of ST2-mediated signaling into donor CD4$^+$ T cells during GVHD initiation. *B*, Representative flow plots of ST2 expression on donor**

$CD4^+CD45.1^+H2\text{-}K^{d-}$ $ST2^{WT}$ (red, quadrant frequencies) and $CD4^+CD45.2^+H2\text{-}K^{d-}YFP^+$ $ST2^{fl/fl}$ (blue) cells from isolated from the spleen of the same allo recipient. *C,* Frequency of ST2 on donor $CD45.1^+$ or $CD45.2^+$ CTV^{lo} donor T cells on d3, 5 and 7. *D-F,* Representative flow plot of $CD45.1^+YFP^-$ and $CD45.2^+YFP^+$ donor $CD4^+$ T cells of an allo recipient (*D*) and total $ST2^{WT}$ (red) *vs.* $ST2^{fl/fl}$ (blue) donor $CD4^+$ T cell counts from the spleen of *E,* allo recipients or *F,* syn recipients on the indicated day. *G,* Representative flow plot of $CD4^+$ donor $ST2^{WT}$ (red) *vs.* $ST2^{fl/fl}$ (blue) from the small intestine (SI) lamina propria of an allo recipient. *H-I,* total $ST2^{WT}$ (red) *vs.* $ST2^{fl/fl}$ (blue) donor $CD4^+$ T cell counts from the SI of *H,* allo recipients or *I,* syn recipients. Data in *A-I* indicate mean+/-SD, *n*=3-4/group, data are representative of 2 independent experiments. *, P<0.05, **, P<0.01, ***, P<0.001, two-way ANOVA (*C-I*).

The frequency of donor $ST2^+$ $CD4^+$ cells steadily increased from day 3 to day 7 in the $ST2^{WT}$ T cell subset isolated from allo BALB/c recipients (**Figure 22 B and C**). BALB/c recipients exhibited a reduced number of presumed-alloantigen specific $ST2^{fl/fl}$ $CD4^+$ T cells compared to $ST2^{WT}$ $CD4^+$ T cells in the spleen of the same recipient on days 3, 5, and 7 (**Figure 22 D and E**). Interestingly, IL-33 signaling was not necessary for lymphopenia-induced proliferation (LIP) in the spleen of syn recipients, as we observed a similar number of $ST2^{fl/fl}$ and $ST2^{WT}$ donor $CD4^+$ T cells (**Figure 22 F**). Additionally, a lack of early IL-33 stimulation presumably in the SLO results in a failure of donor $ST2^{fl/fl}$ $CD4^+$ T cells to infiltrate GVHD target tissues in allo recipients (**Figure 22 G, H**). This was not the case in the syn recipients where both the $ST2^{fl/fl}$ $CD4^+$ T cells and $ST2^{WT}$ $CD4^+$ T cells successfully infiltrated the small intestine by day 7 (**Figure 22 I**). Thus, IL-33 does not appear to function like IL-7, which augments weak TCR signaling to self-peptides presented on self MHC to support LIP after irradiation (318). Instead, IL-33 predominantly promotes the expansion of alloreactive $CD4^+$ T cells, suggesting that IL-33 augments the expansion of $CD4^+$ T cells following TCR recognition of allogeneic MHC or miH.

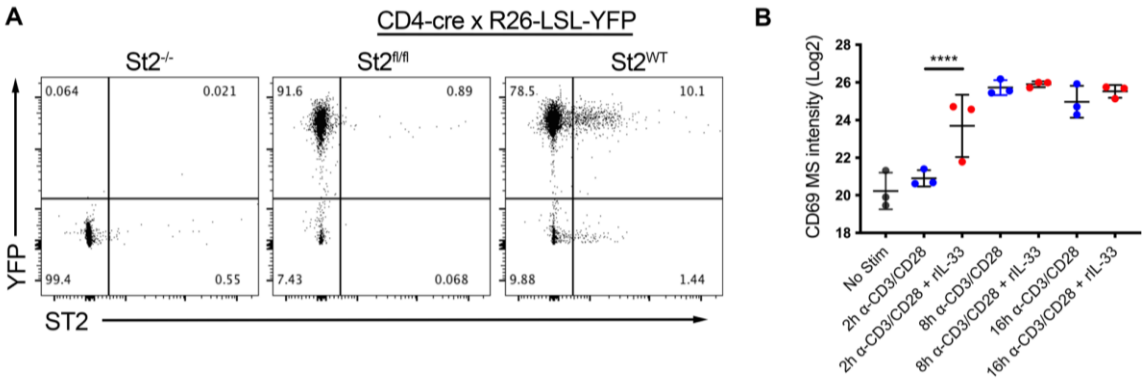

Figure 23. CD4$^+$ T cells from CD4-Cre x R26-LSL-YFP x *St2$^{fl/fl}$* mice do not express ST2 and IL-33 induces early activation marker protein expression.

***A*, B6 *St2$^{-/-}$*, *CD4-Cre x R26-LSL-YFP x St2$^{fl/fl}$*, and *CD4-Cre x R26-LSL-YFP* mice were treated with 0.5 μg IL-33 for 10 days to expand the CD4$^+$ST2$^+$ population. On day 11 splenocytes were harvested and assessed by flow cytometry. Plots are representative of two mice per group, gated on CD4$^+$CD25$^+$CD44$^+$ T cells. *B*, Mass spectrometry analysis of CD69 protein expression in naïve CD4$^+$ T cells following activation with anti-CD3/CD28 plate-bound antibodies with or without rIL-33 co-stimulation. Data in *A* *n*=2/group. Data in *B* indicate mean+/-SD, *n*=3/group. ****, P<0.0001, one-way ANOVA (*B*).**

3.4.4 Early T cell activation is enhanced by IL-33

Another sensitive marker of TCR engagement is the upregulation of CD69, which can be detected by 2-3 hours after TCR engagement (319) by a non-self-antigen (320). As early as day 1 post-alloHCT, ST2^{WT} CD4$^+$ T cells have a higher CD69 MFI and an increased frequency of CD4$^+$ ST2^{WT} donor T cells expressing CD69 relative to ST2$^{fl/fl}$ cells from the same allo recipient spleens (**Figure 24 A-C**). There was no appreciable difference in CD69 MFI or frequency of donor CD69$^+$CD4$^+$ T cells in the spleens of TBI conditioned syn recipients (**Figure 24 B and C**). These data support the conclusion that IL-33 is acting to enhance the activation of only alloreactive T cells. These data are strengthened by our assessment of the total proteome of anti-CD3, anti-CD28,

and IL-33 *in vitro* stimulated $CD4^+$ T cells. Two hours of stimulation with anti-CD3 and anti-CD28 along with IL-33 resulted in a significant upregulation of CD69 protein compared to stimulation with anti-CD3 and anti-CD28 alone (**Figure 23 B**). In addition to these noticeable differences in early activation marker CD69, $ST2^{fl/fl}$ $CD4^+$ T cells retained their expression of CD62L through day 5 above expression levels of $ST2^{WT}$ $CD4^+$ T cells from allo recipients (**Figure 24 D and E**). $CD4^+$ $ST2^{WT}$ donor T cells also expressed higher levels of the activation marker, CD44, compared to $CD4^+$ $ST2^{fl/fl}$ T cells isolated from the same allo recipient (**Figure 24 F and G**). These results suggest that IL-33 is acting to enhance the early activation of alloreactive donor $CD4^+$ T cells.

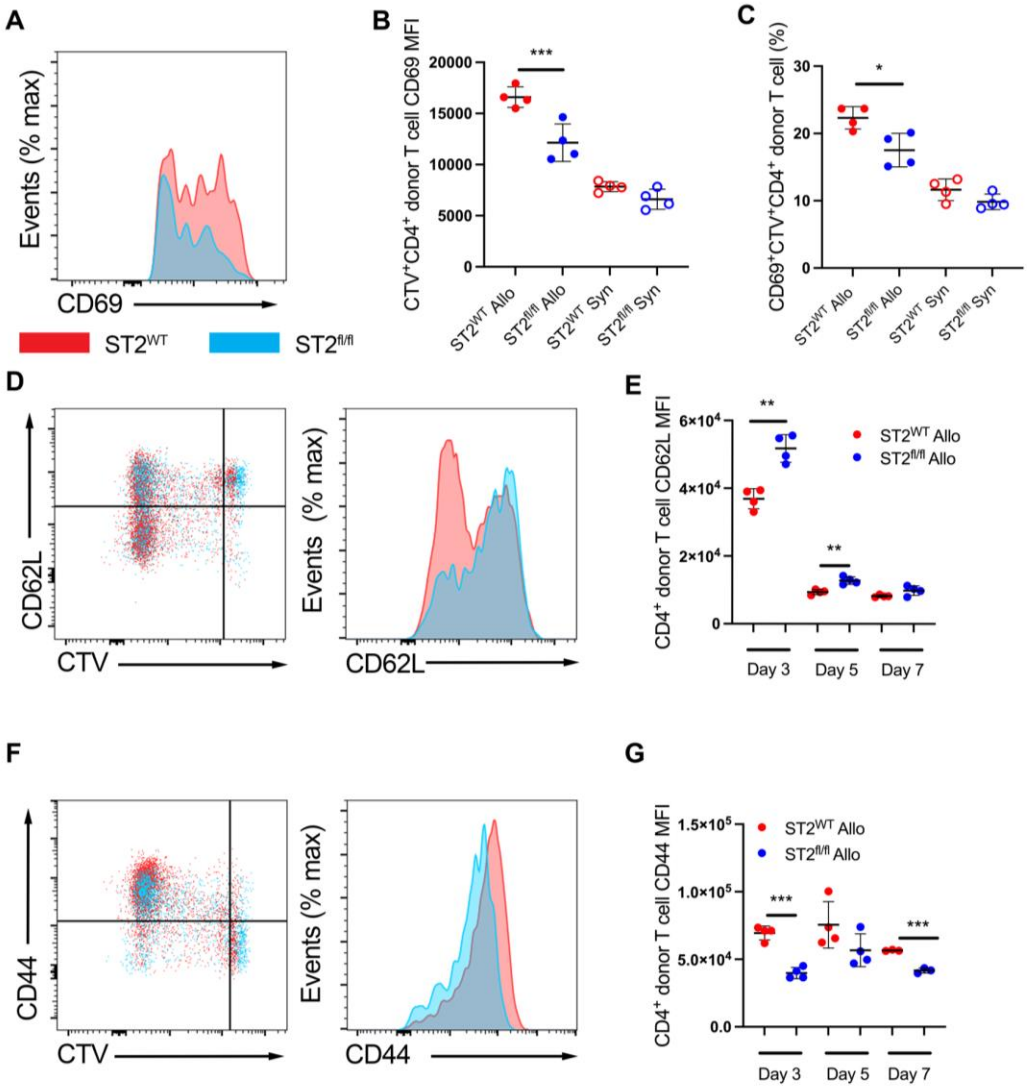

Figure 24. IL-33 stimulation augments early donor CD4$^+$ T cell activation.

***A-G*, CD3$^+$ T cells from CD45.2$^+$ *CD4-Cre x R26-LSL-YFP x St2$^{fl/fl}$* (ST2$^{fl/fl}$) B6 (1x10^6) and *St2$^{+/+}$* CD45.1$^+$ (ST2^{WT}) B6 (1x10^6) mice were labeled with CTV and co-transferred with 1x10^7 WT B6 TCD-BM into lethally irradiated BALB/c and B6 recipients. T cells were harvested from the spleens on d1, 2, 3, 5 and 7 and assessed by flow cytometry. *A*, Representative histogram of CD69 expression on ST2^{WT} (red) CD45.1$^+$ CTV$^+$ or ST2$^{fl/fl}$ (blue) CD45.2$^+$ CTV$^+$ donor CD4$^+$ T cells from the same allo recipient spleen on d1. *B*, Quantification of CD69 MFI on CD45.1$^+$ or CD45.2$^+$ CTV$^+$ donor CD4$^+$ T cells from allo recipient spleens on d1. *C*, Quantification of frequency of CD45.1$^+$ or CD45.2$^+$ CTV$^+$ donor CD69$^+$ CD4$^+$ T cells at d1. *D*, Representative flow plot (CTV vs. CD62L) and histogram of CD62L expression on ST2^{WT} (red) or ST2$^{fl/fl}$ (blue) donor CD4$^+$ T cells from an allo**

recipient spleen on d3. *E*, Quantification of CD62L MFI on d3, 5 and 7. *F*, Representative flow plot (CTV vs. CD44) and histogram of CD44 expression on $ST2^{WT}$ (red) or $ST2^{fl/fl}$ (blue) donor $CD4^+$ T cells from an allo recipient spleen on d3. *E*, Quantification of CD44 MFI on d3, 5 and 7. Data in *B*-*G* indicate mean+/-SD, *n*=3-4/group, data are representative of 2 experiments. *, P<0.05, **, P<0.01, ***, P <0.001, one-way ANOVA (*B*, *C*) two-way ANOVA (*E*, *G*).

3.4.5 IL-33 drives Th1 differentiation while inhibiting regulatory/Th2 gene expression in $CD4^+$ T cells after alloHCT

Further comparison of donor T cells in the SLO at early time points of T cell activation established that $ST2^{WT}$ $CD4^+$ T cells expressed more Tbet than $ST2^{fl/fl}$ $CD4^+$ T cells from the same spleen of allo recipients through day 5 post-alloHCT (**Figure 25 A and B**). Tbet induces the expression of the Th1 cytokine IFNγ and is critical for upregulation of CXCR3, which controls the alloreactive T cell trafficking to GVHD target tissues (321). CXCR3 was expressed at higher levels on donor $ST2^{WT}$ $CD4^+$ T cells than $ST2^{fl/fl}$ T cells in the same spleen of allo recipients through day 7 post-alloHCT (**Figure 25 C and D**). This decrease in CXCR3 matched our earlier finding of decreased infiltration of $ST2^{fl/fl}$ $CD4^+$ T cells into the small intestine, a key GVHD target tissue. Our data establish that alloreactive $ST2^{WT}$ T cells are more proliferative, more highly activated, and prone to differentiate into Th1 cells. To better understand the pathways IL-33 is controlling post-alloHCT in allo recipients, we performed RNAseq on sorted splenic $ST2^{fl/fl}$ and $ST2^{WT}$ donor $CD4^+$ T cells co-transferred into the same lethally irradiated BALB/c allo recipients on day 5 post-alloHCT (**Figure 25 E**). As anticipated from the above studies, the gene profile of the $ST2^{WT}$ donor $CD4^+$ T cells from our RNAseq analysis indicated that IL-33 promotes metabolic activity and Myc activation (**Figure 26 A and B**) needed for robust T cells proliferation following TCR stimulation with cognate antigen (322). Interestingly, the $ST2^{fl/fl}$ donor $CD4^+$ T cells from the same allo

recipients, represented by the negative Normalized Enrichment Scores (NES) on the left side of curves, were more enriched by predetermined Gene Set Enrichment Analysis (GSEA) pathways for genes expressed in T helper cell differentiation and T cell anergy and tolerance (**Figure 25 F-I**). The heat map of genes representative of T cell anergy and tolerance and T helper cell differentiation shows that $ST2^{WT}$ donor $CD4^+$ T cells (red bar) expressed higher levels of Th1 genes, including *Ifng, Tbx21, Cxcr3,* and IFNγ-induced *Cd70* (**Figure 25 F and G**). Surprisingly, $ST2^{fl/fl}$ donor $CD4^+$ T cells (blue bar) have enriched expression of Th2 genes and regulatory genes including, *Foxp3, Ctla4, Tnfrsf18,* and *Il10* (**Figure 25 F and G**), which cause the GSEA results for the T helper differentiation pathway and T cell anergy and tolerance to be enriched in $ST2^{fl/fl}$ donor $CD4^+$ T cells (**Figure 25 H and I**).

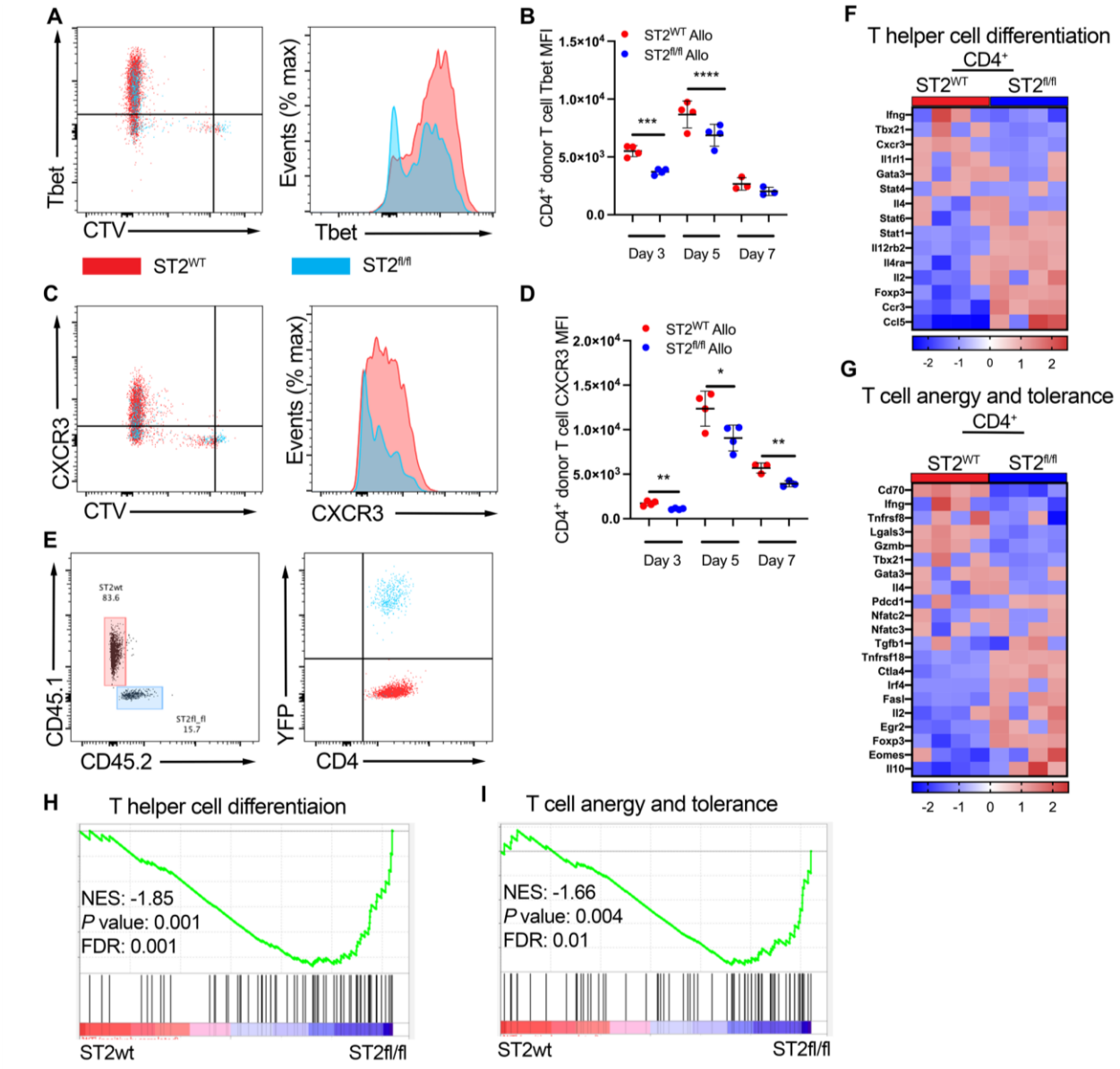

Figure 25. IL-33 stimulation of donor CD4$^+$ T cells drives Th1 differentiation while inhibiting regulatory/Th2 gene expression.

***A-D*, CTV labeled CD3$^+$ T cells from CD45.2$^+$ *CD4-Cre x R26-LSL-YFP x St2$^{fl/fl}$* (ST2$^{fl/fl}$) B6 (1x10^6) and *St2$^{+/+}$* CD45.1$^+$ (ST2^{WT}) B6 (1x10^6) mice were co-transferred with 1x10^7 WT B6 TCD-BM into irradiated BALB/c and B6 recipients. Splenocytes were harvested on d1, 2, 3, 5 and 7 for flow analysis. *A*, Representative flow plot (CTV vs. Tbet) and histogram of Tbet expression on ST2^{WT} (red) or ST2$^{fl/fl}$ (blue) donor CD4$^+$ T cells from the same allo spleen (d5). *B*, Quantification of Tbet MFI on d3, 5 and 7. *C*, Representative flow plot (CTV vs. CXCR3) and histogram of CXCR3 expression on ST2^{WT} (red) or ST2$^{fl/fl}$ (blue) donor CD4$^+$ T cells from the**

same allo spleen (d7). *D*, Quantification of CXCR3 MFI on d3, 5 and 7. E-I, CTV labeled CD3$^+$ T cells from ST2$^{fl/fl}$ and ST2^{WT} B6 mice were co-transferred into irradiated BALB/c as described in *A-D*. CD4$^+$ T cells were sorted from the same spleen on d5 for *St2*$^{+/+}$ H2-Kd$^-$CD45.1$^+$YFP$^-$ (ST2^{WT}) and *St2*$^{fl/fl}$ H2-Kd$^-$CD45.2$^+$YFP$^+$ (ST2$^{fl/fl}$) directly into cDNA prep cell lysis buffer. *E*, Representative sort plot of CD4$^+$CD45.1$^+$YFP$^-$ and CD4$^+$CD45.2$^+$YFP$^+$ donor cells. *F,G*, Heatmap of T helper cell differentiation and T cell anergy and tolerance associated genes enriched in ST2^{WT} (red) and ST2$^{fl/fl}$ (blue) donor CD4$^+$ T cells. *H,I*, Leading edge plots of GSEA of ST2^{WT} (red) or ST2$^{fl/fl}$ (blue) donor CD4$^+$ T cells compared with transcriptional profiles of T helper cell differentiation and T cell anergy and tolerance. FDR, false discovery rate. NES, normalized enrichment score. Data in *A-D* indicate mean+/-SD, *n*=3-4/group, representative of 2 independent experiments. Data in *E-I* *n*=4/group. *, P<0.05, **, P<0.01, ***, P< 0.001, ****, P<0.0001, two-way ANOVA (*B, D*).

These RNAseq findings reflected serum cytokine data in GVHD studies where *Il33*$^{-/-}$ B6 recipients of WT BALB/c T cells (**Figure 26 C**) display reduced levels of IFNγ compared to WT recipients (**Figure 26 D**) and increased levels of IL-10 in the serum of *Il33*$^{-/-}$ recipients compared to the *Il33*$^{+/+}$ recipients (**Figure 26 E**). The increase in IL-10 was mostly reversed by treating the *Il33*$^{-/-}$ recipients with rIL-33 from day 3-6 post-alloHCT (**Figure 26 C and E**). These findings suggest that IL-33 is not only supporting alloreactive T cell activation and Th1 differentiation, but also limiting regulatory gene expression by alloreactive donor CD4$^+$ T cells in the SLO after alloHCT.

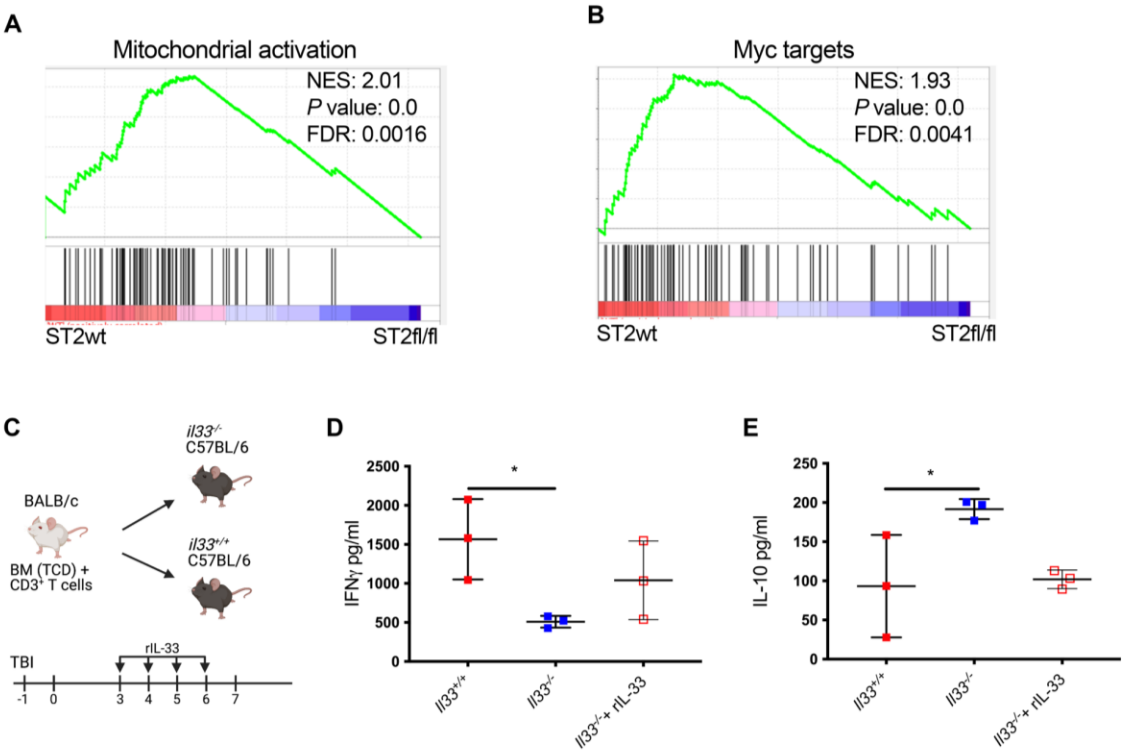

Figure 26. Recipient IL-33 stimulations drives T cell metabolism and cell cycle gene expression and suppresses regulatory cytokine production.

***A,B*, Leading edge plots of GSEA of ST2^{WT} (red) or ST2$^{fl/fl}$ (blue) donor CD4^{+} T cells from an allogeneic recipient RNA-seq (described in Fig 24 *E-I*) compared with transcriptional profiles of Mitochondrial activation and Myc targets. *C-E*, On d-1 CD90.1^{+} *Il33*$^{-/-}$ or CD90.1^{+} *Il33*$^{+/+}$ B6 recipient mice received lethal TBI. On d0, mice received 1x10^{7} CD90.2^{+} BALB/c TCD-BM with 2x10^{6} CD90.2^{+} BALB/c CD3^{+} T cells. Mice were treated with rIL-33 (from d +3 to +6 after HCT; 0.5 µg/mouse/d) or phosphate-buffered saline (PBS) as control. *C*, Schematic of BALB/c to B6 GVHD model as it relates to rIL-33 treatments. *D*, Donor serum was collected on d7 and assessed for systemic IFNγ by Luminex array. *E*, Donor serum was assessed for systemic IL-10 by Luminex array. FDR, false discovery rate. NES, normalized enrichment score. Data in *A,B*, indicate mean+/-SD, *n*=4/group. Data in *D,E*, indicate mean+/-SD, *n*=3/group.*, P<0.05, one-way ANOVA (*D,E*).**

3.4.6 Alloantigen TCR activation is augmented by IL-33 stimulation

Successful $CD4^+$ T cell activation and differentiation requires an initial signal generated through a robust TCR interaction with cognate antigen/MHC and a second, antigen-independent costimulatory signal (323). While Th1 differentiation is typically thought to be dominated by innate cell-derived cytokine IL-12, the strength of TCR and costimulation signaling are highly influential in dictating $CD4^+$ T cells differentiation fates (324-326). Strong TCR signals supports Th1 generation and limits Foxp3 expression (327-329), whereas an attenuated TCR signal results in $CD4^+$ T cell Foxp3 expression (330). Costimulatory molecules feed into TCR signaling pathways to limit Foxp3 expression in newly activated $CD4^+$ T cells (331, 332). Our RNAseq data revealed that IL-33 stimulation of $CD4^+$ donor T cells augmented expression of *Ifng* and *Cd70,* while limiting the expression of *Foxp3* and *Il10* **(Figure 25 G)**. These data suggest that IL-33 may be acting as a novel costimulatory molecule that amplifies alloreactive TCR signaling after alloHCT.

Our data looking at early-activation time points also points to IL-33-mediated augmentation of alloantigen-driven TCR signaling, as we saw that IL-33 stimulation augmented the frequency of $CD69^+CD4^+$ donor T cells and the expression of CD69 on B6 $ST2^{+/+}$ donor T cells **(Figure 24 A-C)**. While CD69 expression is representative of TCR signaling, CD69 expression can be influenced by inflammatory stimuli (333). Nur77 has been identified as an immediate-early response gene expressed in T cells following TCR stimulation (334, 335) and is unique from CD69 in that Nur77 expression is not induced unless the TCR has been engaged (333). We investigated the impact of IL-33 stimulation on TCR signaling by quantifying Nur77 expression post-alloHCT by adoptively transferring *Nur77-GFP* B6 donor $CD4^+$ T cells into *Bm12*

Il33$^{+/+}$ and *Bm12 Il33*$^{-/-}$ recipients. By using the B6 CD4^{+} T cell to Bm12 recipients alloHCT model, we could precisely assess how the absence of IL-33 modulated Nur77 upregulation in donor CD4^{+} T cells in response to a single MHCII mismatch in a model where GVHD is CD4^{+} T cell driven (336, 337). In these studies, CD45.2^{+} *Nur77-GFP* and CD45.1^{+} B6 donor CD4^{+} T cells were labeled with CTV and co-transferred into the same lethally irradiated *Bm12 Il33*$^{+/+}$ or *Bm12 Il33*$^{-/-}$ recipients (**Figures 27 A and 28 A and B**).

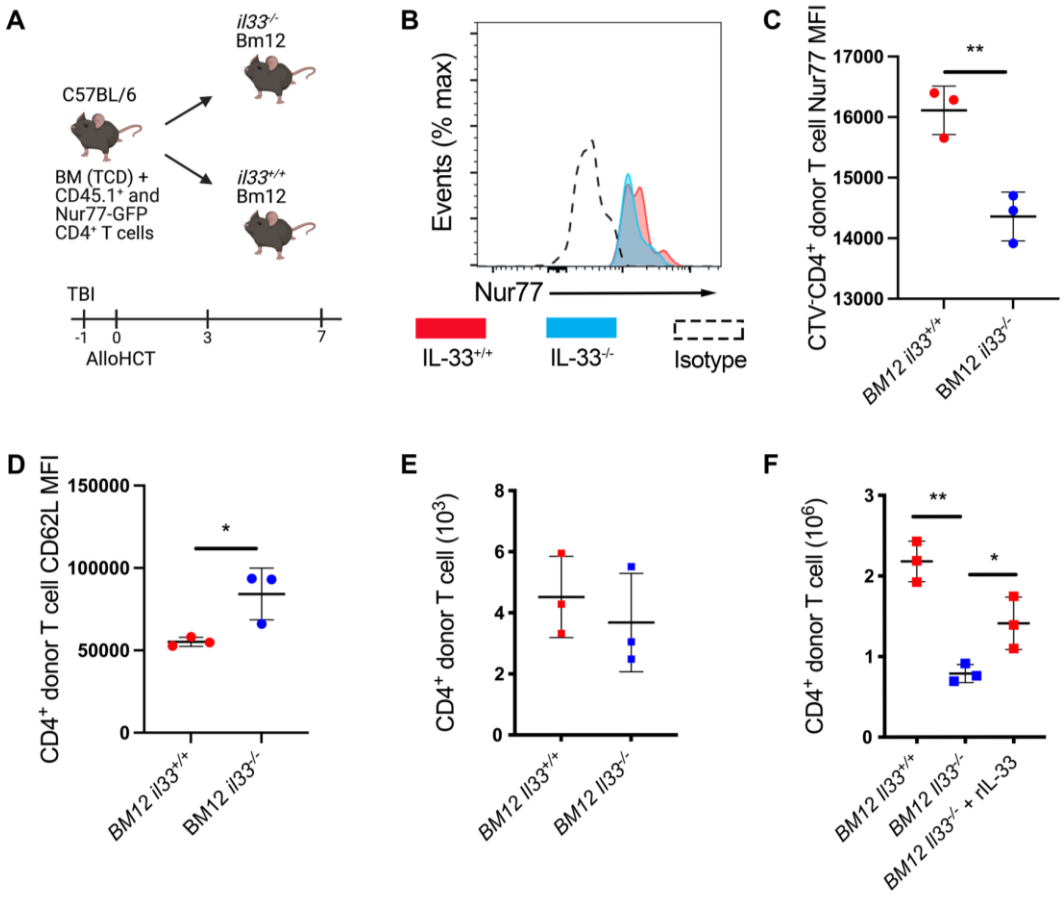

Figure 27. IL-33 stimulation augments immediate-early response gene, Nur77, expression.

***A-C*, Bm12 *Il33*$^{+/+}$ and Bm12 *Il33*$^{-/-}$ recipient mice received lethal TBI (9Gy) on d-1. On d0 recipient mice received 1x10^7 WT Bm12 *Il33*$^{+/+}$ TCD-BM with 5x10^4 Nur77-GFP B6 CD4$^+$ T cells and 5x10^4 CD45.1$^+$ B6 CD4+ T cells. Donor T cells were labeled with CTV prior to adoptive transfer. T cells were harvested from the spleen on d3 and d7 post-alloHCT. *A*, Schematic of mechanistic examination of the impact of recipient IL-33 stimulation of donor CD4$^+$ T cells during GVHD initiation. *B*, Representative histogram of donor CD4$^+$ T cells Nur77-GFP expression from Bm12 *Il33*$^{+/+}$ and Bm12 *Il33*$^{-/-}$ recipient spleens d3. *C*, Quantification of Nur77-GFP MFI on d3. *D*, Quantification of CD62L MFI on Nur77-GFP$^+$ donor CD4$^+$ T cells on d3. *E*, Donor CD45.1$^+$ and CD45.2$^+$ CD4$^+$ T cell counts from the spleen on d3. *F*, Donor CD45.1$^+$ and CD45.2$^+$ CD4$^+$ T cell counts from the spleen on d7. Data in *B-F* indicate mean+/-SD, *n*=3/group. *, P<0.05, **, P<0.01, ***, P<0.001, Student's t test (*C-E*) and one-way ANOVA (*F*).**

Flow cytometric analysis of donor T cells isolated from the spleen of *Bm12 Il33*$^{+/+}$ recipients at day 3 post-alloHCT had increased Nur77 expression in the CD45.2^{+}CD4^{+}CTV^{lo}Nur77^{+} subset compared to the same group of donor T cells isolated from *Bm12 Il33*$^{-/-}$ recipients (**Figures 27 B and C, and 28 B**). The CD45.2^{+}CD4^{+}CTV^{lo}Nur77^{+} from *Bm12 Il33*$^{-/-}$ recipients also had increased retention of CD62L expression on day 3 post-alloHCT (**Figure 27 D**). There was no difference in donor CD4^{+} T cell numbers at day 3 (**Figure 27 E**), but similar to the GVHD model where donor T cells lack the ST2 receptor, by day 7 we see a significant decrease in donor CD4^{+} T cells in the *Bm12 Il33*$^{-/-}$ recipients (**Figure 27 F**). This decrease in donor CD4^{+} expansion could be partially corrected by delivery of rIL-33 (**Figure 27 F**).

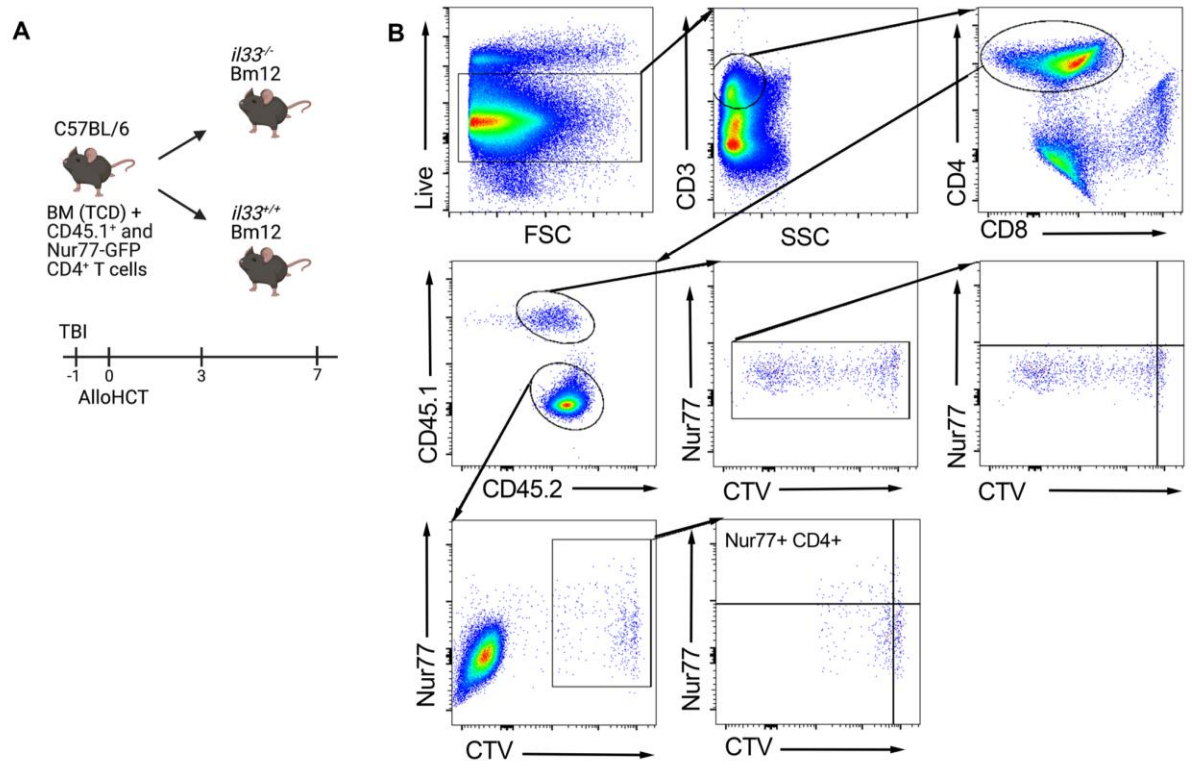

Figure 28. Donor CD4$^+$ T cells upregulated Nur77 by day 3 and are identifiable in the spleen as early as day 1. ***A-B,*** **Bm12 *Il33*$^{+/+}$ and Bm12 *Il33*$^{-/-}$ recipient mice received lethal TBI (9Gy) on d-1. On d0 recipient mice received 1x10^7 WT Bm12 *Il33*$^{+/+}$ TCD-BM with 5x10^4 Nur77-GFP B6 CD4$^+$ T cells and 5x10^4 CD45.1$^+$ B6 CD4$^+$ T cells. Donor T cells were labeled with CTV prior to adoptive transfer. T cells were harvested from the spleen on d3 and d7 post-alloHCT.** ***A,*** **Schematic of mechanistic examination of the impact of recipient IL-33 stimulation of donor CD4$^+$ T cells during GVHD initiation.** ***B,*** **Representative flow plot gating to identify donor CD45.1$^+$CD4$^+$Nur77-GFP$^-$ and CD45.2$^+$CD4$^+$ Nur77-GFP$^+$ T cells. Data in *A,B,* indicate mean+/-SD, *n*=3/group.**

We further verified that IL-33 modulated early TCR signaling by assessing phosphorylation of pathway intermediates involved in TCR signaling after alloHCT (**Figure 29 A and B**). Phosphorylation of important kinases downstream of TCR and ST2 were measured by flow cytometry in donor CD4$^+$ T cells from ST2$^{fl/fl}$ and ST2^{WT} mice, which were labeled with CTV and co-transferred into the same lethally irradiated BALB/c (allo) recipients (**Figures 29 A and**

B, and 30 C and D). Splenocytes were harvested and assessed on day 1 post-alloHCT (**Figure 30 A and B**). $ST2^{WT}$ donor $CD4^+$ T cells had increased levels of phosphorylated (p) p38 and ERK, as well as the MTORC1 target S6 compared to $ST2^{fl/fl}$ donor $CD4^+$ T cells from the same allo recipient (Fig. 8 C-E). These findings establish that ST2 augments activation of p38, ERK, and mTOR pathways that are common to the TCR pathway. We also show the importance of the p38 pathways to Th1 effector function, as p38 inhibition negates IL-33-mediated IFNγ production by $CD4^+$ T cells (**Figure 29 F**).

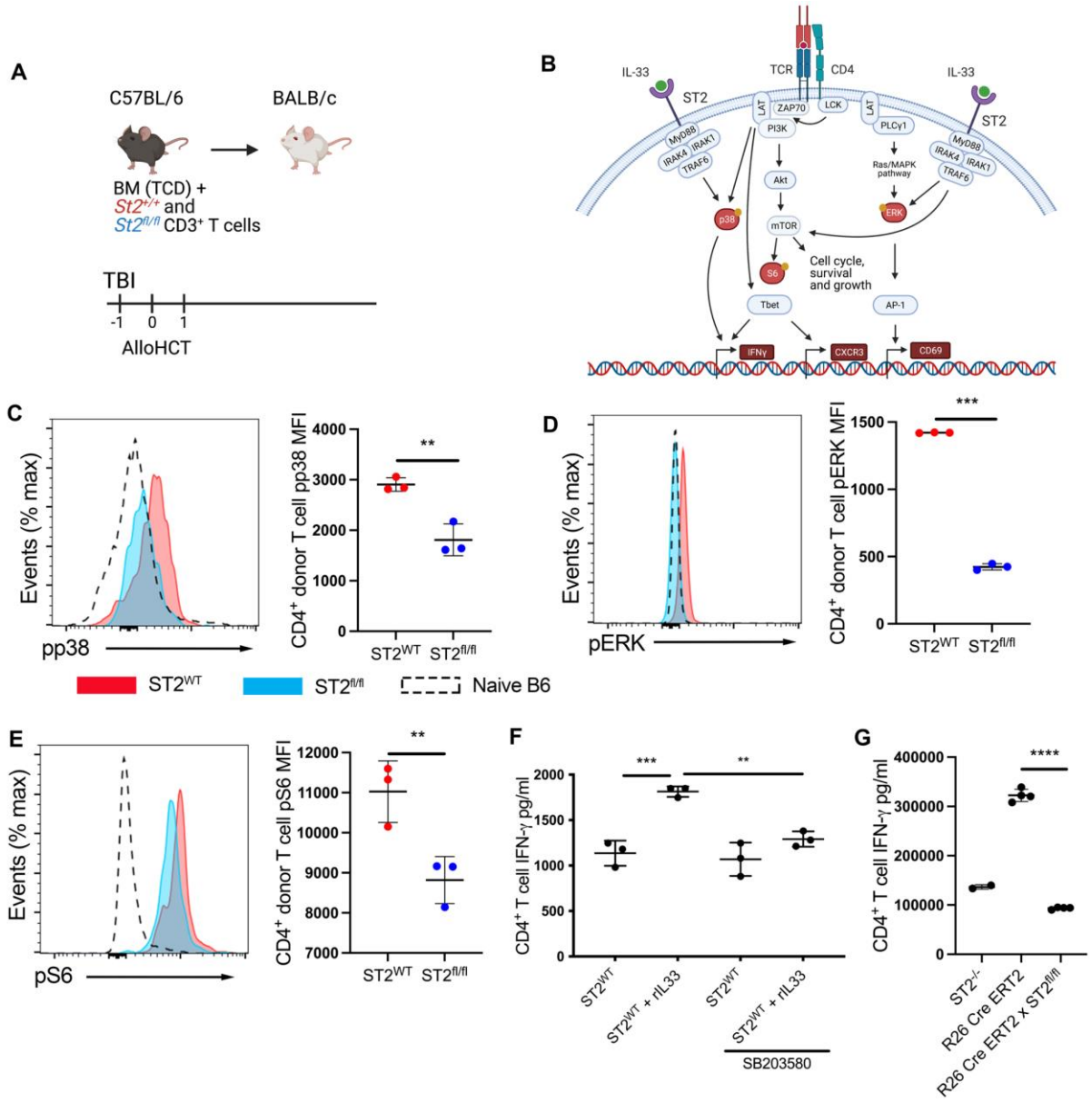

Figure 29. Alloantigen driven TCR signaling networks are enhanced by IL-33 stimulation.

***A*, Schematic of mechanistic examination of the impact of ST2-mediated signaling into donor CD4$^+$ T cells during GVHD initiation. *B*, Diagram of overlap between TCR and ST2 signaling pathways. *C-E*, CTV labeled CD3$^+$ T cells from CD45.2$^+$ *CD4-Cre x R26-LSL-YFP x St2$^{fl/fl}$* B6 (1x10^6) and *St2$^{+/+}$* CD45.1$^+$ B6 (1x10^6) mice were co-transferred with 1x10^7 WT B6 TCD-BM into lethally irradiated BALB/c recipients. ST2^{WT} (red) and ST2$^{fl/fl}$ (blue) CD4$^+$ T cells from the same spleen were assessed by flow cytometry on d1. *C*, Representative histograms of phosphorylated p38 expression and quantification of pp38 MFI, *D*, phosphorylated ERK expression and quantification of pERK MFI, *E*, phosphorylated S6 expression and quantification of pS6 MFI,**

on d1 from ST2^{WT} (red) and ST2$^{fl/fl}$ (blue) donor CD4^{+} T cells (C-E). *F*, Sorted naïve CD4^{+} T cells from *St2*$^{+/+}$ B6 were stimulated in vitro with anti-CD3/CD28 beads, IL-12, IL-2 and anti-IL-4 for 4 days, followed by a 3hr rest and 24hr IL-33 stimulation (or no stim) with or without p38 inhibitions. IFNγ concentration in culture supernatants were assessed by ELISA. *G*, Sorted naïve CD4+ T cells from *St2*$^{+/+}$ B6 were stimulated in vitro with anti-CD3/CD28 beads, IL-12, IL-2, anti-IL-4, IL-33 and 4-hydroxytamoxifen (TAM) for 4 days. IFNγ concentration in culture supernatants were assessed by ELISA. Data in *C-F* indicate mean+/-SD, n=3-4/group, data are representative of 2 experiments. Data in *G* n=2-4/group. *, P<0.05, **, P<0.01, ***, P<0.001, ****, P<0.0001, Student's t test (*C-E*) and one-way ANOVA (*F,G*).

To demonstrate ST2 deficient T cells are not intrinsically defective from a lack of IL-33 stimulation early during T cell development, we used ST2 inducible knockout mice to delete ST2 at the time of activation and Th1 differentiation. Specifically, when B6 *R26-cre*^{ERT2}*x St2*$^{fl/fl}$ and B6 *R26-cre*^{ERT2} were Th1 skewed *in vitro* and treated with 4-hydroxytamoxifen (Tam) and rIL-33, *R26-cre*^{ERT2} mice produced IFNγ in response to IL-33 stimulation but Tam-treated *R26-cre*^{ERT2}*x St2*$^{fl/fl}$ whose ST2 would be deleted, produced IFNγ at levels comparable to CD4^{+} B6 *St2*$^{-/-}$ controls (**Figure 29 G**). Thus, the observed differences are not due to a lack of ST2 signaling during development, but to the loss of IL-33 stimulation of donor T cells following alloHCT. In total, our data indicates that early after alloHCT IL-33 acts as a potent costimulatory signal that augments TCR signaling pathways to support alloreactive CD4^{+} T cell activation, proliferation and Th1 differentiation.

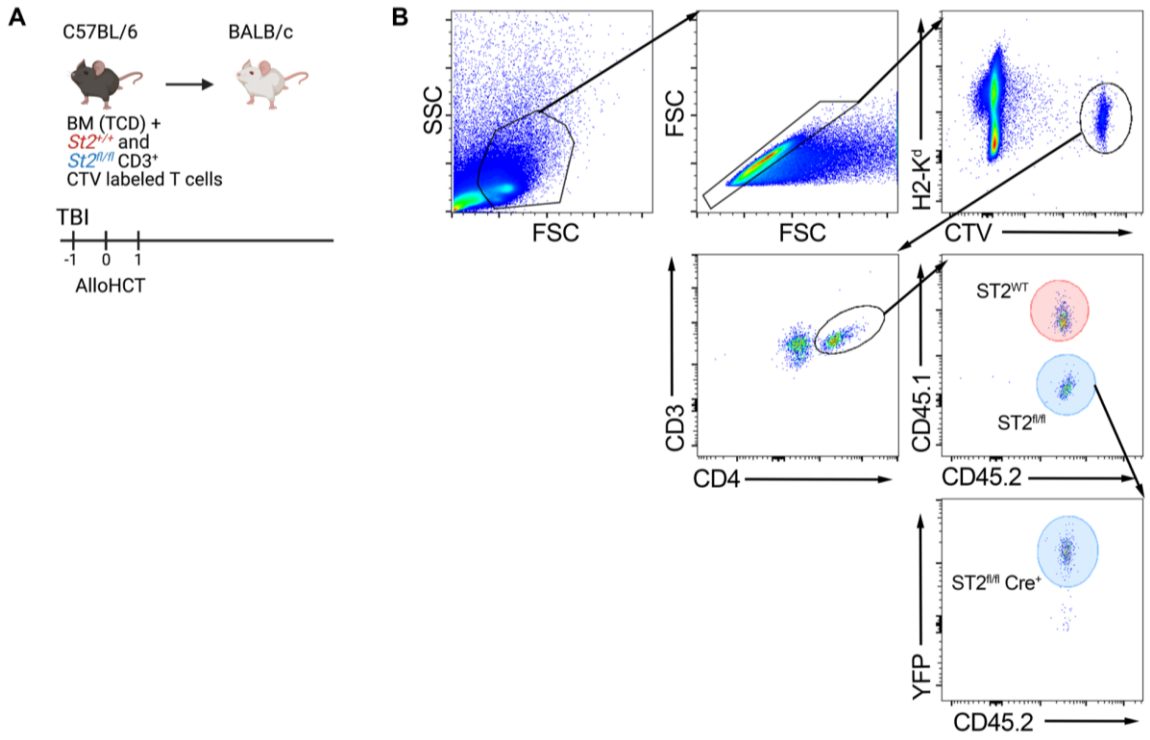

Figure 30. Donor CD4$^+$ T cells are identifiable in the spleen as early as day 1.

A-B, **CD3$^+$ T cells from CD45.2$^+$ *CD4-Cre x R26-LSL-YFP x St2$^{fl/fl}$* B6 (1x10^6) and *St2$^{+/+}$* CD45.1$^+$ B6 (1x10^6) mice were labeled with CTV and adoptively transferred with 1x10^7 WT B6 TCD-BM into lethally irradiated BALB/c recipients. ST2^{WT} (red) and ST2$^{fl/fl}$ (blue) CD4$^+$ T cells from the same spleen were assessed by flow cytometry on d1. *A,* Schematic of mechanistic examination of the impact of ST2-mediated signaling into donor CD4$^+$ T cells during GVHD initiation. *B,* Representative flow plot gating to identify donor CD45.1$^+$CD4$^+$YFP$^-$ and CD45.2$^+$CD4$^+$ YFP$^+$ T cells. Data in *A,B,* indicate mean+/-SD, *n*=3-4/group, data are representative of 2 experiments.**

3.5 Discussion

In the current studies we provide novel mechanistic insights into IL-33-mediated CD4$^+$ T cell immunobiology after alloHCT and build on our past observation that IL-33 is a clinically

relevant, recipient-derived stimuli that drives lethal GVHD (36). Specifically, we reveal that the stromal cell-derived DAMP, IL-33, contributes to the generation of alloreactive Th1 cells by functioning as a costimulatory signal that acts directly on donor $CD4^+$ T cells to augment TCR-related signaling pathways. Another significant finding was that IL-33 promoted early Th1 differentiation independently of IL-12. IL-33 has been described as a DAMP released from epithelial barrier tissues and perivascular regions of the lung to aid parasite clearance and contribute to allergy through the antigen-independent functions of Type 2 innate lymphoid cells and Th2 cells (4, 28). In contrast, our current findings suggest an important function for IL-33 in contributing to antigen-dependent activation and differentiation of alloreactive $CD4^+$ T cells into Th1 cells by augmenting TCR signaling pathways. Our identification of IL-33 as a stromal cell-derived DAMP that is a costimulatory signal driving the activation and differentiation of alloreactive Th1 cells independently of the indirect PAMP-stimulated innate cytokine, IL-12, provides new insights into targetable APC-independent signals supporting early GVHD initiation.

ST2 is a member of the IL-1R/TLR superfamily expressed constitutively or induced on a wide range of immune and non-hematopoietic cells (4, 338). Evidence is emerging supporting costimulatory roles for IL-1R/TLR ligands that directly promote T cell proliferation, survival, and differentiation (339-341). IL-1 family members, like IL-33 and IL-1, can work synergistically with STAT stimulators to enhance T cell effector responses (342, 343). Likewise, IL-1β has been described as an adjuvant that can directly boost T cell expansion and survival following cognate antigen stimulation, independent of IL-6 and CD28 signaling (177, 344). Recently, Matsuoka et al. demonstrate that MyD88 signaling in T cells was needed for donor T cell survival and Th1, Tc1, and Th17 differentiation leading to GVHD lethality (189). A lack of MyD88 signaling in donor T cells also facilitated $Foxp3^+$ Treg expansion after alloHCT to reduce GVHD lethality

(189). ST2, like other IL-1R/TLR superfamily members, relies on MyD88 to convey IL-33 stimulation (2, 4, 338, 345). Our current findings regarding IL-33 promoting Th1 differentiation while limiting *Foxp3* and *Il10* expression are highly compatible with those of Matsuoka et al (189). Likewise, the demonstration by these investigators that GVHD-promoting effects were independent of TLR2 and TLR7 support our conclusion that IL-33 is a critical T cell-stimulating DAMP after alloHCT. Griesenauer et al. have also recently demonstrated similar findings with *Myd88*$^{-/-}$ donor T cells conferring protection. While not pinpointing the specific ligand activating MyD88 signaling in T cells, they determined that the reduced GVHD lethality was independent of signaling through IL-1R and TLR4, since knocking out these receptors on donor T cells did not provide the same protection (188). Our studies now provide a definitive ligand that explains the phenotypes of *Myd88*$^{-/-}$ T cell in GVHD. When these and our current studies are looked at in total, it can be safely concluded that IL-33 released from recipient tissues ligates MyD88-dependent ST2 to act as a potent donor T cell costimulatory factor that supports Th1 differentiation and expansion, while regulating the induction and function of Treg.

Our data are divergent from findings using a lymphocytic choriomeningitis virus (LCMV) mouse model where *Stat4*$^{-/-}$ and *Tbet*$^{-/-}$ T cells did not upregulate ST2 following an LCMV challenge (105). Likewise, we had previously observed that IL-12 increased CD8^{+} T cell ST2 expression *in vitro*, in a Tbet dependent manner (36, 107). In the current studies, neutralization of IL-12p40 did not modulate ST2 expression on donor T cells. Given the rapid response of donor CD4^{+} T cells to IL-33, it is most likely that a low level of ST2 exists on naïve T cells that initiate immediate response to IL-33, with alloHCT-associated stimuli like IFNγ or TCR stimuli augmenting subsequent ST2 expression as these T cells are activated and proliferate. Identifying how ST2 is regulated on donor CD4^{+} T cells will be an important area of investigation moving

forward that may lead to the identification of therapeutics that are able to limit the potency of the IL-33/ST2 axis after alloHCT.

Our data emphasize the importance of IL-33 for early activation and differentiation of $CD4^+$ T cells into Th1 cells expressing Tbet and CXCR3 in the SLO. While we do not precisely rule out a role for IL-33 expressed in other locations, such as the barrier tissues or GVHD target organs, our data establish a profound augmentation of IL-33 in the SLO after radiation exposure at times when donor T cells will almost exclusively be found in the SLO (346-348). It has been shown that radiation and alloHCT change the SLO structure and increases the relative density of FRC-like stromal cells that support GVHD development (349). Our data suggest these changes contribute to acute GVHD by augmented IL-33 availability that then increase donor Th1 responses. This concept and our current findings align with past studies identifying radiation-resistant cells in splenic T cell zones as the critical source of IL-33 in LCMV infections (106) and the described radiation-resistant nature of FRC (350, 351). Yet, conditions of sustained IL-33 in the SLO seem unique to alloHCT and the radiation conditioning recipients receive as compared to IL-33 expression patterns during pathogen responses. In recent studies by Aparicio-Domingo et al. (39), they detailed how IL-33 expression by $CCL19^+$ FRC was important for the expansion of virus reactive $CD8^+$ T cells secreting IFNγ. They described, however, a rapid depletion of IL-33 in the FRC of the SLO during LCMV infections (39). These authors concluded that FRC frequency was not altered, but pre-stored nuclear IL-33 protein was released into the SLO after viral infection (39). Thus, this controlled period of critical IL-33 stimulation of T cells appears prolonged or augmented after alloHCT. In total, these data would indicate that the conditioning necessary for alloHCT alters typical IL-33 expression patterns to cause a sustained and augmented presence of IL-33 in the SLO. This increased IL-33 then promotes pathological Th1 alloimmune responses

leading to GVHD. Our current studies raise several outstanding questions regarding IL-33 expression and release. First, how is IL-33, sequestered in the nucleus, being released from FRC to stimulate Th1 responses and can this process be modulated to control GVHD. Second, our data using ST2 deficient donors and recipients lacking IL-33 clearly establish that IL-33 is important after alloHCT to promote Tbet induction and CXCR3 expression that initiates Th1 cell infiltration into GVHD target tissues. Yet, IL-33 is upregulated by alloHCT in epithelial cells and mesenchymal cells of barrier tissues, particularly the small intestine (36). Future studies utilizing inducible ST2 deletion on donor T cells or targeted deletion of IL-33 in the GVHD target tissues will be important to answer if there is a role for IL-33 sustaining Th1 responses over the prolonged course of GVHD.

A number of factors influence the lineage-specific differentiation of naïve $CD4^+$ T cells; these include the type of APC, concentration of antigen, duration of TCR ligation, costimulatory signals, and local cytokine environment (352). Early amplification of Tbet transcription involves p38 (353, 354), a signaling pathway activated by IL-33 ligation of ST2 (103). Several studies have suggested that Th1 subsets preferentially differentiate in response to high-affinity antigen or high antigen dose, whereas lower affinity antigen and low antigen dose favors Th2 responses (355, 356). Weak affinity peptides used to stimulate TCR-transgenic T cells or low concentration of their cognate peptide instead induce Th2 differentiation through transient activation of extracellular signal-regulated kinase (ERK), which is associated with IL-4 production and GATA3 expression (357-359). In contrast, high concentrations of cognate antigen or high-affinity peptide stimulation of TCR-transgenic T cells results in strong and prolonged ERK activation, which suppresses GATA3 expression (359). We show that IL-33 augments $Tbet^+$ T cells during a $CD4^+$ donor T cell response to alloantigen; we also show that IL-33 stimulation intensifies p38, ERK,

and s6 phosphorylation *in vivo*. Together these data suggest that IL-33 is boosting TCR signaling to support $CD4^+$ differentiation into Th1 cells. While alloantigen is ubiquitous in GVHD, the antigen affinity of alloreactive T cells causing GVHD is poorly defined. This makes it difficult to clarify if IL-33 is augmenting weak TCR signals to diversify and broaden the alloresponse or acting to complement strong TCR signals to support the survival of potent alloreactive clones (360).

GVHD occurs even if recipient cells do not express the CD28 ligands CD80 and 86 and is ablated if only donor APC can present antigen to donor T cells (177, 361, 362). This suggests that there are recipient signals, such as IL-33, that can provide the costimulation necessary for donor T cell activation after alloHCT. We initially identified that IL-33 upregulated the early activation marker CD69 in allogeneic, but not syngeneic recipients, suggesting that CD69 was being upregulated in response to TCR stimulation and IL-33 stimulation. Yet, CD69 on T cells has been shown to be upregulated by inflammatory stimuli, particularly IFNγ or innate cytokines released following TLR ligation (333, 335). A better marker of TCR-engagement is thought to be the orphan nuclear hormone receptor Nur77, which is rapidly transcribed in response to antigen receptor signaling but does not respond to general inflammatory stimuli *in vivo* (333). (335) Earlier studies identified Nur77 as a critical signal during T cell development, and the expression of Nur77 was dependent on TCR engagement and on simultaneous costimulation, since anti-CD3 stimulation alone did not upregulate Nur77 expression (363). On day 3 post-alloHCT we show an increase expression of Nur77-GFP donor T cell transferred into allogeneic $Il33^{+/+}$ recipients relative to those transferred into $Il33^{-/-}$ recipients. These data then support the conclusion that recipient IL-33 is acting as a costimulatory factor that augments TCR signaling pathways to support early activation and differentiation in to Th1 cells.

Despite evolving immunoprophylaxis regimens after alloHCT, donor T cell responses to MHC mismatches or allogeneic minor histocompatibility antigens on matched MHC results in GVHD in 30-70% of recipients (295). It is well appreciated how the excessive expansion of alloreactive Th1 cells producing high levels of the pro-inflammatory cytokines IFNγ and TNFα is central to GVHD pathology. Interestingly, IL-33 promoted early Th1 differentiation and infiltration of recipient GVHD target tissues independently of IL-12. This finding suggests that the combined targeting of IL-33 and IL-12 using antibodies undergoing clinical testing (184, 364) immediately after alloHCT would target two distinct Th1-driving pathways and thus be highly effective in limiting early donor Th1 responses. Our data indicate that IL-33 does not, however, appear to be involved in LIP. We have previously shown that B6 *St2*$^{-/-}$ deficient T cells retain the ability to clear BALB/c A20 B cell lymphoma, even though they do not cause GVHD in BALB/c recipients (36). These data suggest that targeting of IL-33 or ST2 signaling would not be expected to disrupt T cell reconstitution or GVL responses, only effectively limit pathologic Th1 alloreactive responses leading to GVHD. It is also of considerable interest that St2$^{fl/fl}$ donor CD4^{+} T cells have a gene transcript suggesting they may be adopting a regulatory phenotype and that *Il33*$^{-/-}$ recipients have increased levels of IL-10 in the serum at day 7. These findings suggest that in the absence of IL-33 augmentation of TCR signaling pathways, alloreactive donor T cells are prone to skewing towards more regulatory subsets, including Treg or Tr1 cells. This increased generation of regulatory cells would have significant therapeutic implication for patients receiving alloHCT. In particular targeting IL-33 or ST2 would be expected to be effective in lowering the risk of GVHD and supporting regulatory responses following alloHCT to induce tolerance to treat autoimmune disease or limit the need for immunosuppression after solid organ transplantation.

4.0 General Discussion and Conclusion

In the above described studies I have identified two unique mechanisms for IL-33 mediated regulation of T cell responses. First, following ALI induced by chemical or viral injury, IL-33 is a crucial local factor necessary to limit the early inflammatory response mediated by IL-33-stimulated IL-13 production by Treg. In contrast to these reparative functions, I have also found that IL-33 is a clinically relevant, recipient-derived stimuli that drives lethal GVHD. In this case, I reveal that IL-33 contributes to the generation of alloreactive Th1 cells by functioning as a costimulatory signal that acts directly on donor $CD4^+$ T cells to augment TCR-related signaling pathways and promote Th1 differentiation independent of IL-12. IL-33 is clearly an important molecule that communicates tissue conditions to a variety of immune cells as they respond to potential threats by non-self or work to restore damaged self.

To understand the role of IL-33 in immunobiology it is critical to recognize the complex pleiotropic effects of IL-33 in immune homeostasis and disease. Our understanding of IL-33 has evolved from the original described role in allergic pathology to active participation in organism development, metabolism, homeostatic functions, injury repair, fibrosis, pathogen responses and immune dysregulation in inflammatory diseases. There are many parts that contribute to the spectrum of IL-33 biology, first the type and quantity of cells expressing IL-33 in a tissue, the tight regulation of IL-33, the kinetics of ST2 expression on the responding cell, the presence of supporting signals and downstream signaling events following ST2 ligation.

IL-33 is widely expressed in many tissues of the body. In the lung, an IL-33-rich environment, IL-33 creates a Type 2 milieu dominated by IL-5 and IL-9 (365) and the early lung is dense with basophils and mast cells, in addition to IL-33-expanded ILC2s and eosinophils (365).

The appearance of IL-13-producing ILC2s coincided with the appearance of alveolar macrophages (AM), which were polarized by IL-13 towards a reparative and regulatory Type 2 subset. It is hypothesized that the Type 2-dominated environment of the lung is poised to support tissue remodeling, while protecting loss of function by limiting excessively destructive Type 1 inflammatory responses to microbes (365, 366). Type 2 homeostatic state in the lung appears to come a cost, as the Type 2-dominated immune responses also contribute to allergy or asthma (366). Following ALI in this Type 2 skewed environment IL-33 release supports further Type 2 and reparative cytokine secretion from the tissue resident immune cells.

In the lung IL-33 is constitutively expressed, but sequestered, in the lung epithelium and Type 2 alveolar cells of both mice and human (27, 34, 37, 284). Following ALI, *IL33* mRNA and protein level increase in lung tissue (165). $ST2^+$ Treg are enriched in the tissues and accumulated rapidly at a higher frequency in injured peripheral tissues, yet there have been little described differences between $ST2^+$ Treg in the tissues versus those in circulation. $ST2^+$ Treg express higher levels of activation and suppressor molecules than $ST2^-$ Treg, yet outside of tissue-imprinted differences (255, 367, 368), $ST2^+$ Treg in the lungs are quite comparable to $ST2^+$ Treg in the spleen (102). Thus, it is likely that $ST2^+$ Treg are a recirculating fraction of tissue resident Treg (255) and could get stimulated by IL-33 in the tissues or in circulation. Yet our findings following ALI support that acute inflammation and resolution following chemical injury is a local response, as we did not observe systemic changes (369). These findings corroborate earlier studies of IL-33 in the lung following parasite infection, potentially due to the numerous regulation mechanisms for IL-33.

Locksley's group determined that IL-33 is important in the parenchymal tissue of the lung for Type 2 effector function, but IL-33 is not critical in the SLO for priming and activation of a

pathogen-clearing Th2 response (370). In contrast the SLO appears to be a critical reservoir for released IL-33 that supports a Type 1 immune response to viral infections (39), or alloimmune responses after alloHCT. During a LCMV infection the FRC of the SLO were identified as the critical source of IL-33 to support $CD8^+$ T cell mediated viral clearance (39). IL-33 has been described to be expressed in the lymphatic endothelial cell and in the FRC of the SLO, but only the FRC were critical sources of IL-33 during a chronic viral infection. IL-33 producing FRC are also precisely located in the medullary and T cell zone, in close proximity to the anti-viral effector T cells (39). In the above described studies our data establishes a profound augmentation of IL-33 in the SLO after radiation exposure at times when donor T cells will almost exclusively be found in the SLO (346-348). FRC in the T cell zone not only express IL-33 and secrete chemokine factors attracting T cells to T cell zone of the lymphoid tissue, but they are also critical for SLO remodeling and enlargement following a viral infection or alloantigen driven donor T cell expansion during the initiation of GVHD (142). It has been shown that radiation and alloHCT change the SLO structure and increases the relative density of FRC-like stromal cells, which are described as a radiation resistant cell that support GVHD development (349-351). Previous findings in fibroblasts determined mechanical strain was sufficient for IL-33 release. Thus, during SLO expansion following an infection or alloHCT, IL-33 may be released through mechanical strain from the FRC as they stretch and proliferate to facilitate T cell activation and priming in the enlarged SLO (44). Another possibility during viral infection or GVHD is that the effector T cells are targeting FRC, since their selective elimination during acute GVHD has recently been described (371). Our current understanding of IL-33 release would suggest this to be the less likely scenario since apoptotic cell death results in IL-33 inactivation through caspase cleavage (4, 5). A third hypothesis is that biologically active IL-33 is released into circulation and can mediate systemic

effects since we do not fully rule out a role for IL-33 expressed in other locations, such as the barrier tissues or GVHD target organs. These studies are underway and will shed light on these scenarios in the future. My findings suggest IL-33 expression is important locally, and in many unique cellular and tissue sources. Ultimately, the location of the immune response and cellular source of IL-33 is impactful on the resulting immune response. The kinetics and mechanism of release are also critical and must coincide with the expression of ST2 on the responding cell, it is likely that this choreographed combination of events determines the type of immune response IL-33 promotes.

How rapidly IL-33 is neutralized will also be an important variable to local versus systemic effects of this potent tissue damage signal. Based on findings from the trauma model and our ALI studies, it is possible that IL-33 is in circulation, but it may not be biologically active. In humans, IL-33 is easily detected in the serum following trauma (83), yet in the mouse IL-33 is less easily detected in the serum even though IL-33 protein expression significantly increases in the lung parenchyma. IL-33 is tightly regulated and quickly inactivated by a decoy receptor, sST2, and by oxidation (5). IL-33 in the tissues is also only active for a brief period and likely acts with the most potency on the neighboring cells.

IL-33 ligation by ST2 is transduced by the adapter molecule MyD88, which is a key downstream adapter for TLRs and IL-1R superfamily members. MyD88 was initially described as a critical signal transducer in innate immune cells, promoting cell activation and effector cytokine production (372). More recently studies have identified a critical role for MyD88-mediated signaling by IL-1 family members to enhance T cell responses (342, 343). $CD4^+$ T cells require signaling through MyD88 for overcoming suppression by Treg (373). Additionally, IL-1 family members are reported to have diverse functional contributions to all T cell effector lineage

commitment and effector function (352). Turka's group reported that MyD88 activates NFκB and PI3K pathways in T cells, promoting their proliferation, IL-2 production, and survival (339, 374). Their group also identified a role of MyD88 signaling in Treg function, where MyD88-deficient Treg were ineffective at restraining allo-effector responses due to a cell-survival-independent defect suggesting a functional defect (375). The above-described studies add to our current understand of IL-1R family/MyD88 signaling to focus on a key stimulus, IL-33, that drives functional programing in both conventional T cells and Tregs. Highlighting the importance of cell-specific targeting of inflammatory pathways. Interestingly even though IL-33 has the capacity to influence T conventional cells and Treg, the mechanism of IL-33-mediated stimulation is distinct. I describe two unique roles for IL-33, first in the potential TCR-independent stimulation of Treg to produce effector cytokines and second in an apparent TCR-dependent manner to augment TCR signaling pathways following alloantigen engagement.

Rudensky's group determined that Treg-secreted Areg is mobilized in response to IL-18 or IL-33 in a TCR-independent manner, unlike Treg suppressor function, which is TCR-dependent (100, 376). They used TCR mutant mice to suggest IL-33 stimulated Areg secretion by Treg is TCR-independent. Similarly, we established that IL-33 acts on $ST2^+$ Treg to mediate secretion of IL-13 in TCR-independent manner. Using $CD90.1^+$ FOXP3-IRES-mRFP (FIR) reporter mice we completed a direct comparison of $ST2^+$ $Foxp3^+$ Treg, $ST2^-$ $Foxp3^+$ Treg, and $ST2^+$ $Foxp3^-$ Th2 cells (102). These FACS-isolated populations were stimulated with anti-CD3/CD28 beads alone or with rIL-33. CD3/CD28–stimulated Th2 cells secreted significant IL-13, however, this was not modulated by IL-33. Thus, Th2 secretion of IL-13 was IL-33–independent. While TCR stimulation alone did not drive potent IL-13 secretion, IL-33 stimulation of $ST2^+$ Treg, however, induced ample secretion of IL-13. Thus, IL-33 mediates TCR-independent secretion of IL-13 by $ST2^+$

mouse Treg. By generating a mouse with Treg deficient for IL-13 (Foxp3^{Cre} x *il4/il13*^{flox}), we established Treg secreted IL-13, while not involved in direct T cell suppression, is critical to control lethal inflammation and support early injury responses after chemical or viral lung injury (102). The Benoist group has supported this finding in a study determining the relative importance of TCR inputs versus cytokine cues for Treg function (377). Their findings suggest that TCR signals are muted in Treg, whereas cytokine signaling pathways are more enhanced (377). Interestingly, the Benoist groups also suggests that ST2 expression on Treg may be at least partially TCR-dependent since ST2 expression is controlled by DUSP4, a phosphatase that is overexpressed in Treg, and has significant modulated gene overlap with TCR dependent signals. ST2 gene expression, *Il1rl1*, was also reduced in Treg following induced TCR knockdown (378). These findings together suggest that Treg may partially depend on TCR signaling to upregulated ST2, but once upregulated, IL-33-mediated effector functions can act outside of the TCR. Also, there may be other mechanisms that maintain ST2 expression, such as GATA3 phosphorylation, which has been shown to enhance ST2 expression on memory Th2 cells and colonic Treg (99, 379). Similar to the relationship uncovered by the Benoist studies, we and others have determined that ST2 expression is transiently expressed on Th1 cells following antigen encounter to act as a costimulatory factor aiding T cell activation (105). In total, these studies suggest a close relationship between ST2 and TCR signaling in CD4$^+$ T cell responses.

The classic view of adaptive T cell responses is that APC integrate signals that identify the nature of the challenge, which program an appropriate T cell response. Consistent with this, recipient conditioning-mediated damage to host tissues, particularly of the GI tract, releases DAMPs and PAMPs to stimulate recipient APC pro-inflammatory activity, including IL-12 secretion. Nevertheless, other mechanisms must also exist to initiate pathogenic alloreactive T

cells responses, as recipients with disrupted PAMP signaling pathways (*MyD88*$^{-/-}$*TRIF*$^{-/-}$) or lacking IL-12, or costimulation molecules still develop GVHD (177). Additionally, Hill's group, demonstrated that nonhematopoietic recipient cells were sufficient for donor T cell activation and expansion (361). These findings challenge current paradigms and suggest that there are other stimulatory signals contributing to T cell activation and differentiation. In the above studies we demonstrate that the information of tissue damage is directly communicated to donor alloreactive T cells via IL-33, which promotes both alloreactive T cell expansion and Th1 differentiation, independent of IL-12. These finding establishes IL-33 as a novel recipient-derived signal that can directly contribute to lethal alloreactive Th1 responses leading to GVHD.

In the above described studies of GVHD, IL-33 acts in a novel costimulatory role to alloreactive Th1 cells, promoting proliferation, enhanced activation, and differentiation. Our data looking at early-activation points of IL-33-mediated augmentation of alloantigen-driven TCR signaling we first saw that IL-33 stimulation augmented the frequency of CD69^{+} CD4^{+} donor T cells. Then we demonstrate an increase expression of Nur77-GFP, which is an early response gene rapidly transcribed in response to antigen receptor signaling but does not respond to general inflammatory stimuli *in vivo*, in donor T cell transferred into allogeneic *Il33*$^{+/+}$ recipients relative to those transferred into *Il33*$^{-/-}$ recipients. Finally, we demonstrate through the phosphorylation of distal TCR and ST2 pathway intermediates that IL-33 acts directly on donor CD4^{+} T cells to augment TCR-related signaling pathways. Unlike traditionally costimulatory receptors, which interact with their respective ligand that are a counter-receptor on the surface of APCs, IL-33 is a stromal cell-derived cytokine. My demonstration that IL-33 has the capacity to act as a costimulatory factor, potentially in the absence of a traditional antigen presentation on an APC is novel. There are very few examples where tissue-secreted molecule can function as a

costimulatory/coinhibitory ligand. Thus, this may be particularly critical during GVHD disease where nonhematopoietic cells have the capacity to present antigen.

A similar costimulatory factor that has been studied in alloimmunity is 4-1BB. 4-1BB is a member of the TNF family of costimulatory receptors and is transiently expressed on activated T cells upon TCR stimulation (380). 4-1BB is a potent costimulator of T cells promoting proliferation, expansion and supports the acquisition of a memory phenotype (381). In the setting of alloimmunity over stimulation of 4-1BB with an agonistic anti-4-1BB antibody accelerates GVHD lethality, whereas recipient mice administered 4-1BB deficient donor T cells had significantly reduced GVHD mortality compared to WT controls (382). Like ST2 expression on Treg, there is a population of Treg that preferentially express 4-1BB. 4-1BB costimulation of Treg expand functional peripheral Treg (383). Yet there is contrasting evidence supporting the role of 4-1BB in immunity and regulation. Stimulating 4-1BB can promote anti-viral immunity, but also can suppress disease symptoms in mouse models of autoimmunity, suggesting a dual function of supporting a Type 1 immune response and a regulatory response, similar to my findings with IL-33 in stimulating Treg following ALI versus Th1 cells during GVHD. Pleiotropic molecules clearly serve an important and powerful role in immunobiology demonstrating that if we can develop targeted therapeutics for these molecules, they can be used in numerous diseases to shape a desired outcome. If we understand the timing and place of IL-33 that directs a desired immune response – we can control it and augment it. Conversely, we can block or be ready to counter any associated pathology mediated by $ST2^+$ cells locally or systemically.

The opposing outcomes of IL-33 stimulation on different $CD4^+$ T cell subsets is likely linked by a fine balance of positive and negative signals that regulating IL-33 release and stimulation of each T cell subset in unique tissue environments. The lung environment is suggested

to be skewed towards a Type 2 immune environment whereas in the SLO the pathogen/antigen response is the determinant signal. It is likely that in both locations IL-33 is likely acting as a costimulatory signal to enhance the immune response similar to the effects of 4-1BB costimulation. The expression of and mechanism of upregulation of ST2 on the cell surface is also critical, since IL-33 stimulation of Treg cytokine production is TCR-independent and IL-33 stimulation of Th1 cells in TCR-dependent. These results suggest that there is an additional signal, like TCR engagement with cognate antigen, for the upregulation of ST2 on Th1 cells adding another layer of control over IL-33 stimulation of Th1 cells.

Recent studies in pathogen immunity in the tissues have suggested the importance of the type of infection in molding the immune response rather than the distinct Th subsets (384). Within the $CD4^+$ T effector gene grouping the accessibility of enhancer elements for master regulators of Th subsets in chromatin were not important readouts of a cell's differentiation state. Instead, transcription factors that were activation drivers, AP-1, IRFs and BACH2 were more important contributors to T effector phenotype and are downstream of PAMP and DAMP signaling receptors as well as costimulatory receptors (384). These data suggest the critical role IL-1R/TLR ligands have in shaping the immune response. Future studies will need to clearly define the necessary signals for ST2 upregulation on Th1 cells. Studying the effect of IL-33 stimulation of naïve ($CD62L^+$) $CD4^+$ T cells compared to effector ($CD44^+$) on ST2 and TCR pathway intermediates will determine if antigen stimulation is necessary coactivation of these pathways. Additionally, *ex vivo* studies of differentiated Th1 cells with and without TCR and IL-33 stimulation will determine if TCR stimulation is necessary for IL-33-mediated Th1 effector/recall function. Determining the critical cellular sources of IL-33 through targeted Cre-deletion, and the mechanism of IL-33

release needs to be more clearly defined to develop relevant therapeutic approaches for maximizing the therapeutic potential of this critical costimulatory molecule.

Another feature that makes IL-33 signaling unique to other PAMP/DAMP is that IL-33 stimulation drives a unique metabolic profile compared to pro-inflammatory TLR stimulation from LPS. We have recently used a heart transplant model to clarify that a critical function of endogenous IL-33 was to promote the generation of reparative macrophage phenotype through a metabolic reprogramming augmenting OXHPOS and FA uptake. IL-33 is unlike other DAMPs like HMGB1 that drives glycolysis and epigenetic modifications enabling inflammatory cytokine production (385). IL-33 instead blocks iNOS expression and, similar to IL-4, IL-10, and IL-13, increases mitochondrial function and FA uptake (386, 387). Additionally, in the above described GVHD studies I identify using RNAseq that IL-33 stimulation may augment phosphorylation of a mTORC1 pathway intermediate, a key drive of immune metabolism. In many settings mTOR has been described to integrate the environmental signals to regulate immune cell metabolism, differentiation, and effector function (388). mTORC1 promotes glycolysis through the activation of HIF1α and c-Myc, which we observed is an enriched pathway in ST2 replete donor T cells (389). Additionally, mTORC1 has a unique role in Treg metabolism, supporting effector Treg suppressor marker ICOS and CTLA-4, but diminishing markers for central memory T cells and decreases *in vivo* longevity (390). We have demonstrated that IL-33-mediated IL-13 production by Treg is inhibited by rapamycin treatment, a potent inhibitor of mTOR (**Appendix**). These data suggest that some of the broad reach of IL-33 effects in homeostasis and immunity may be the result of a common thread of metabolic pathway modulation. Determining the key IL-33-driven metabolic signals will also be critical for fully understand the mechanism of IL-33 immunobiology.

Given the emerging evidence that IL-33 is an important mediator of both early inflammation, injury resolution and repair there is significant therapeutic potential in manipulating the expression or delivery of IL-33 during the course of disease. We have shown that the delivery of regulatory biomolecules, such as one-dose of exogenous rIL-33 or rIL-13 decreases lethality after bleo-induced ALI. In contrast we have also shown the detrimental effects of administering rIL-33 shortly after alloHCT, suggesting that limiting IL-33 activity early may ameliorate GVHD (36). There has been significant progress in the development of IL-33/ST2 blocking tools. There are three major therapeutic strategies that neutralize IL-33 directly, implement soluble decoy receptors or use anti-ST2 antibodies. Etokimab, an anti-IL-33 biologic was recently published in a placebo-controlled phase 2a clinical trial in peanut allergy where the active participants had reduced Type 2 cytokines and IgE following peanut challenge (391). Astegolimab, a human IgG mAb that blocks ST2 was tested in a placebo-controlled phase 2b trial in asthma with an endpoint of reduced annual asthma exacerbation rate (AER). Astegolimab reduced AER compared to placebo and had a comparable efficacy in patients with low eosinophils (392). These clinical trials suggest that a there is a clear clinical role for neutralizing IL-33. Future studies will be needed to establish the best timing and mechanism of therapeutic delivery of regulatory IL-33 in balance with limiting the detrimental effects of IL-33 during disease, since too much IL-33 may promote pathological Type 2 or Type 1 immunity.

Appendix

mTOR signaling is necessary for ST2$^+$ Treg IL-13 production

We have previously established that IL-33 supports the expansion of ST2$^+$ Treg through the MAPK/p38 pathway (103). We have recently identified ST2$^+$ Treg are abundant producers of IL-10, yet this was IL-33-independent (102). We also determined that IL-33 stimulation of ST2$^+$ Treg combined with TCR stimulation significantly increases their secretion of IL-13 (102), yet the mechanism of IL-10 and IL-13 secretion had not been identified. To determine this, we utilized Foxp3$^+$ reporter mice to characterize the intermediate signaling pathways in cytokine production induced by IL-33 in ST2$^+$ Treg. We sorted splenic CD4$^+$ T cells based on their expression of CD25, Foxp3, and ST2, into ST2$^+$ Treg (CD4$^+$ CD25^{hi} ST2$^+$ Foxp3$^+$), and ST2$^-$ Treg (CD4$^+$ CD25^{hi} ST2$^-$ Foxp3$^+$). Anti-CD3/CD28-stimulated or anti-CD3/CD28/IL-33- stimulated ST2$^-$ Treg, we have previously shown secrete IL-10, yet less than ST2$^+$ Treg, they also secrete very little IL-13 (**Figure 10**). ST2$^+$ Treg are abundant producers of IL-10, and this is mediated by the MAPK/p38 pathways since inhibition completely obliterated IL-10 secretion and partially mediated by mTOR signaling since rapamycin reduced IL-10 secretion to levels secreted by ST2$^-$ Treg (**Figure 31**). IL-33 stimulation of ST2$^+$ Treg combined with anti-CD3/CD28-exposure significantly increases their secretion of IL-13 (**Figure 10**). IL-33-mediated IL-13 secretion by Treg is mediated by mTOR signaling since rapamycin inhibition of mTORC1 reduces IL-13 secretion down to levels secreted by ST2$^-$ Treg (**Figure 31**).

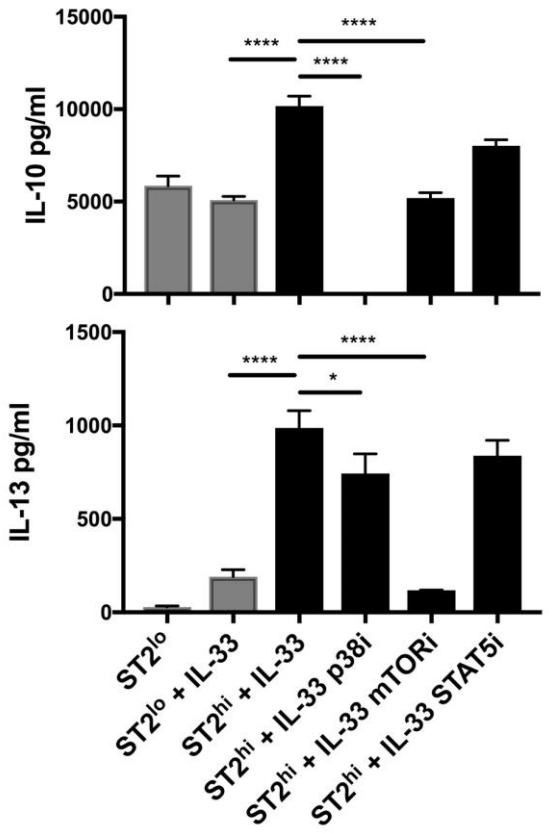

Figure 31. IL-33-mediated signaling pathways in Treg.

Assessment of cytokine secretion by ST2^{-} or ST2^{+} Foxp3^{+} CD4^{+} T cell populations from sorted CD4^{+} CD25^{+} Foxp3^{+} (RFP^{+}) ST2^{-} or ST2^{+} cells from PBS or IL-33-treated Foxp3-IRES-mRFP reporter mice after culture with or without IL-33 (20 ng/ml) and indicated inhibitors (p38-SB203580 5μM, mTOR-rapamycin 25nM, STAT5-CAS 285986-31-4 1 μM). Supernatants were harvested on day 3 of culture with anti-CD3, -CD28 and IL-2 stimulation and assessed by Cytometric Bead Array (CBA) for IL-10 and IL-13. Statistical analysis with ANOVA was used to establish significance between values indicated. *P < 0.05, **P < 0.01, ***P < 0.001, ****P < 0.0001.

A major mechanism of rapamycin is the induction and expansion of Treg cell populations (393, 394). Treatments with rapamycin following bleo induced systemic sclerosis in a mouse model results in reduced lung and skin fibrosis and attenuated levels of profibrotic cytokines (395). Liew's group determined that treatment with rapamycin significantly reduced IL-33 mediated

airway inflammation and reduced IL-13 products in BAL fluids, and secretion by ILC2s and Th2s (396). Suggesting that mTOR is a primary mediator of IL-33-induced IL-13 production.

Bibliography

1. Baekkevold ES, Roussigne M, Yamanaka T, Johansen FE, Jahnsen FL, Amalric F, et al. Molecular characterization of NF-HEV, a nuclear factor preferentially expressed in human high endothelial venules. *Am J Pathol.* 2003;163(1):69-79.

2. Schmitz J, Owyang A, Oldham E, Song Y, Murphy E, McClanahan TK, et al. IL-33, an interleukin-1-like cytokine that signals via the IL-1 receptor-related protein ST2 and induces T helper type 2-associated cytokines. *Immunity.* 2005;23(5):479-90.

3. Carriere V, Roussel L, Ortega N, Lacorre DA, Americh L, Aguilar L, et al. IL-33, the IL-1-like cytokine ligand for ST2 receptor, is a chromatin-associated nuclear factor in vivo. *Proc Natl Acad Sci U S A.* 2007;104(1):282-7.

4. Liew FY, Girard JP, and Turnquist HR. Interleukin-33 in health and disease. *Nat Rev Immunol.* 2016;16(11):676-89.

5. Cayrol C, and Girard JP. Interleukin-33 (IL-33): A nuclear cytokine from the IL-1 family. *Immunol Rev.* 2018;281(1):154-68.

6. Martin NT, and Martin MU. Interleukin 33 is a guardian of barriers and a local alarmin. *Nat Immunol.* 2016;17(2):122-31.

7. Onda H, Kasuya H, Takakura K, Hori T, Imaizumi T, Takeuchi T, et al. Identification of genes differentially expressed in canine vasospastic cerebral arteries after subarachnoid hemorrhage. *J Cereb Blood Flow Metab.* 1999;19(11):1279-88.

8. Tsuda H, Komine M, Tominaga SI, and Ohtsuki M. Identification of the promoter region of human IL-33 responsive to induction by IFNgamma. *J Dermatol Sci.* 2017;85(2):137-40.

9. Talabot-Ayer D, Calo N, Vigne S, Lamacchia C, Gabay C, and Palmer G. The mouse interleukin (Il)33 gene is expressed in a cell type- and stimulus-dependent manner from two alternative promoters. *J Leukoc Biol.* 2012;91(1):119-25.

10. Grotenboer NS, Ketelaar ME, Koppelman GH, and Nawijn MC. Decoding asthma: translating genetic variation in IL33 and IL1RL1 into disease pathophysiology. *J Allergy Clin Immunol.* 2013;131(3):856-65.

11. Gudbjartsson DF, Bjornsdottir US, Halapi E, Helgadottir A, Sulem P, Jonsdottir GM, et al. Sequence variants affecting eosinophil numbers associate with asthma and myocardial infarction. *Nat Genet.* 2009;41(3):342-7.

12. Moffatt MF, Gut IG, Demenais F, Strachan DP, Bouzigon E, Heath S, et al. A large-scale, consortium-based genomewide association study of asthma. *N Engl J Med.* 2010;363(13):1211-21.

13. Torgerson DG, Ampleford EJ, Chiu GY, Gauderman WJ, Gignoux CR, Graves PE, et al. Meta-analysis of genome-wide association studies of asthma in ethnically diverse North American populations. *Nat Genet.* 2011;43(9):887-92.

14. Smith D, Helgason H, Sulem P, Bjornsdottir US, Lim AC, Sveinbjornsson G, et al. A rare IL33 loss-of-function mutation reduces blood eosinophil counts and protects from asthma. *PLoS Genet.* 2017;13(3):e1006659.

15. Gordon ED, Simpson LJ, Rios CL, Ringel L, Lachowicz-Scroggins ME, Peters MC, et al. Alternative splicing of interleukin-33 and type 2 inflammation in asthma. *Proc Natl Acad Sci U S A.* 2016;113(31):8765-70.

16. Hardman CS, Panova V, and McKenzie AN. IL-33 citrine reporter mice reveal the temporal and spatial expression of IL-33 during allergic lung inflammation. *Eur J Immunol.* 2013;43(2):488-98.

17. Bessa J, Meyer CA, de Vera Mudry MC, Schlicht S, Smith SH, Iglesias A, et al. Altered subcellular localization of IL-33 leads to non-resolving lethal inflammation. *J Autoimmun.* 2014;55:33-41.

18. Ito R, Maruoka S, Soda K, Katano I, Kawai K, Yagoto M, et al. A humanized mouse model to study asthmatic airway inflammation via the human IL-33/IL-13 axis. *JCI Insight.* 2018;3(21).

19. Hong J, Bae S, Jhun H, Lee S, Choi J, Kang T, et al. Identification of constitutively active interleukin 33 (IL-33) splice variant. *J Biol Chem.* 2011;286(22):20078-86.

20. Tsuda H, Komine M, Karakawa M, Etoh T, Tominaga S, and Ohtsuki M. Novel splice variants of IL-33: differential expression in normal and transformed cells. *J Invest Dermatol.* 2012;132(11):2661-4.

21. Roussel L, Erard M, Cayrol C, and Girard JP. Molecular mimicry between IL-33 and KSHV for attachment to chromatin through the H2A-H2B acidic pocket. *EMBO Rep.* 2008;9(10):1006-12.

22. Garlanda C, Dinarello CA, and Mantovani A. The interleukin-1 family: back to the future. *Immunity.* 2013;39(6):1003-18.

23. Lingel A, Weiss TM, Niebuhr M, Pan B, Appleton BA, Wiesmann C, et al. Structure of IL-33 and its interaction with the ST2 and IL-1RAcP receptors--insight into heterotrimeric IL-1 signaling complexes. *Structure.* 2009;17(10):1398-410.

24. Liu X, Hammel M, He Y, Tainer JA, Jeng US, Zhang L, et al. Structural insights into the interaction of IL-33 with its receptors. *Proc Natl Acad Sci U S A.* 2013;110(37):14918-23.

25. Veerapandian B. Structure and function of interleukin-1, based on crystallographic and modeling studies. *Biophys J.* 1992;62(1):112-5.

26. Moussion C, Ortega N, and Girard JP. The IL-1-like cytokine IL-33 is constitutively expressed in the nucleus of endothelial cells and epithelial cells in vivo: a novel 'alarmin'? *PLoS One.* 2008;3(10):e3331.

27. Pichery M, Mirey E, Mercier P, Lefrancais E, Dujardin A, Ortega N, et al. Endogenous IL-33 is highly expressed in mouse epithelial barrier tissues, lymphoid organs, brain, embryos, and inflamed tissues: in situ analysis using a novel Il-33-LacZ gene trap reporter strain. *J Immunol.* 2012;188(7):3488-95.

28. Dahlgren MW, Jones SW, Cautivo KM, Dubinin A, Ortiz-Carpena JF, Farhat S, et al. Adventitial Stromal Cells Define Group 2 Innate Lymphoid Cell Tissue Niches. *Immunity.* 2019;50(3):707-22 e6.

29. Gadani SP, Walsh JT, Smirnov I, Zheng J, and Kipnis J. The glia-derived alarmin IL-33 orchestrates the immune response and promotes recovery following CNS injury. *Neuron.* 2015;85(4):703-9.

30. Kuchler AM, Pollheimer J, Balogh J, Sponheim J, Manley L, Sorensen DR, et al. Nuclear interleukin-33 is generally expressed in resting endothelium but rapidly lost upon angiogenic or proinflammatory activation. *Am J Pathol.* 2008;173(4):1229-42.

31. Nguyen PT, Dorman LC, Pan S, Vainchtein ID, Han RT, Nakao-Inoue H, et al. Microglial Remodeling of the Extracellular Matrix Promotes Synapse Plasticity. *Cell.* 2020;182(2):388-403 e15.

32. Vainchtein ID, Chin G, Cho FS, Kelley KW, Miller JG, Chien EC, et al. Astrocyte-derived interleukin-33 promotes microglial synapse engulfment and neural circuit development. *Science.* 2018;359(6381):1269-73.

33. Xi H, Katschke KJ, Jr., Li Y, Truong T, Lee WP, Diehl L, et al. IL-33 amplifies an innate immune response in the degenerating retina. *J Exp Med.* 2016;213(2):189-207.

34. Byers DE, Alexander-Brett J, Patel AC, Agapov E, Dang-Vu G, Jin X, et al. Long-term IL-33-producing epithelial progenitor cells in chronic obstructive lung disease. *J Clin Invest.* 2013;123(9):3967-82.

35. Prefontaine D, Nadigel J, Chouiali F, Audusseau S, Semlali A, Chakir J, et al. Increased IL-33 expression by epithelial cells in bronchial asthma. *J Allergy Clin Immunol.* 2010;125(3):752-4.

36. Reichenbach DK, Schwarze V, Matta BM, Tkachev V, Lieberknecht E, Liu Q, et al. The IL-33/ST2 axis augments effector T-cell responses during acute GVHD. *Blood.* 2015;125(20):3183-92.

37. Kearley J, Silver JS, Sanden C, Liu Z, Berlin AA, White N, et al. Cigarette smoke silences innate lymphoid cell function and facilitates an exacerbated type I interleukin-33-dependent response to infection. *Immunity.* 2015;42(3):566-79.

38. Yasuda K, Muto T, Kawagoe T, Matsumoto M, Sasaki Y, Matsushita K, et al. Contribution of IL-33-activated type II innate lymphoid cells to pulmonary eosinophilia in intestinal nematode-infected mice. *Proc Natl Acad Sci U S A.* 2012;109(9):3451-6.

39. Aparicio-Domingo P, Cannelle H, Buechler MB, Nguyen S, Kallert SM, Favre S, et al. Fibroblast-derived IL-33 is dispensable for lymph node homeostasis but critical for CD8 T-cell responses to acute and chronic viral infection. *Eur J Immunol.* 2021;51(1):76-90.

40. Sponheim J, Pollheimer J, Olsen T, Balogh J, Hammarstrom C, Loos T, et al. Inflammatory bowel disease-associated interleukin-33 is preferentially expressed in ulceration-associated myofibroblasts. *Am J Pathol.* 2010;177(6):2804-15.

41. Seltmann J, Werfel T, and Wittmann M. Evidence for a regulatory loop between IFN-gamma and IL-33 in skin inflammation. *Exp Dermatol.* 2013;22(2):102-7.

42. Sundlisaeter E, Edelmann RJ, Hol J, Sponheim J, Kuchler AM, Weiss M, et al. The alarmin IL-33 is a notch target in quiescent endothelial cells. *Am J Pathol.* 2012;181(3):1099-111.

43. Chang J, Xia Y, Wasserloos K, Deng M, Blose KJ, Vorp DA, et al. Cyclic stretch induced IL-33 production through HMGB1/TLR-4 signaling pathway in murine respiratory epithelial cells. *PLoS One.* 2017;12(9):e0184770.

44. Kakkar R, Hei H, Dobner S, and Lee RT. Interleukin 33 as a mechanically responsive cytokine secreted by living cells. *J Biol Chem.* 2012;287(9):6941-8.

45. Hung LY, Pastore CF, Douglas B, and Herbert DR. Myeloid-Derived IL-33 Limits the Severity of Dextran Sulfate Sodium-Induced Colitis. *Am J Pathol.* 2021;191(2):266-73.

46. Hung LY, Tanaka Y, Herbine K, Pastore C, Singh B, Ferguson A, et al. Cellular context of IL-33 expression dictates impact on anti-helminth immunity. *Sci Immunol.* 2020;5(53).

47. Stier MT, Mitra R, Nyhoff LE, Goleniewska K, Zhang J, Puccetti MV, et al. IL-33 Is a Cell-Intrinsic Regulator of Fitness during Early B Cell Development. *J Immunol.* 2019;203(6):1457-67.

48. Hatzioannou A, Banos A, Sakelaropoulos T, Fedonidis C, Vidali MS, Kohne M, et al. An intrinsic role of IL-33 in Treg cell-mediated tumor immunoevasion. *Nat Immunol.* 2020;21(1):75-85.

49. Chen WY, Hong J, Gannon J, Kakkar R, and Lee RT. Myocardial pressure overload induces systemic inflammation through endothelial cell IL-33. *Proc Natl Acad Sci U S A.* 2015;112(23):7249-54.

50. Molofsky AB, Van Gool F, Liang HE, Van Dyken SJ, Nussbaum JC, Lee J, et al. Interleukin-33 and Interferon-gamma Counter-Regulate Group 2 Innate Lymphoid Cell Activation during Immune Perturbation. *Immunity.* 2015;43(1):161-74.

51. Ali S, Mohs A, Thomas M, Klare J, Ross R, Schmitz ML, et al. The dual function cytokine IL-33 interacts with the transcription factor NF-kappaB to dampen NF-kappaB-stimulated gene transcription. *J Immunol.* 2011;187(4):1609-16.

52. Choi YS, Park JA, Kim J, Rho SS, Park H, Kim YM, et al. Nuclear IL-33 is a transcriptional regulator of NF-kappaB p65 and induces endothelial cell activation. *Biochem Biophys Res Commun.* 2012;421(2):305-11.

53. Lee EJ, So MW, Hong S, Kim YG, Yoo B, and Lee CK. Interleukin-33 acts as a transcriptional repressor and extracellular cytokine in fibroblast-like synoviocytes in patients with rheumatoid arthritis. *Cytokine.* 2016;77:35-43.

54. Ni Y, Tao L, Chen C, Song H, Li Z, Gao Y, et al. The Deubiquitinase USP17 Regulates the Stability and Nuclear Function of IL-33. *Int J Mol Sci.* 2015;16(11):27956-66.

55. Gautier V, Cayrol C, Farache D, Roga S, Monsarrat B, Burlet-Schiltz O, et al. Extracellular IL-33 cytokine, but not endogenous nuclear IL-33, regulates protein expression in endothelial cells. *Sci Rep.* 2016;6:34255.

56. Travers J, Rochman M, Miracle CE, Habel JE, Brusilovsky M, Caldwell JM, et al. Chromatin regulates IL-33 release and extracellular cytokine activity. *Nat Commun.* 2018;9(1):3244.

57. Serrels B, McGivern N, Canel M, Byron A, Johnson SC, McSorley HJ, et al. IL-33 and ST2 mediate FAK-dependent antitumor immune evasion through transcriptional networks. *Sci Signal.* 2017;10(508).

58. Griffith BGC, Upstill-Goddard R, Brunton H, Grimes GR, Biankin AV, Serrels B, et al. FAK regulates IL-33 expression by controlling chromatin accessibility at c-Jun motifs. *Sci Rep.* 2021;11(1):229.

59. Cayrol C, and Girard JP. The IL-1-like cytokine IL-33 is inactivated after maturation by caspase-1. *Proc Natl Acad Sci U S A.* 2009;106(22):9021-6.

60. Palm NW, Rosenstein RK, Yu S, Schenten DD, Florsheim E, and Medzhitov R. Bee venom phospholipase A2 induces a primary type 2 response that is dependent on the receptor ST2 and confers protective immunity. *Immunity.* 2013;39(5):976-85.

61. Rickard JA, O'Donnell JA, Evans JM, Lalaoui N, Poh AR, Rogers T, et al. RIPK1 regulates RIPK3-MLKL-driven systemic inflammation and emergency hematopoiesis. *Cell.* 2014;157(5):1175-88.

62. Rose WA, 2nd, Okragly AJ, Patel CN, and Benschop RJ. IL-33 released by alum is responsible for early cytokine production and has adjuvant properties. *Sci Rep.* 2015;5:13146.

63. Fux M, Pecaric-Petkovic T, Odermatt A, Hausmann OV, Lorentz A, Bischoff SC, et al. IL-33 is a mediator rather than a trigger of the acute allergic response in humans. *Allergy.* 2014;69(2):216-22.

64. Hristova M, Habibovic A, Veith C, Janssen-Heininger YM, Dixon AE, Geiszt M, et al. Airway epithelial dual oxidase 1 mediates allergen-induced IL-33 secretion and activation of type 2 immune responses. *J Allergy Clin Immunol.* 2016;137(5):1545-56 e11.

65. Kouzaki H, Iijima K, Kobayashi T, O'Grady SM, and Kita H. The danger signal, extracellular ATP, is a sensor for an airborne allergen and triggers IL-33 release and innate Th2-type responses. *J Immunol.* 2011;186(7):4375-87.

66. Uchida M, Anderson EL, Squillace DL, Patil N, Maniak PJ, Iijima K, et al. Oxidative stress serves as a key checkpoint for IL-33 release by airway epithelium. *Allergy.* 2017;72(10):1521-31.

67. Snelgrove RJ, Gregory LG, Peiro T, Akthar S, Campbell GA, Walker SA, et al. Alternaria-derived serine protease activity drives IL-33-mediated asthma exacerbations. *J Allergy Clin Immunol.* 2014;134(3):583-92 e6.

68. Sanada S, Hakuno D, Higgins LJ, Schreiter ER, McKenzie AN, and Lee RT. IL-33 and ST2 comprise a critical biomechanically induced and cardioprotective signaling system. *J Clin Invest.* 2007;117(6):1538-49.

69. Momota M, Nagayama M, Okude H, Ishii KJ, Ori D, Kawasaki T, et al. The Ca(2+)-dependent pathway contributes to changes in the subcellular localization and extracellular release of interleukin-33. *Biochem Biophys Res Commun.* 2020;530(4):699-705.

70. Lefrancais E, Roga S, Gautier V, Gonzalez-de-Peredo A, Monsarrat B, Girard JP, et al. IL-33 is processed into mature bioactive forms by neutrophil elastase and cathepsin G. *Proc Natl Acad Sci U S A.* 2012;109(5):1673-8.

71. Lefrancais E, Duval A, Mirey E, Roga S, Espinosa E, Cayrol C, et al. Central domain of IL-33 is cleaved by mast cell proteases for potent activation of group-2 innate lymphoid cells. *Proc Natl Acad Sci U S A.* 2014;111(43):15502-7.

72. Scott IC, Majithiya JB, Sanden C, Thornton P, Sanders PN, Moore T, et al. Interleukin-33 is activated by allergen- and necrosis-associated proteolytic activities to regulate its alarmin activity during epithelial damage. *Sci Rep.* 2018;8(1):3363.

73. Cohen ES, Scott IC, Majithiya JB, Rapley L, Kemp BP, England E, et al. Oxidation of the alarmin IL-33 regulates ST2-dependent inflammation. *Nat Commun.* 2015;6:8327.

74. Mohapatra A, Van Dyken SJ, Schneider C, Nussbaum JC, Liang HE, and Locksley RM. Group 2 innate lymphoid cells utilize the IRF4-IL-9 module to coordinate epithelial cell maintenance of lung homeostasis. *Mucosal Immunol.* 2016;9(1):275-86.

75. Ali S, Nguyen DQ, Falk W, and Martin MU. Caspase 3 inactivates biologically active full length interleukin-33 as a classical cytokine but does not prohibit nuclear translocation. *Biochem Biophys Res Commun.* 2010;391(3):1512-6.

76. Luthi AU, Cullen SP, McNeela EA, Duriez PJ, Afonina IS, Sheridan C, et al. Suppression of interleukin-33 bioactivity through proteolysis by apoptotic caspases. *Immunity.* 2009;31(1):84-98.

77. Kim LK, Morita R, Kobayashi Y, Eisenbarth SC, Lee CG, Elias J, et al. AMCase is a crucial regulator of type 2 immune responses to inhaled house dust mites. *Proc Natl Acad Sci U S A.* 2015;112(22):E2891-9.

78. Lamkanfi M, Kanneganti TD, Van Damme P, Vanden Berghe T, Vanoverberghe I, Vandekerckhove J, et al. Targeted peptidecentric proteomics reveals caspase-7 as a substrate of the caspase-1 inflammasomes. *Mol Cell Proteomics.* 2008;7(12):2350-63.

79. Bandara G, Beaven MA, Olivera A, Gilfillan AM, and Metcalfe DD. Activated mast cells synthesize and release soluble ST2-a decoy receptor for IL-33. *Eur J Immunol.* 2015;45(11):3034-44.

80. Hayakawa H, Hayakawa M, Kume A, and Tominaga S. Soluble ST2 blocks interleukin-33 signaling in allergic airway inflammation. *J Biol Chem.* 2007;282(36):26369-80.

81. Billiar IM, Guardado J, Abdul-Malak O, Vodovotz Y, Billiar TR, and Namas RA. Elevations in Circulating sST2 Levels Are Associated With In-Hospital Mortality and Adverse Clinical Outcomes After Blunt Trauma. *J Surg Res.* 2019;244:23-33.

82. Lipsky BP, Toy DY, Swart DA, Smithgall MD, and Smith D. Deletion of the ST2 proximal promoter disrupts fibroblast-specific expression but does not reduce the amount of soluble ST2 in circulation. *Eur J Immunol.* 2012;42(7):1863-9.

83. Xu J, Guardado J, Hoffman R, Xu H, Namas R, Vodovotz Y, et al. IL33-mediated ILC2 activation and neutrophil IL5 production in the lung response after severe trauma: A reverse translation study from a human cohort to a mouse trauma model. *PLoS Med.* 2017;14(7):e1002365.

84. Li T, Zhang Z, Bartolacci JG, Dwyer GK, Liu Q, Mathews LR, et al. Graft IL-33 regulates infiltrating macrophages to protect against chronic rejection. *J Clin Invest.* 2020;130(10):5397-412.

85. Kumar S, Tzimas MN, Griswold DE, and Young PR. Expression of ST2, an interleukin-1 receptor homologue, is induced by proinflammatory stimuli. *Biochem Biophys Res Commun.* 1997;235(3):474-8.

86. Mildner M, Storka A, Lichtenauer M, Mlitz V, Ghannadan M, Hoetzenecker K, et al. Primary sources and immunological prerequisites for sST2 secretion in humans. *Cardiovasc Res.* 2010;87(4):769-77.

87. Zhao J, Wei J, Mialki RK, Mallampalli DF, Chen BB, Coon T, et al. F-box protein FBXL19-mediated ubiquitination and degradation of the receptor for IL-33 limits pulmonary inflammation. *Nat Immunol.* 2012;13(7):651-8.

88. Bulek K, Swaidani S, Qin J, Lu Y, Gulen MF, Herjan T, et al. The essential role of single Ig IL-1 receptor-related molecule/Toll IL-1R8 in regulation of Th2 immune response. *J Immunol.* 2009;182(5):2601-9.

89. Humphreys NE, Xu D, Hepworth MR, Liew FY, and Grencis RK. IL-33, a potent inducer of adaptive immunity to intestinal nematodes. *J Immunol.* 2008;180(4):2443-9.

90. Kondo Y, Yoshimoto T, Yasuda K, Futatsugi-Yumikura S, Morimoto M, Hayashi N, et al. Administration of IL-33 induces airway hyperresponsiveness and goblet cell hyperplasia in the lungs in the absence of adaptive immune system. *Int Immunol.* 2008;20(6):791-800.

91. Miller AM, Xu D, Asquith DL, Denby L, Li Y, Sattar N, et al. IL-33 reduces the development of atherosclerosis. *J Exp Med.* 2008;205(2):339-46.

92. Alvarez F, Fritz JH, and Piccirillo CA. Pleiotropic Effects of IL-33 on CD4(+) T Cell Differentiation and Effector Functions. *Front Immunol.* 2019;10:522.

93. Griesenauer B, and Paczesny S. The ST2/IL-33 Axis in Immune Cells during Inflammatory Diseases. *Front Immunol.* 2017;8:475.

94. Komai-Koma M, Xu D, Li Y, McKenzie AN, McInnes IB, and Liew FY. IL-33 is a chemoattractant for human Th2 cells. *Eur J Immunol.* 2007;37(10):2779-86.

95. Lohning M, Stroehmann A, Coyle AJ, Grogan JL, Lin S, Gutierrez-Ramos JC, et al. T1/ST2 is preferentially expressed on murine Th2 cells, independent of interleukin 4, interleukin 5, and interleukin 10, and important for Th2 effector function. *Proc Natl Acad Sci U S A.* 1998;95(12):6930-5.

96. Guo L, Wei G, Zhu J, Liao W, Leonard WJ, Zhao K, et al. IL-1 family members and STAT activators induce cytokine production by Th2, Th17, and Th1 cells. *Proc Natl Acad Sci U S A.* 2009;106(32):13463-8.

97. Xu D, Chan WL, Leung BP, Huang F, Wheeler R, Piedrafita D, et al. Selective expression of a stable cell surface molecule on type 2 but not type 1 helper T cells. *J Exp Med.* 1998;187(5):787-94.

98. Siede J, Frohlich A, Datsi A, Hegazy AN, Varga DV, Holecska V, et al. IL-33 Receptor-Expressing Regulatory T Cells Are Highly Activated, Th2 Biased and Suppress CD4 T Cell Proliferation through IL-10 and TGFbeta Release. *PLoS One.* 2016;11(8):e0161507.

99. Schiering C, Krausgruber T, Chomka A, Frohlich A, Adelmann K, Wohlfert EA, et al. The alarmin IL-33 promotes regulatory T-cell function in the intestine. *Nature.* 2014;513(7519):564-8.

100. Arpaia N, Green JA, Moltedo B, Arvey A, Hemmers S, Yuan S, et al. A Distinct Function of Regulatory T Cells in Tissue Protection. *Cell.* 2015;162(5):1078-89.

101. Burzyn D, Kuswanto W, Kolodin D, Shadrach JL, Cerletti M, Jang Y, et al. A special population of regulatory T cells potentiates muscle repair. *Cell.* 2013;155(6):1282-95.

102. Liu Q, Dwyer GK, Zhao Y, Li H, Mathews LR, Chakka AB, et al. IL-33-mediated IL-13 secretion by ST2+ Tregs controls inflammation after lung injury. *JCI Insight.* 2019;4(6).

103. Matta BM, Reichenbach DK, Zhang X, Mathews L, Koehn BH, Dwyer GK, et al. Peri-alloHCT IL-33 administration expands recipient T-regulatory cells that protect mice against acute GVHD. *Blood.* 2016;128(3):427-39.

104. Turnquist HR, Zhao Z, Rosborough BR, Liu Q, Castellaneta A, Isse K, et al. IL-33 expands suppressive CD11b+ Gr-1(int) and regulatory T cells, including ST2L+ Foxp3+ cells, and mediates regulatory T cell-dependent promotion of cardiac allograft survival. *J Immunol.* 2011;187(9):4598-610.

105. Baumann C, Bonilla WV, Frohlich A, Helmstetter C, Peine M, Hegazy AN, et al. T-bet- and STAT4-dependent IL-33 receptor expression directly promotes antiviral Th1 cell responses. *Proc Natl Acad Sci U S A.* 2015;112(13):4056-61.

106. Bonilla WV, Frohlich A, Senn K, Kallert S, Fernandez M, Johnson S, et al. The alarmin interleukin-33 drives protective antiviral CD8(+) T cell responses. *Science.* 2012;335(6071):984-9.

107. Yang Q, Li G, Zhu Y, Liu L, Chen E, Turnquist H, et al. IL-33 synergizes with TCR and IL-12 signaling to promote the effector function of CD8+ T cells. *Eur J Immunol.* 2011;41(11):3351-60.

108. Hoyler T, Klose CS, Souabni A, Turqueti-Neves A, Pfeifer D, Rawlins EL, et al. The transcription factor GATA-3 controls cell fate and maintenance of type 2 innate lymphoid cells. *Immunity.* 2012;37(4):634-48.

109. Mjosberg J, Bernink J, Golebski K, Karrich JJ, Peters CP, Blom B, et al. The transcription factor GATA3 is essential for the function of human type 2 innate lymphoid cells. *Immunity.* 2012;37(4):649-59.

110. Moro K, Yamada T, Tanabe M, Takeuchi T, Ikawa T, Kawamoto H, et al. Innate production of T(H)2 cytokines by adipose tissue-associated c-Kit(+)Sca-1(+) lymphoid cells. *Nature.* 2010;463(7280):540-4.

111. Neill DR, Wong SH, Bellosi A, Flynn RJ, Daly M, Langford TK, et al. Nuocytes represent a new innate effector leukocyte that mediates type-2 immunity. *Nature.* 2010;464(7293):1367-70.

112. Price AE, Liang HE, Sullivan BM, Reinhardt RL, Eisley CJ, Erle DJ, et al. Systemically dispersed innate IL-13-expressing cells in type 2 immunity. *Proc Natl Acad Sci U S A.* 2010;107(25):11489-94.

113. Yagi R, Zhong C, Northrup DL, Yu F, Bouladoux N, Spencer S, et al. The transcription factor GATA3 is critical for the development of all IL-7Ralpha-expressing innate lymphoid cells. *Immunity.* 2014;40(3):378-88.

114. Spits H, Artis D, Colonna M, Diefenbach A, Di Santo JP, Eberl G, et al. Innate lymphoid cells--a proposal for uniform nomenclature. *Nat Rev Immunol.* 2013;13(2):145-9.

115. Oboki K, Ohno T, Kajiwara N, Arae K, Morita H, Ishii A, et al. IL-33 is a crucial amplifier of innate rather than acquired immunity. *Proc Natl Acad Sci U S A.* 2010;107(43):18581-6.

116. He Z, Song J, Hua J, Yang M, Ma Y, Yu T, et al. Mast cells are essential intermediaries in regulating IL-33/ST2 signaling for an immune network favorable to mucosal healing in experimentally inflamed colons. *Cell Death Dis.* 2018;9(12):1173.

117. Wang JX, Kaieda S, Ameri S, Fishgal N, Dwyer D, Dellinger A, et al. IL-33/ST2 axis promotes mast cell survival via BCLXL. *Proc Natl Acad Sci U S A.* 2014;111(28):10281-6.

118. Pecaric-Petkovic T, Didichenko SA, Kaempfer S, Spiegl N, and Dahinden CA. Human basophils and eosinophils are the direct target leukocytes of the novel IL-1 family member IL-33. *Blood.* 2009;113(7):1526-34.

119. Cohen M, Giladi A, Gorki AD, Solodkin DG, Zada M, Hladik A, et al. Lung Single-Cell Signaling Interaction Map Reveals Basophil Role in Macrophage Imprinting. *Cell.* 2018;175(4):1031-44 e18.

120. Joshi AD, Oak SR, Hartigan AJ, Finn WG, Kunkel SL, Duffy KE, et al. Interleukin-33 contributes to both M1 and M2 chemokine marker expression in human macrophages. *BMC Immunol.* 2010;11:52.

121. Kurowska-Stolarska M, Stolarski B, Kewin P, Murphy G, Corrigan CJ, Ying S, et al. IL-33 amplifies the polarization of alternatively activated macrophages that contribute to airway inflammation. *J Immunol.* 2009;183(10):6469-77.

122. Suzukawa M, Koketsu R, Iikura M, Nakae S, Matsumoto K, Nagase H, et al. Interleukin-33 enhances adhesion, CD11b expression and survival in human eosinophils. *Lab Invest.* 2008;88(11):1245-53.

123. Wang Y, Yang Y, Wang M, Wang S, Jeong JM, Xu L, et al. Eosinophils attenuate hepatic ischemia-reperfusion injury in mice through ST2-dependent IL-13 production. *Sci Transl Med.* 2021;13(579).

124. Matta BM, Lott JM, Mathews LR, Liu Q, Rosborough BR, Blazar BR, et al. IL-33 is an unconventional Alarmin that stimulates IL-2 secretion by dendritic cells to selectively expand IL-33R/ST2+ regulatory T cells. *J Immunol.* 2014;193(8):4010-20.

125. Monticelli LA, Osborne LC, Noti M, Tran SV, Zaiss DM, and Artis D. IL-33 promotes an innate immune pathway of intestinal tissue protection dependent on amphiregulin-EGFR interactions. *Proc Natl Acad Sci U S A.* 2015;112(34):10762-7.

126. Lu Y, Basatemur G, Scott IC, Chiarugi D, Clement M, Harrison J, et al. Interleukin-33 Signaling Controls the Development of Iron-Recycling Macrophages. *Immunity.* 2020;52(5):782-93 e5.

127. Grencis RK. Immunity to helminths: resistance, regulation, and susceptibility to gastrointestinal nematodes. *Annu Rev Immunol.* 2015;33:201-25.

128. Hung LY, Lewkowich IP, Dawson LA, Downey J, Yang Y, Smith DE, et al. IL-33 drives biphasic IL-13 production for noncanonical Type 2 immunity against hookworms. *Proc Natl Acad Sci U S A.* 2013;110(1):282-7.

129. Townsend MJ, Fallon PG, Matthews DJ, Jolin HE, and McKenzie AN. T1/ST2-deficient mice demonstrate the importance of T1/ST2 in developing primary T helper cell type 2 responses. *J Exp Med.* 2000;191(6):1069-76.

130. Wilson S, Jones FM, Fofana HK, Landoure A, Kimani G, Mwatha JK, et al. A late IL-33 response after exposure to Schistosoma haematobium antigen is associated with an up-regulation of IL-13 in human eosinophils. *Parasite Immunol.* 2013;35(7-8):224-8.

131. Le HT, Tran VG, Kim W, Kim J, Cho HR, and Kwon B. IL-33 priming regulates multiple steps of the neutrophil-mediated anti-Candida albicans response by modulating TLR and dectin-1 signals. *J Immunol.* 2012;189(1):287-95.

132. Tran VG, Kim HJ, Kim J, Kang SW, Moon UJ, Cho HR, et al. IL-33 Enhances Host Tolerance to Candida albicans Kidney Infections through Induction of IL-13 Production by CD4+ T Cells. *J Immunol.* 2015;194(10):4871-9.

133. Rostan O, Gangneux JP, Piquet-Pellorce C, Manuel C, McKenzie AN, Guiguen C, et al. The IL-33/ST2 axis is associated with human visceral leishmaniasis and suppresses Th1 responses in the livers of BALB/c mice infected with Leishmania donovani. *mBio.* 2013;4(5):e00383-13.

134. Lamberet A, Rostan O, Dion S, Jan A, Guegan H, Manuel C, et al. IL-33/ST2 axis is involved in disease progression in the spleen during Leishmania donovani infection. *Parasit Vectors.* 2020;13(1):320.

135. Baumann C, Frohlich A, Brunner TM, Holecska V, Pinschewer DD, and Lohning M. Memory CD8(+) T Cell Protection From Viral Reinfection Depends on Interleukin-33 Alarmin Signals. *Front Immunol.* 2019;10:1833.

136. McLaren JE, Clement M, Marsden M, Miners KL, Llewellyn-Lacey S, Grant EJ, et al. IL-33 Augments Virus-Specific Memory T Cell Inflation and Potentiates the Efficacy of an Attenuated Cytomegalovirus-Based Vaccine. *J Immunol.* 2019;202(3):943-55.

137. Nabekura T, Girard JP, and Lanier LL. IL-33 receptor ST2 amplifies the expansion of NK cells and enhances host defense during mouse cytomegalovirus infection. *J Immunol.* 2015;194(12):5948-52.

138. Rood JE, Rao S, Paessler M, Kreiger PA, Chu N, Stelekati E, et al. ST2 contributes to T-cell hyperactivation and fatal hemophagocytic lymphohistiocytosis in mice. *Blood.* 2016;127(4):426-35.

139. Bourgeois E, Van LP, Samson M, Diem S, Barra A, Roga S, et al. The pro-Th2 cytokine IL-33 directly interacts with invariant NKT and NK cells to induce IFN-gamma production. *Eur J Immunol.* 2009;39(4):1046-55.

140. Smithgall MD, Comeau MR, Yoon BR, Kaufman D, Armitage R, and Smith DE. IL-33 amplifies both Th1- and Th2-type responses through its activity on human basophils, allergen-reactive Th2 cells, iNKT and NK cells. *Int Immunol.* 2008;20(8):1019-30.

141. Mueller SN, and Rouse BT. Immune responses to viruses. *Clinical Immunology.* 2008:421-31.

142. Acton SE, Farrugia AJ, Astarita JL, Mourao-Sa D, Jenkins RP, Nye E, et al. Dendritic cells control fibroblastic reticular network tension and lymph node expansion. *Nature.* 2014;514(7523):498-502.

143. Flaczyk A, Duerr CU, Shourian M, Lafferty EI, Fritz JH, and Qureshi ST. IL-33 signaling regulates innate and adaptive immunity to Cryptococcus neoformans. *J Immunol.* 2013;191(5):2503-13.

144. Piehler D, Eschke M, Schulze B, Protschka M, Muller U, Grahnert A, et al. The IL-33 receptor (ST2) regulates early IL-13 production in fungus-induced allergic airway inflammation. *Mucosal Immunol.* 2016;9(4):937-49.

145. Piehler D, Grahnert A, Eschke M, Richter T, Kohler G, Stenzel W, et al. T1/ST2 promotes T helper 2 cell activation and polyfunctionality in bronchopulmonary mycosis. *Mucosal Immunol.* 2013;6(2):405-14.

146. Alvarez F, Istomine R, Shourian M, Pavey N, Al-Aubodah TA, Qureshi S, et al. The alarmins IL-1 and IL-33 differentially regulate the functional specialisation of Foxp3(+) regulatory T cells during mucosal inflammation. *Mucosal Immunol.* 2019;12(3):746-60.

147. Palmieri V, Ebel JF, Ngo Thi Phuong N, Klopfleisch R, Vu VP, Adamczyk A, et al. Interleukin-33 signaling exacerbates experimental infectious colitis by enhancing gut permeability and inhibiting protective Th17 immunity. *Mucosal Immunol.* 2021;14(4):923-36.

148. Alves-Filho JC, Sonego F, Souto FO, Freitas A, Verri WA, Jr., Auxiliadora-Martins M, et al. Interleukin-33 attenuates sepsis by enhancing neutrophil influx to the site of infection. *Nat Med.* 2010;16(6):708-12.

149. Brunner M, Krenn C, Roth G, Moser B, Dworschak M, Jensen-Jarolim E, et al. Increased levels of soluble ST2 protein and IgG1 production in patients with sepsis and trauma. *Intensive Care Med.* 2004;30(7):1468-73.

150. Cekmez F, Fidanci MK, Ayar G, Saldir M, Karaoglu A, Gunduz RC, et al. Diagnostic Value of Upar, IL-33, and ST2 Levels in Childhood Sepsis. *Clin Lab.* 2016;62(5):751-5.

151. Hoogerwerf JJ, Tanck MW, van Zoelen MA, Wittebole X, Laterre PF, and van der Poll T. Soluble ST2 plasma concentrations predict mortality in severe sepsis. *Intensive Care Med.* 2010;36(4):630-7.

152. Morrow KN, Coopersmith CM, and Ford ML. IL-17, IL-27, and IL-33: A Novel Axis Linked to Immunological Dysfunction During Sepsis. *Front Immunol.* 2019;10:1982.

153. Nascimento DC, Melo PH, Pineros AR, Ferreira RG, Colon DF, Donate PB, et al. IL-33 contributes to sepsis-induced long-term immunosuppression by expanding the regulatory T cell population. *Nat Commun.* 2017;8:14919.

154. Li C, Li H, Jiang Z, Zhang T, Wang Y, Li Z, et al. Interleukin-33 increases antibacterial defense by activation of inducible nitric oxide synthase in skin. *PLoS Pathog.* 2014;10(2):e1003918.

155. Yin H, Li X, Hu S, Liu T, Yuan B, Ni Q, et al. IL-33 promotes Staphylococcus aureus-infected wound healing in mice. *Int Immunopharmacol.* 2013;17(2):432-8.

156. Matute-Bello G, Frevert CW, and Martin TR. Animal models of acute lung injury. *Am J Physiol Lung Cell Mol Physiol.* 2008;295(3):L379-99.

157. Ashbaugh DG, Bigelow DB, Petty TL, and Levine BE. Acute respiratory distress in adults. *Lancet.* 1967;2(7511):319-23.

158. Ware LB, and Matthay MA. The acute respiratory distress syndrome. *N Engl J Med.* 2000;342(18):1334-49.

159. Hudson LD, Milberg JA, Anardi D, and Maunder RJ. Clinical risks for development of the acute respiratory distress syndrome. *Am J Respir Crit Care Med.* 1995;151(2 Pt 1):293-301.

160. Pepe PE, Potkin RT, Reus DH, Hudson LD, and Carrico CJ. Clinical predictors of the adult respiratory distress syndrome. *Am J Surg.* 1982;144(1):124-30.

161. Pittet JF, Mackersie RC, Martin TR, and Matthay MA. Biological markers of acute lung injury: prognostic and pathogenetic significance. *Am J Respir Crit Care Med.* 1997;155(4):1187-205.

162. Moore BB, and Hogaboam CM. Murine models of pulmonary fibrosis. *Am J Physiol Lung Cell Mol Physiol.* 2008;294(2):L152-60.

163. Cavarra E, Carraro F, Fineschi S, Naldini A, Bartalesi B, Pucci A, et al. Early response to bleomycin is characterized by different cytokine and cytokine receptor profiles in lungs. *Am J Physiol Lung Cell Mol Physiol.* 2004;287(6):L1186-92.

164. Shen AS, Haslett C, Feldsien DC, Henson PM, and Cherniack RM. The intensity of chronic lung inflammation and fibrosis after bleomycin is directly related to the severity of acute injury. *Am Rev Respir Dis.* 1988;137(3):564-71.

165. Luzina IG, Kopach P, Lockatell V, Kang PH, Nagarsekar A, Burke AP, et al. Interleukin-33 potentiates bleomycin-induced lung injury. *Am J Respir Cell Mol Biol.* 2013;49(6):999-1008.

166. Hendrickson CM, and Matthay MA. Viral pathogens and acute lung injury: investigations inspired by the SARS epidemic and the 2009 H1N1 influenza pandemic. *Semin Respir Crit Care Med.* 2013;34(4):475-86.

167. Amato MB, Barbas CS, Medeiros DM, Magaldi RB, Schettino GP, Lorenzi-Filho G, et al. Effect of a protective-ventilation strategy on mortality in the acute respiratory distress syndrome. *N Engl J Med.* 1998;338(6):347-54.

168. Acute Respiratory Distress Syndrome N, Brower RG, Matthay MA, Morris A, Schoenfeld D, Thompson BT, et al. Ventilation with lower tidal volumes as compared with traditional tidal volumes for acute lung injury and the acute respiratory distress syndrome. *N Engl J Med.* 2000;342(18):1301-8.

169. Girard TD, and Bernard GR. Mechanical ventilation in ARDS: a state-of-the-art review. *Chest.* 2007;131(3):921-9.

170. Anderson BE, McNiff J, Yan J, Doyle H, Mamula M, Shlomchik MJ, et al. Memory CD4+ T cells do not induce graft-versus-host disease. *J Clin Invest.* 2003;112(1):101-8.

171. Zeiser R, and Blazar BR. Acute Graft-versus-Host Disease — Biologic Process, Prevention, and Therapy. *New England Journal of Medicine.* 2017;377(22):2167-79.

172. Bayraktar UD, de Lima M, Saliba RM, Maloy M, Castro-Malaspina HR, Chen J, et al. Ex vivo T cell-depleted versus unmodified allografts in patients with acute myeloid leukemia in first complete remission. *Biol Blood Marrow Transplant.* 2013;19(6):898-903.

173. Bleakley M, Heimfeld S, Loeb KR, Jones LA, Chaney C, Seropian S, et al. Outcomes of acute leukemia patients transplanted with naive T cell-depleted stem cell grafts. *J Clin Invest.* 2015;125(7):2677-89.

174. Klein OR, Buddenbaum J, Tucker N, Chen AR, Gamper CJ, Loeb D, et al. Nonmyeloablative Haploidentical Bone Marrow Transplantation with Post-Transplantation Cyclophosphamide for Pediatric and Young Adult Patients with High-Risk Hematologic Malignancies. *Biol Blood Marrow Transplant.* 2017;23(2):325-32.

175. Busque S, Scandling JD, Lowsky R, Shizuru J, Jensen K, Waters J, et al. Mixed chimerism and acceptance of kidney transplants after immunosuppressive drug withdrawal. *Sci Transl Med.* 2020;12(528).

176. Matte-Martone C, Liu J, Zhou M, Chikina M, Green DR, Harty JT, et al. Differential requirements for myeloid leukemia IFN-gamma conditioning determine graft-versus-leukemia resistance and sensitivity. *J Clin Invest.* 2017;127(7):2765-76.

177. Li H, Matte-Martone C, Tan HS, Venkatesan S, McNiff J, Demetris AJ, et al. Graft-versus-host disease is independent of innate signaling pathways triggered by pathogens in host hematopoietic cells. *J Immunol.* 2011;186(1):230-41.

178. Markey KA, MacDonald KP, and Hill GR. The biology of graft-versus-host disease: experimental systems instructing clinical practice. *Blood.* 2014;124(3):354-62.

179. MacDonald KP, Shlomchik WD, and Reddy P. Biology of graft-versus-host responses: recent insights. *Biol Blood Marrow Transplant.* 2013;19(1 Suppl):S10-4.

180. Shlomchik WD. Graft-versus-host disease. *Nat Rev Immunol.* 2007;7(5):340-52.

181. Lazarevic V, Glimcher LH, and Lord GM. T-bet: a bridge between innate and adaptive immunity. *Nat Rev Immunol.* 2013;13(11):777-89.

182. Fu J, Wang D, Yu Y, Heinrichs J, Wu Y, Schutt S, et al. T-bet is critical for the development of acute graft-versus-host disease through controlling T cell differentiation and function. *J Immunol.* 2015;194(1):388-97.

183. Lord GM, Rao RM, Choe H, Sullivan BM, Lichtman AH, Luscinskas FW, et al. T-bet is required for optimal proinflammatory CD4+ T-cell trafficking. *Blood.* 2005;106(10):3432-9.

184. Pidala J, Beato F, Kim J, Betts B, Jim H, Sagatys E, et al. In vivo IL-12/IL-23p40 neutralization blocks Th1/Th17 response after allogeneic hematopoietic cell transplantation. *Haematologica.* 2018;103(3):531-9.

185. Hartwell MJ, Ozbek U, Holler E, Renteria AS, Major-Monfried H, Reddy P, et al. An early-biomarker algorithm predicts lethal graft-versus-host disease and survival. *JCI Insight.* 2017;2(3):e89798.

186. Ponce DM, Hilden P, Mumaw C, Devlin SM, Lubin M, Giralt S, et al. High day 28 ST2 levels predict for acute graft-versus-host disease and transplant-related mortality after cord blood transplantation. *Blood.* 2015;125(1):199-205.

187. Vander Lugt MT, Braun TM, Hanash S, Ritz J, Ho VT, Antin JH, et al. ST2 as a marker for risk of therapy-resistant graft-versus-host disease and death. *N Engl J Med.* 2013;369(6):529-39.

188. Griesenauer B, Jiang H, Yang J, Zhang J, Ramadan AM, Egbosiuba J, et al. ST2/MyD88 Deficiency Protects Mice against Acute Graft-versus-Host Disease and Spares Regulatory T Cells. *J Immunol.* 2019;202(10):3053-64.

189. Matsuoka S, Hashimoto D, Kadowaki M, Ohigashi H, Hayase E, Yokoyama E, et al. Myeloid differentiation factor 88 signaling in donor T cells accelerates graft-versus-host disease. *Haematologica.* 2020;105(1):226-34.

190. Beers MF, and Morrisey EE. The three R's of lung health and disease: repair, remodeling, and regeneration. *J Clin Invest.* 2011;121(6):2065-73.

191. Lechner AJ, Driver IH, Lee J, Conroy CM, Nagle A, Locksley RM, et al. Recruited Monocytes and Type 2 Immunity Promote Lung Regeneration following Pneumonectomy. *Cell Stem Cell.* 2017;21(1):120-34 e7.

192. Dagher R, Copenhaver AM, Besnard V, Berlin A, Hamidi F, Maret M, et al. IL-33-ST2 axis regulates myeloid cell differentiation and activation enabling effective club cell regeneration. *Nat Commun.* 2020;11(1):4786.

193. Lai D, Tang J, Chen L, Fan EK, Scott MJ, Li Y, et al. Group 2 innate lymphoid cells protect lung endothelial cells from pyroptosis in sepsis. *Cell Death Dis.* 2018;9(3):369.

194. Mahapatro M, Foersch S, Hefele M, He GW, Giner-Ventura E, McHedlidze T, et al. Programming of Intestinal Epithelial Differentiation by IL-33 Derived from Pericryptal Fibroblasts in Response to Systemic Infection. *Cell Rep.* 2016;15(8):1743-56.

195. Sun M, He C, Wu W, Zhou G, Liu F, Cong Y, et al. Hypoxia inducible factor-1alpha-induced interleukin-33 expression in intestinal epithelia contributes to mucosal homeostasis in inflammatory bowel disease. *Clin Exp Immunol.* 2017;187(3):428-40.

196. Waddell A, Vallance JE, Hummel A, Alenghat T, and Rosen MJ. IL-33 Induces Murine Intestinal Goblet Cell Differentiation Indirectly via Innate Lymphoid Cell IL-13 Secretion. *J Immunol.* 2019;202(2):598-607.

197. Sattler S, Ling GS, Xu D, Hussaarts L, Romaine A, Zhao H, et al. IL-10-producing regulatory B cells induced by IL-33 (Breg(IL-33)) effectively attenuate mucosal inflammatory responses in the gut. *J Autoimmun.* 2014;50:107-22.

198. Lopetuso LR, De Salvo C, Pastorelli L, Rana N, Senkfor HN, Petito V, et al. IL-33 promotes recovery from acute colitis by inducing miR-320 to stimulate epithelial restitution and repair. *Proc Natl Acad Sci U S A.* 2018;115(40):E9362-E70.

199. Zaiss DMW, Gause WC, Osborne LC, and Artis D. Emerging functions of amphiregulin in orchestrating immunity, inflammation, and tissue repair. *Immunity.* 2015;42(2):216-26.

200. Matthay MA, Ware LB, and Zimmerman GA. The acute respiratory distress syndrome. *J Clin Invest.* 2012;122(8):2731-40.

201. Wheeler AP, and Bernard GR. Acute lung injury and the acute respiratory distress syndrome: a clinical review. *Lancet.* 2007;369(9572):1553-64.

202. Bellani G, Laffey JG, Pham T, Fan E, Brochard L, Esteban A, et al. Epidemiology, Patterns of Care, and Mortality for Patients With Acute Respiratory Distress Syndrome in Intensive Care Units in 50 Countries. *JAMA.* 2016;315(8):788-800.

203. Bauer TT, Monton C, Torres A, Cabello H, Fillela X, Maldonado A, et al. Comparison of systemic cytokine levels in patients with acute respiratory distress syndrome, severe pneumonia, and controls. *Thorax.* 2000;55(1):46-52.

204. Aggarwal NR, King LS, and D'Alessio FR. Diverse macrophage populations mediate acute lung inflammation and resolution. *Am J Physiol Lung Cell Mol Physiol.* 2014;306(8):L709-25.

205. Zemans RL, and Matthay MA. What drives neutrophils to the alveoli in ARDS? *Thorax.* 2017;72(1):1-3.

206. Thompson BT, Chambers RC, and Liu KD. Acute Respiratory Distress Syndrome. *N Engl J Med.* 2017;377(19):1904-5.

207. McAuley DF, Laffey JG, O'Kane CM, Perkins GD, Mullan B, Trinder TJ, et al. Simvastatin in the acute respiratory distress syndrome. *N Engl J Med.* 2014;371(18):1695-703.

208. National Heart L, Blood Institute ACTN, Truwit JD, Bernard GR, Steingrub J, Matthay MA, et al. Rosuvastatin for sepsis-associated acute respiratory distress syndrome. *N Engl J Med.* 2014;370(23):2191-200.

209. Ferguson ND, Cook DJ, Guyatt GH, Mehta S, Hand L, Austin P, et al. High-frequency oscillation in early acute respiratory distress syndrome. *N Engl J Med.* 2013;368(9):795-805.

210. Young D, Lamb SE, Shah S, MacKenzie I, Tunnicliffe W, Lall R, et al. High-frequency oscillation for acute respiratory distress syndrome. *N Engl J Med.* 2013;368(9):806-13.

211. Spragg RG, Lewis JF, Walmrath HD, Johannigman J, Bellingan G, Laterre PF, et al. Effect of recombinant surfactant protein C-based surfactant on the acute respiratory distress syndrome. *N Engl J Med.* 2004;351(9):884-92.

212. Paine R, 3rd, Standiford TJ, Dechert RE, Moss M, Martin GS, Rosenberg AL, et al. A randomized trial of recombinant human granulocyte-macrophage colony stimulating factor for patients with acute lung injury. *Critical care medicine.* 2012;40(1):90-7.

213. Steinberg KP, Hudson LD, Goodman RB, Hough CL, Lanken PN, Hyzy R, et al. Efficacy and safety of corticosteroids for persistent acute respiratory distress syndrome. *N Engl J Med.* 2006;354(16):1671-84.

214. Bernard GR, Luce JM, Sprung CL, Rinaldo JE, Tate RM, Sibbald WJ, et al. High-dose corticosteroids in patients with the adult respiratory distress syndrome. *N Engl J Med.* 1987;317(25):1565-70.

215. Bernard GR, Wheeler AP, Arons MM, Morris PE, Paz HL, Russell JA, et al. A trial of antioxidants N-acetylcysteine and procysteine in ARDS. The Antioxidant in ARDS Study Group. *Chest.* 1997;112(1):164-72.

216. Fan E, Brodie D, and Slutsky AS. Acute Respiratory Distress Syndrome: Advances in Diagnosis and Treatment. *JAMA.* 2018;319(7):698-710.

217. Tremblay L, Valenza F, Ribeiro SP, Li J, and Slutsky AS. Injurious ventilatory strategies increase cytokines and c-fos m-RNA expression in an isolated rat lung model. *J Clin Invest.* 1997;99(5):944-52.

218. Parsons PE, Eisner MD, Thompson BT, Matthay MA, Ancukiewicz M, Bernard GR, et al. Lower tidal volume ventilation and plasma cytokine markers of inflammation in patients with acute lung injury. *Critical care medicine.* 2005;33(1):1-6; discussion 230-2.

219. Izbicki G, Segel MJ, Christensen TG, Conner MW, and Breuer R. Time course of bleomycin-induced lung fibrosis. *Int J Exp Pathol.* 2002;83(3):111-9.

220. Chaudhary NI, Schnapp A, and Park JE. Pharmacologic differentiation of inflammation and fibrosis in the rat bleomycin model. *Am J Respir Crit Care Med.* 2006;173(7):769-76.

221. Mouratis MA, and Aidinis V. Modeling pulmonary fibrosis with bleomycin. *Curr Opin Pulm Med.* 2011;17(5):355-61.

222. Gasse P, Mary C, Guenon I, Noulin N, Charron S, Schnyder-Candrian S, et al. IL-1R1/MyD88 signaling and the inflammasome are essential in pulmonary inflammation and fibrosis in mice. *J Clin Invest.* 2007;117(12):3786-99.

223. Misharin AV, Morales-Nebreda L, Mutlu GM, Budinger GR, and Perlman H. Flow cytometric analysis of macrophages and dendritic cell subsets in the mouse lung. *Am J Respir Cell Mol Biol.* 2013;49(4):503-10.

224. Gibbons MA, MacKinnon AC, Ramachandran P, Dhaliwal K, Duffin R, Phythian-Adams AT, et al. Ly6Chi monocytes direct alternatively activated profibrotic macrophage regulation of lung fibrosis. *Am J Respir Crit Care Med.* 2011;184(5):569-81.

225. Wynn TA, and Vannella KM. Macrophages in Tissue Repair, Regeneration, and Fibrosis. *Immunity.* 2016;44(3):450-62.

226. D'Alessio FR, Tsushima K, Aggarwal NR, West EE, Willett MH, Britos MF, et al. CD4+CD25+Foxp3+ Tregs resolve experimental lung injury in mice and are present in humans with acute lung injury. *J Clin Invest.* 2009;119(10):2898-913.

227. Misharin AV, Morales-Nebreda L, Reyfman PA, Cuda CM, Walter JM, McQuattie-Pimentel AC, et al. Monocyte-derived alveolar macrophages drive lung fibrosis and persist in the lung over the life span. *J Exp Med.* 2017;214(8):2387-404.

228. Klune JR, Dhupar R, Cardinal J, Billiar TR, and Tsung A. HMGB1: endogenous danger signaling. *Mol Med.* 2008;14(7-8):476-84.

229. Hirsiger S, Simmen HP, Werner CM, Wanner GA, and Rittirsch D. Danger signals activating the immune response after trauma. *Mediators Inflamm.* 2012;2012:315941.

230. Namas RA, Mi Q, Namas R, Almahmoud K, Zaaqoq AM, Abdul-Malak O, et al. Insights into the Role of Chemokines, Damage-Associated Molecular Patterns, and Lymphocyte-Derived Mediators from Computational Models of Trauma-Induced Inflammation. *Antioxid Redox Signal.* 2015;23(17):1370-87.

231. Matta BM, Reichenbach DK, Blazar BR, and Turnquist HR. Alarmins and Their Receptors as Modulators and Indicators of Alloimmune Responses. *Am J Transplant.* 2017;17(2):320-7.

232. Marvie P, Lisbonne M, L'Helgoualc'h A, Rauch M, Turlin B, Preisser L, et al. Interleukin-33 overexpression is associated with liver fibrosis in mice and humans. *J Cell Mol Med.* 2010;14(6B):1726-39.

233. Manetti M, Ibba-Manneschi L, Liakouli V, Guiducci S, Milia AF, Benelli G, et al. The IL1-like cytokine IL33 and its receptor ST2 are abnormally expressed in the affected skin and visceral organs of patients with systemic sclerosis. *Ann Rheum Dis.* 2010;69(3):598-605.

234. Molofsky AB, Savage AK, and Locksley RM. Interleukin-33 in Tissue Homeostasis, Injury, and Inflammation. *Immunity.* 2015;42(6):1005-19.

235. Chen CC, Kobayashi T, Iijima K, Hsu FC, and Kita H. IL-33 dysregulates regulatory T cells and impairs established immunologic tolerance in the lungs. *J Allergy Clin Immunol.* 2017;140(5):1351-63 e7.

236. MacDonald KG, Dawson NA, Huang Q, Dunne JV, Levings MK, and Broady R. Regulatory T cells produce profibrotic cytokines in the skin of patients with systemic sclerosis. *J Allergy Clin Immunol.* 2015;135(4):946- e9.

237. Wing K, Onishi Y, Prieto-Martin P, Yamaguchi T, Miyara M, Fehervari Z, et al. CTLA-4 control over Foxp3+ regulatory T cell function. *Science.* 2008;322(5899):271-5.

238. Robinson KM, Ramanan K, Clay ME, McHugh KJ, Rich HE, and Alcorn JF. Novel protective mechanism for interleukin-33 at the mucosal barrier during influenza-associated bacterial superinfection. *Mucosal Immunol.* 2018;11(1):199-208.

239. Ashcroft T, Simpson JM, and Timbrell V. Simple method of estimating severity of pulmonary fibrosis on a numerical scale. *J Clin Pathol.* 1988;41(4):467-70.

240. Macedo C, Turnquist HR, Castillo-Rama M, Zahorchak AF, Shapiro R, Thomson AW, et al. Rapamycin augments human DC IL-12p70 and IL-27 secretion to promote allogeneic Type 1 polarization modulated by NK cells. *Am J Transplant.* 2013;13(9):2322-33.

241. Liang J, Jung Y, Tighe RM, Xie T, Liu N, Leonard M, et al. A macrophage subpopulation recruited by CC chemokine ligand-2 clears apoptotic cells in noninfectious lung injury. *Am J Physiol Lung Cell Mol Physiol.* 2012;302(9):L933-40.

242. Fan MH, Zhu Q, Li HH, Ra HJ, Majumdar S, Gulick DL, et al. Fibroblast Activation Protein (FAP) Accelerates Collagen Degradation and Clearance from Lungs in Mice. *J Biol Chem.* 2016;291(15):8070-89.

243. Martin M. Cutadapt removes adapter sequences from high-througput sequencing reads. *EMBnetjournal.* 2011;17(1):10-2.

244. Kim D, Pertea G, Trapnell C, Pimentel H, Kelley R, and Salzberg SL. TopHat2: accurate alignment of transcriptomes in the presence of insertions, deletions and gene fusions. *Genome Biol.* 2013;14(4):R36.

245. Langmead B, and Salzberg SL. Fast gapped-read alignment with Bowtie 2. *Nat Methods.* 2012;9(4):357-9.

246. Trapnell C, Williams BA, Pertea G, Mortazavi A, Kwan G, van Baren MJ, et al. Transcript assembly and quantification by RNA-Seq reveals unannotated transcripts and isoform switching during cell differentiation. *Nat Biotechnol.* 2010;28(5):511-5.

247. Trapnell C, Hendrickson DG, Sauvageau M, Goff L, Rinn JL, and Pachter L. Differential analysis of gene regulation at transcript resolution with RNA-seq. *Nat Biotechnol.* 2013;31(1):46-53.

248. Livak KJ, and Schmittgen TD. Analysis of relative gene expression data using real-time quantitative PCR and the 2(-Delta Delta C(T)) Method. *Methods.* 2001;25(4):402-8.

249. Li D, Guabiraba R, Besnard AG, Komai-Koma M, Jabir MS, Zhang L, et al. IL-33 promotes ST2-dependent lung fibrosis by the induction of alternatively activated macrophages and innate lymphoid cells in mice. *J Allergy Clin Immunol.* 2014;134(6):1422-32 e11.

250. Russo RC, Guabiraba R, Garcia CC, Barcelos LS, Roffe E, Souza AL, et al. Role of the chemokine receptor CXCR2 in bleomycin-induced pulmonary inflammation and fibrosis. *Am J Respir Cell Mol Biol.* 2009;40(4):410-21.

251. Tsukui T, Ueha S, Abe J, Hashimoto S, Shichino S, Shimaoka T, et al. Qualitative rather than quantitative changes are hallmarks of fibroblasts in bleomycin-induced pulmonary fibrosis. *Am J Pathol.* 2013;183(3):758-73.

252. Arnold L, Henry A, Poron F, Baba-Amer Y, van Rooijen N, Plonquet A, et al. Inflammatory monocytes recruited after skeletal muscle injury switch into antiinflammatory macrophages to support myogenesis. *J Exp Med.* 2007;204(5):1057-69.

253. Kuswanto W, Burzyn D, Panduro M, Wang KK, Jang YC, Wagers AJ, et al. Poor Repair of Skeletal Muscle in Aging Mice Reflects a Defect in Local, Interleukin-33-Dependent Accumulation of Regulatory T Cells. *Immunity.* 2016;44(2):355-67.

254. Kim JM, Rasmussen JP, and Rudensky AY. Regulatory T cells prevent catastrophic autoimmunity throughout the lifespan of mice. *Nat Immunol.* 2007;8(2):191-7.

255. Delacher M, Imbusch CD, Weichenhan D, Breiling A, Hotz-Wagenblatt A, Trager U, et al. Genome-wide DNA-methylation landscape defines specialization of regulatory T cells in tissues. *Nat Immunol.* 2017;18(10):1160-72.

256. Zhu J, and Paul WE. Heterogeneity and plasticity of T helper cells. *Cell Res.* 2010;20(1):4-12.

257. Nakayama T, Hirahara K, Onodera A, Endo Y, Hosokawa H, Shinoda K, et al. Th2 Cells in Health and Disease. *Annu Rev Immunol.* 2017;35:53-84.

258. Voehringer D, Wu D, Liang HE, and Locksley RM. Efficient generation of long-distance conditional alleles using recombineering and a dual selection strategy in replicate plates. *BMC Biotechnol.* 2009;9:69.

259. Walkin L, Herrick SE, Summers A, Brenchley PE, Hoff CM, Korstanje R, et al. The role of mouse strain differences in the susceptibility to fibrosis: a systematic review. *Fibrogenesis Tissue Repair.* 2013;6(1):18.

260. Murray PJ, Allen JE, Biswas SK, Fisher EA, Gilroy DW, Goerdt S, et al. Macrophage activation and polarization: nomenclature and experimental guidelines. *Immunity.* 2014;41(1):14-20.

261. Veglia F, Perego M, and Gabrilovich D. Myeloid-derived suppressor cells coming of age. *Nat Immunol.* 2018;19(2):108-19.

262. Ostrand-Rosenberg S, and Fenselau C. Myeloid-Derived Suppressor Cells: Immune-Suppressive Cells That Impair Antitumor Immunity and Are Sculpted by Their Environment. *J Immunol.* 2018;200(2):422-31.

263. Wills-Karp M, Luyimbazi J, Xu X, Schofield B, Neben TY, Karp CL, et al. Interleukin-13: central mediator of allergic asthma. *Science.* 1998;282(5397):2258-61.

264. Lee CG, Homer RJ, Zhu Z, Lanone S, Wang X, Koteliansky V, et al. Interleukin-13 induces tissue fibrosis by selectively stimulating and activating transforming growth factor beta(1). *J Exp Med.* 2001;194(6):809-21.

265. Kaviratne M, Hesse M, Leusink M, Cheever AW, Davies SJ, McKerrow JH, et al. IL-13 activates a mechanism of tissue fibrosis that is completely TGF-beta independent. *J Immunol.* 2004;173(6):4020-9.

266. Fichtner-Feigl S, Strober W, Kawakami K, Puri RK, and Kitani A. IL-13 signaling through the IL-13alpha2 receptor is involved in induction of TGF-beta1 production and fibrosis. *Nat Med.* 2006;12(1):99-106.

267. Heredia JE, Mukundan L, Chen FM, Mueller AA, Deo RC, Locksley RM, et al. Type 2 innate signals stimulate fibro/adipogenic progenitors to facilitate muscle regeneration. *Cell.* 2013;153(2):376-88.

268. Bosurgi L, Cao YG, Cabeza-Cabrerizo M, Tucci A, Hughes LD, Kong Y, et al. Macrophage function in tissue repair and remodeling requires IL-4 or IL-13 with apoptotic cells. *Science.* 2017;356(6342):1072-6.

269. Gieseck RL, 3rd, Wilson MS, and Wynn TA. Type 2 immunity in tissue repair and fibrosis. *Nat Rev Immunol.* 2018;18(1):62-76.

270. Bruce DW, Stefanski HE, Vincent BG, Dant TA, Reisdorf S, Bommiasamy H, et al. Type 2 innate lymphoid cells treat and prevent acute gastrointestinal graft-versus-host disease. *J Clin Invest.* 2017;127(5):1813-25.

271. Highfill SL, Rodriguez PC, Zhou Q, Goetz CA, Koehn BH, Veenstra R, et al. Bone marrow myeloid-derived suppressor cells (MDSCs) inhibit graft-versus-host disease (GVHD) via an arginase-1-dependent mechanism that is up-regulated by interleukin-13. *Blood.* 2010;116(25):5738-47.

272. Proto JD, Doran AC, Gusarova G, Yurdagul A, Jr., Sozen E, Subramanian M, et al. Regulatory T Cells Promote Macrophage Efferocytosis during Inflammation Resolution. *Immunity.* 2018;49(4):666-77 e6.

273. Panduro M, Benoist C, and Mathis D. Tissue Tregs. *Annu Rev Immunol.* 2016;34:609-33.

274. Gomez Perdiguero E, Klapproth K, Schulz C, Busch K, Azzoni E, Crozet L, et al. Tissue-resident macrophages originate from yolk-sac-derived erythro-myeloid progenitors. *Nature.* 2015;518(7540):547-51.

275. Fan X, and Rudensky AY. Hallmarks of Tissue-Resident Lymphocytes. *Cell.* 2016;164(6):1198-211.

276. Zheng T, Zhu Z, Liu W, Lee CG, Chen Q, Homer RJ, et al. Cytokine regulation of IL-13Ralpha2 and IL-13Ralpha1 in vivo and in vitro. *J Allergy Clin Immunol.* 2003;111(4):720-8.

277. Bonfield TL, Konstan MW, and Berger M. Altered respiratory epithelial cell cytokine production in cystic fibrosis. *J Allergy Clin Immunol.* 1999;104(1):72-8.

278. Fischader G, Roder-Stolinski C, Wichmann G, Nieber K, and Lehmann I. Release of MCP-1 and IL-8 from lung epithelial cells exposed to volatile organic compounds. *Toxicol In Vitro.* 2008;22(2):359-66.

279. Saba S, Soong G, Greenberg S, and Prince A. Bacterial stimulation of epithelial G-CSF and GM-CSF expression promotes PMN survival in CF airways. *Am J Respir Cell Mol Biol.* 2002;27(5):561-7.

280. Karo-Atar D, Bordowitz A, Wand O, Pasmanik-Chor M, Fernandez IE, Itan M, et al. A protective role for IL-13 receptor alpha 1 in bleomycin-induced pulmonary injury and repair. *Mucosal Immunol.* 2016;9(1):240-53.

281. D'Alessio FR, Craig JM, Singer BD, Files DC, Mock JR, Garibaldi BT, et al. Enhanced resolution of experimental ARDS through IL-4-mediated lung macrophage reprogramming. *Am J Physiol Lung Cell Mol Physiol.* 2016;310(8):L733-46.

282. Ito M, Komai K, Mise-Omata S, Iizuka-Koga M, Noguchi Y, Kondo T, et al. Brain regulatory T cells suppress astrogliosis and potentiate neurological recovery. *Nature.* 2019;565(7738):246-50.

283. Noble PW, Barkauskas CE, and Jiang D. Pulmonary fibrosis: patterns and perpetrators. *J Clin Invest.* 2012;122(8):2756-62.

284. Prefontaine D, Lajoie-Kadoch S, Foley S, Audusseau S, Olivenstein R, Halayko AJ, et al. Increased expression of IL-33 in severe asthma: evidence of expression by airway smooth muscle cells. *J Immunol.* 2009;183(8):5094-103.

285. Hrusch CL, Manns ST, Bryazka D, Casaos J, Bonham CA, Jaffery MR, et al. ICOS protects against mortality from acute lung injury through activation of IL-5(+) ILC2s. *Mucosal Immunol.* 2018;11(1):61-70.

286. Jones SA, Scheller J, and Rose-John S. Therapeutic strategies for the clinical blockade of IL-6/gp130 signaling. *J Clin Invest.* 2011;121(9):3375-83.

287. Le TT, Karmouty-Quintana H, Melicoff E, Le TT, Weng T, Chen NY, et al. Blockade of IL-6 Trans signaling attenuates pulmonary fibrosis. *J Immunol.* 2014;193(7):3755-68.

288. Tadokoro T, Wang Y, Barak LS, Bai Y, Randell SH, and Hogan BL. IL-6/STAT3 promotes regeneration of airway ciliated cells from basal stem cells. *Proc Natl Acad Sci U S A.* 2014;111(35):E3641-9.

289. Liang J, Zhang Y, Xie T, Liu N, Chen H, Geng Y, et al. Hyaluronan and TLR4 promote surfactant-protein-C-positive alveolar progenitor cell renewal and prevent severe pulmonary fibrosis in mice. *Nat Med.* 2016;22(11):1285-93.

290. Campbell IK, Leong D, Edwards KM, Rayzman V, Ng M, Goldberg GL, et al. Therapeutic Targeting of the G-CSF Receptor Reduces Neutrophil Trafficking and Joint Inflammation in Antibody-Mediated Inflammatory Arthritis. *J Immunol.* 2016;197(11):4392-402.

291. Maus UA, Waelsch K, Kuziel WA, Delbeck T, Mack M, Blackwell TS, et al. Monocytes are potent facilitators of alveolar neutrophil emigration during lung inflammation: role of the CCL2-CCR2 axis. *J Immunol.* 2003;170(6):3273-8.

292. Kreisel D, Nava RG, Li W, Zinselmeyer BH, Wang B, Lai J, et al. In vivo two-photon imaging reveals monocyte-dependent neutrophil extravasation during pulmonary inflammation. *Proc Natl Acad Sci U S A.* 2010;107(42):18073-8.

293. Baran CP, Opalek JM, McMaken S, Newland CA, O'Brien JM, Jr., Hunter MG, et al. Important roles for macrophage colony-stimulating factor, CC chemokine ligand 2, and mononuclear phagocytes in the pathogenesis of pulmonary fibrosis. *Am J Respir Crit Care Med.* 2007;176(1):78-89.

294. Rosseau S, Hammerl P, Maus U, Walmrath HD, Schutte H, Grimminger F, et al. Phenotypic characterization of alveolar monocyte recruitment in acute respiratory distress syndrome. *Am J Physiol Lung Cell Mol Physiol.* 2000;279(1):L25-35.

295. Hill GR, Betts BC, Tkachev V, Kean LS, and Blazar BR. Current Concepts and Advances in Graft-Versus-Host Disease Immunology. *Annu Rev Immunol.* 2021.

296. Leventhal JR, and Ildstad ST. Tolerance induction in HLA disparate living donor kidney transplantation by facilitating cell-enriched donor stem cell Infusion: The importance of durable chimerism. *Hum Immunol.* 2018;79(5):272-6.

297. Spitzer TR, Sykes M, Tolkoff-Rubin N, Kawai T, McAfee SL, Dey BR, et al. Long-term follow-up of recipients of combined human leukocyte antigen-matched bone marrow and kidney transplantation for multiple myeloma with end-stage renal disease. *Transplantation.* 2011;91(6):672-6.

298. Schmaltz C, Alpdogan O, Horndasch KJ, Muriglan SJ, Kappel BJ, Teshima T, et al. Differential use of Fas ligand and perforin cytotoxic pathways by donor T cells in graft-versus-host disease and graft-versus-leukemia effect. *Blood.* 2001;97(9):2886-95.

299. Takashima S, Martin ML, Jansen SA, Fu Y, Bos J, Chandra D, et al. T cell-derived interferon-gamma programs stem cell death in immune-mediated intestinal damage. *Sci Immunol.* 2019;4(42).

300. Yi T, Chen Y, Wang L, Du G, Huang D, Zhao D, et al. Reciprocal differentiation and tissue-specific pathogenesis of Th1, Th2, and Th17 cells in graft-versus-host disease. *Blood.* 2009;114(14):3101-12.

301. Hill GR, and Koyama M. Cytokines and costimulation in acute graft-versus-host disease. *Blood.* 2020;136(4):418-28.

302. Bastian D, Wu Y, Betts BC, and Yu XZ. The IL-12 Cytokine and Receptor Family in Graft-vs.-Host Disease. *Front Immunol.* 2019;10:988.

303. Blecher-Gonen R, Bost P, Hilligan KL, David E, Salame TM, Roussel E, et al. Single-Cell Analysis of Diverse Pathogen Responses Defines a Molecular Roadmap for Generating Antigen-Specific Immunity. *Cell Syst.* 2019;8(2):109-21 e6.

304. Kapsenberg ML. Dendritic-cell control of pathogen-driven T-cell polarization. *Nat Rev Immunol.* 2003;3(12):984-93.

305. Pasare C, and Medzhitov R. Toll-dependent control mechanisms of CD4 T cell activation. *Immunity.* 2004;21(5):733-41.

306. Gauthier SD, Moutuou MM, Daudelin F, Leboeuf D, and Guimond M. IL-7 Is the Limiting Homeostatic Factor that Constrains Homeostatic Proliferation of CD8(+) T Cells after Allogeneic Stem Cell Transplantation and Graft-versus-Host Disease. *Biol Blood Marrow Transplant.* 2019;25(4):648-55.

307. Zeiser R, and Blazar BR. Acute Graft-versus-Host Disease - Biologic Process, Prevention, and Therapy. *N Engl J Med.* 2017;377(22):2167-79.

308. Kulak NA, Pichler G, Paron I, Nagaraj N, and Mann M. Minimal, encapsulated proteomic-sample processing applied to copy-number estimation in eukaryotic cells. *Nat Methods.* 2014;11(3):319-24.

309. Balasubramani A, Shibata Y, Crawford GE, Baldwin AS, Hatton RD, and Weaver CT. Modular utilization of distal cis-regulatory elements controls Ifng gene expression in T cells activated by distinct stimuli. *Immunity.* 2010;33(1):35-47.

310. Hertweck A, Evans CM, Eskandarpour M, Lau JC, Oleinika K, Jackson I, et al. T-bet Activates Th1 Genes through Mediator and the Super Elongation Complex. *Cell Rep.* 2016;15(12):2756-70.

311. Koyama M, Mukhopadhyay P, Schuster IS, Henden AS, Hulsdunker J, Varelias A, et al. MHC Class II Antigen Presentation by the Intestinal Epithelium Initiates Graft-versus-Host Disease and Is Influenced by the Microbiota. *Immunity.* 2019;51(5):885-98 e7.

312. Williamson E, Garside P, Bradley JA, More IA, and Mowat AM. Neutralizing IL-12 during induction of murine acute graft-versus-host disease polarizes the cytokine profile toward a Th2-type alloimmune response and confers long term protection from disease. *J Immunol.* 1997;159(3):1208-15.

313. Tominaga S. A putative protein of a growth specific cDNA from BALB/c-3T3 cells is highly similar to the extracellular portion of mouse interleukin 1 receptor. *FEBS Lett.* 1989;258(2):301-4.

314. Beilhack A, Schulz S, Baker J, Beilhack GF, Wieland CB, Herman EI, et al. In vivo analyses of early events in acute graft-versus-host disease reveal sequential infiltration of T-cell subsets. *Blood.* 2005;106(3):1113-22.

315. Mahlakoiv T, Flamar AL, Johnston LK, Moriyama S, Putzel GG, Bryce PJ, et al. Stromal cells maintain immune cell homeostasis in adipose tissue via production of interleukin-33. *Sci Immunol.* 2019;4(35).

316. Vasanthakumar A, and Kallies A. Interleukin (IL)-33 and the IL-1 Family of Cytokines-Regulators of Inflammation and Tissue Homeostasis. *Cold Spring Harb Perspect Biol.* 2019;11(3).

317. Reddy P, Negrin R, and Hill GR. Mouse models of bone marrow transplantation. *Biol Blood Marrow Transplant.* 2008;14(1 Suppl 1):129-35.

318. Surh CD, and Sprent J. Homeostasis of naive and memory T cells. *Immunity.* 2008;29(6):848-62.

319. Cibrian D, and Sanchez-Madrid F. CD69: from activation marker to metabolic gatekeeper. *Eur J Immunol.* 2017;47(6):946-53.

320. O'Donoghue GP, Bugaj LJ, Anderson W, Daniels KG, Rawlings DJ, and Lim WA. T cells selectively filter oscillatory signals on the minutes timescale. *Proc Natl Acad Sci U S A.* 2021;118(9).

321. Choi J, Ziga ED, Ritchey J, Collins L, Prior JL, Cooper ML, et al. IFNgammaR signaling mediates alloreactive T-cell trafficking and GVHD. *Blood.* 2012;120(19):4093-103.

322. Geltink RIK, Kyle RL, and Pearce EL. Unraveling the Complex Interplay Between T Cell Metabolism and Function. *Annu Rev Immunol.* 2018;36:461-88.

323. Ruterbusch M, Pruner KB, Shehata L, and Pepper M. In Vivo CD4(+) T Cell Differentiation and Function: Revisiting the Th1/Th2 Paradigm. *Annu Rev Immunol.* 2020;38:705-25.

324. Acuto O, and Michel F. CD28-mediated co-stimulation: a quantitative support for TCR signalling. *Nat Rev Immunol.* 2003;3(12):939-51.

325. Coquet JM, Rausch L, and Borst J. The importance of co-stimulation in the orchestration of T helper cell differentiation. *Immunol Cell Biol.* 2015;93(9):780-8.

326. Wei SC, Sharma R, Anang NAS, Levine JH, Zhao Y, Mancuso JJ, et al. Negative Co-stimulation Constrains T Cell Differentiation by Imposing Boundaries on Possible Cell States. *Immunity.* 2019;50(4):1084-98 e10.

327. Bhattacharyya ND, and Feng CG. Regulation of T Helper Cell Fate by TCR Signal Strength. *Front Immunol.* 2020;11:624.

328. Tubo NJ, and Jenkins MK. TCR signal quantity and quality in CD4(+) T cell differentiation. *Trends Immunol.* 2014;35(12):591-6.

329. van Panhuys N, Klauschen F, and Germain RN. T-cell-receptor-dependent signal intensity dominantly controls CD4(+) T cell polarization In Vivo. *Immunity.* 2014;41(1):63-74.

330. Gomez-Rodriguez J, Wohlfert EA, Handon R, Meylan F, Wu JZ, Anderson SM, et al. Itk-mediated integration of T cell receptor and cytokine signaling regulates the balance between Th17 and regulatory T cells. *J Exp Med.* 2014;211(3):529-43.

331. Mikami N, Kawakami R, Chen KY, Sugimoto A, Ohkura N, and Sakaguchi S. Epigenetic conversion of conventional T cells into regulatory T cells by CD28 signal deprivation. *Proc Natl Acad Sci U S A.* 2020;117(22):12258-68.

332. Semple K, Nguyen A, Yu Y, Wang H, Anasetti C, and Yu XZ. Strong CD28 costimulation suppresses induction of regulatory T cells from naive precursors through Lck signaling. *Blood.* 2011;117(11):3096-103.

333. Ashouri JF, and Weiss A. Endogenous Nur77 Is a Specific Indicator of Antigen Receptor Signaling in Human T and B Cells. *J Immunol.* 2017;198(2):657-68.

334. Cunningham NR, Artim SC, Fornadel CM, Sellars MC, Edmonson SG, Scott G, et al. Immature CD4+CD8+ thymocytes and mature T cells regulate Nur77 distinctly in response to TCR stimulation. *J Immunol.* 2006;177(10):6660-6.

335. Moran AE, Holzapfel KL, Xing Y, Cunningham NR, Maltzman JS, Punt J, et al. T cell receptor signal strength in Treg and iNKT cell development demonstrated by a novel fluorescent reporter mouse. *J Exp Med.* 2011;208(6):1279-89.

336. McKenzie IF, Morgan GM, Sandrin MS, Michaelides MM, Melvold RW, and Kohn HI. B6.C-H-2bm12. A new H-2 mutation in the I region in the mouse. *J Exp Med.* 1979;150(6):1323-38.

337. Sprent J, Schaefer M, Lo D, and Korngold R. Properties of purified T cell subsets. II. In vivo responses to class I vs. class II H-2 differences. *J Exp Med.* 1986;163(4):998-1011.

338. Mantovani A, Dinarello CA, Molgora M, and Garlanda C. Interleukin-1 and Related Cytokines in the Regulation of Inflammation and Immunity. *Immunity.* 2019;50(4):778-95.

339. Gelman AE, Zhang J, Choi Y, and Turka LA. Toll-like receptor ligands directly promote activated CD4+ T cell survival. *J Immunol.* 2004;172(10):6065-73.

340. Imanishi T, Hara H, Suzuki S, Suzuki N, Akira S, and Saito T. Cutting edge: TLR2 directly triggers Th1 effector functions. *J Immunol.* 2007;178(11):6715-9.

341. Reynolds JM, Pappu BP, Peng J, Martinez GJ, Zhang Y, Chung Y, et al. Toll-like receptor 2 signaling in CD4(+) T lymphocytes promotes T helper 17 responses and regulates the pathogenesis of autoimmune disease. *Immunity.* 2010;32(5):692-702.

342. Hu W, Troutman TD, Edukulla R, and Pasare C. Priming microenvironments dictate cytokine requirements for T helper 17 cell lineage commitment. *Immunity.* 2011;35(6):1010-22.

343. Zhu J, Yamane H, and Paul WE. Differentiation of effector CD4 T cell populations (*). *Annu Rev Immunol.* 2010;28:445-89.

344. Ben-Sasson SZ, Hu-Li J, Quiel J, Cauchetaux S, Ratner M, Shapira I, et al. IL-1 acts directly on CD4 T cells to enhance their antigen-driven expansion and differentiation. *Proc Natl Acad Sci U S A.* 2009;106(17):7119-24.

345. Martin MU. Special aspects of interleukin-33 and the IL-33 receptor complex. *Semin Immunol.* 2013;25(6):449-57.

346. Duffner U, Lu B, Hildebrandt GC, Teshima T, Williams DL, Reddy P, et al. Role of CXCR3-induced donor T-cell migration in acute GVHD. *Exp Hematol.* 2003;31(10):897-902.

347. Kim YM, Sachs T, Asavaroengchai W, Bronson R, and Sykes M. Graft-versus-host disease can be separated from graft-versus-lymphoma effects by control of lymphocyte trafficking with FTY720. *J Clin Invest.* 2003;111(5):659-69.

348. Panoskaltsis-Mortari A, Price A, Hermanson JR, Taras E, Lees C, Serody JS, et al. In vivo imaging of graft-versus-host-disease in mice. *Blood.* 2004;103(9):3590-8.

349. Chung J, Ebens CL, Perkey E, Radojcic V, Koch U, Scarpellino L, et al. Fibroblastic niches prime T cell alloimmunity through Delta-like Notch ligands. *J Clin Invest.* 2017;127(4):1574-88.

350. Cremasco V, Woodruff MC, Onder L, Cupovic J, Nieves-Bonilla JM, Schildberg FA, et al. B cell homeostasis and follicle confines are governed by fibroblastic reticular cells. *Nat Immunol.* 2014;15(10):973-81.

351. Neely HR, and Flajnik MF. Emergence and Evolution of Secondary Lymphoid Organs. *Annu Rev Cell Dev Biol.* 2016;32:693-711.

352. Jain A, Song R, Wakeland EK, and Pasare C. T cell-intrinsic IL-1R signaling licenses effector cytokine production by memory CD4 T cells. *Nat Commun.* 2018;9(1):3185.

353. Jirmanova L, Giardino Torchia ML, Sarma ND, Mittelstadt PR, and Ashwell JD. Lack of the T cell-specific alternative p38 activation pathway reduces autoimmunity and inflammation. *Blood.* 2011;118(12):3280-9.

354. Jones DC, Ding X, Zhang TY, and Daynes RA. Peroxisome proliferator-activated receptor alpha negatively regulates T-bet transcription through suppression of p38 mitogen-activated protein kinase activation. *J Immunol.* 2003;171(1):196-203.

355. Ariga H, Shimohakamada Y, Nakada M, Tokunaga T, Kikuchi T, Kariyone A, et al. Instruction of naive CD4+ T-cell fate to T-bet expression and T helper 1 development: roles of T-cell receptor-mediated signals. *Immunology.* 2007;122(2):210-21.

356. Keck S, Schmaler M, Ganter S, Wyss L, Oberle S, Huseby ES, et al. Antigen affinity and antigen dose exert distinct influences on CD4 T-cell differentiation. *Proc Natl Acad Sci U S A.* 2014;111(41):14852-7.

357. Jorritsma PJ, Brogdon JL, and Bottomly K. Role of TCR-induced extracellular signal-regulated kinase activation in the regulation of early IL-4 expression in naive CD4+ T cells. *J Immunol.* 2003;170(5):2427-34.

358. Tao X, Grant C, Constant S, and Bottomly K. Induction of IL-4-producing CD4+ T cells by antigenic peptides altered for TCR binding. *J Immunol.* 1997;158(9):4237-44.

359. Yamane H, Zhu J, and Paul WE. Independent roles for IL-2 and GATA-3 in stimulating naive CD4+ T cells to generate a Th2-inducing cytokine environment. *J Exp Med.* 2005;202(6):793-804.

360. Kishimoto H, and Sprent J. Strong TCR ligation without costimulation causes rapid onset of Fas-dependent apoptosis of naive murine CD4+ T cells. *J Immunol.* 1999;163(4):1817-26.

361. Koyama M, Kuns RD, Olver SD, Raffelt NC, Wilson YA, Don AL, et al. Recipient nonhematopoietic antigen-presenting cells are sufficient to induce lethal acute graft-versus-host disease. *Nat Med.* 2011;18(1):135-42.

362. Anderson BE, McNiff JM, Jain D, Blazar BR, Shlomchik WD, and Shlomchik MJ. Distinct roles for donor- and host-derived antigen-presenting cells and costimulatory molecules in murine chronic graft-versus-host disease: requirements depend on target organ. *Blood.* 2005;105(5):2227-34.

363. Amsen D, Revilla Calvo C, Osborne BA, and Kruisbeek AM. Costimulatory signals are required for induction of transcription factor Nur77 during negative selection of CD4(+)CD8(+) thymocytes. *Proc Natl Acad Sci U S A.* 1999;96(2):622-7.

364. Chen YL, Gutowska-Owsiak D, Hardman CS, Westmoreland M, MacKenzie T, Cifuentes L, et al. Proof-of-concept clinical trial of etokimab shows a key role for IL-33 in atopic dermatitis pathogenesis. *Sci Transl Med.* 2019;11(515).

365. Saluzzo S, Gorki AD, Rana BMJ, Martins R, Scanlon S, Starkl P, et al. First-Breath-Induced Type 2 Pathways Shape the Lung Immune Environment. *Cell Rep.* 2017;18(8):1893-905.

366. de Kleer IM, Kool M, de Bruijn MJ, Willart M, van Moorleghem J, Schuijs MJ, et al. Perinatal Activation of the Interleukin-33 Pathway Promotes Type 2 Immunity in the Developing Lung. *Immunity.* 2016;45(6):1285-98.

367. Vasanthakumar A, Moro K, Xin A, Liao Y, Gloury R, Kawamoto S, et al. The transcriptional regulators IRF4, BATF and IL-33 orchestrate development and maintenance of adipose tissue-resident regulatory T cells. *Nat Immunol.* 2015;16(3):276-85.

368. Li C, DiSpirito JR, Zemmour D, Spallanzani RG, Kuswanto W, Benoist C, et al. TCR Transgenic Mice Reveal Stepwise, Multi-site Acquisition of the Distinctive Fat-Treg Phenotype. *Cell.* 2018;174(2):285-99 e12.

369. Altman MC, Lai Y, Nolin JD, Long S, Chen CC, Piliponsky AM, et al. Airway epithelium-shifted mast cell infiltration regulates asthmatic inflammation via IL-33 signaling. *J Clin Invest.* 2019;129(11):4979-91.

370. Van Dyken SJ, Nussbaum JC, Lee J, Molofsky AB, Liang HE, Pollack JL, et al. A tissue checkpoint regulates type 2 immunity. *Nat Immunol.* 2016;17(12):1381-7.

371. Dertschnig S, Evans P, Santos ESP, Manzo T, Ferrer IR, Stauss HJ, et al. Graft-versus-host disease reduces lymph node display of tissue-restricted self-antigens and promotes autoimmunity. *J Clin Invest.* 2020;130(4):1896-911.

372. Medzhitov R, and Janeway CA, Jr. Decoding the patterns of self and nonself by the innate immune system. *Science.* 2002;296(5566):298-300.

373. Schenten D, Nish SA, Yu S, Yan X, Lee HK, Brodsky I, et al. Signaling through the adaptor molecule MyD88 in CD4+ T cells is required to overcome suppression by regulatory T cells. *Immunity.* 2014;40(1):78-90.

374. Gelman AE, LaRosa DF, Zhang J, Walsh PT, Choi Y, Sunyer JO, et al. The adaptor molecule MyD88 activates PI-3 kinase signaling in CD4+ T cells and enables CpG oligodeoxynucleotide-mediated costimulation. *Immunity.* 2006;25(5):783-93.

375. Borges CM, Reichenbach DK, Kim BS, Misra A, Blazar BR, and Turka LA. Regulatory T cell expressed MyD88 is critical for prolongation of allograft survival. *Transpl Int.* 2016;29(8):930-40.

376. Levine AG, Arvey A, Jin W, and Rudensky AY. Continuous requirement for the TCR in regulatory T cell function. *Nat Immunol.* 2014;15(11):1070-8.

377. Yan D, Farache J, Mingueneau M, Mathis D, and Benoist C. Imbalanced signal transduction in regulatory T cells expressing the transcription factor FoxP3. *Proc Natl Acad Sci U S A.* 2015;112(48):14942-7.

378. Vahl JC, Drees C, Heger K, Heink S, Fischer JC, Nedjic J, et al. Continuous T cell receptor signals maintain a functional regulatory T cell pool. *Immunity.* 2014;41(5):722-36.

379. Endo Y, Hirahara K, Iinuma T, Shinoda K, Tumes DJ, Asou HK, et al. The interleukin-33-p38 kinase axis confers memory T helper 2 cell pathogenicity in the airway. *Immunity.* 2015;42(2):294-308.

380. Humphreys IR, Lee SW, Jones M, Loewendorf A, Gostick E, Price DA, et al. Biphasic role of 4-1BB in the regulation of mouse cytomegalovirus-specific CD8(+) T cells. *Eur J Immunol.* 2010;40(10):2762-8.

381. Willoughby JE, Kerr JP, Rogel A, Taraban VY, Buchan SL, Johnson PW, et al. Differential impact of CD27 and 4-1BB costimulation on effector and memory CD8 T cell generation following peptide immunization. *J Immunol.* 2014;193(1):244-51.

382. Blazar BR, Kwon BS, Panoskaltsis-Mortari A, Kwak KB, Peschon JJ, and Taylor PA. Ligation of 4-1BB (CDw137) regulates graft-versus-host disease, graft-versus-leukemia,

and graft rejection in allogeneic bone marrow transplant recipients. *J Immunol.* 2001;166(5):3174-83.

383. Zheng G, Wang B, and Chen A. The 4-1BB costimulation augments the proliferation of CD4+CD25+ regulatory T cells. *J Immunol.* 2004;173(4):2428-34.

384. Kiner E, Willie E, Vijaykumar B, Chowdhary K, Schmutz H, Chandler J, et al. Gut CD4(+) T cell phenotypes are a continuum molded by microbes, not by TH archetypes. *Nat Immunol.* 2021;22(2):216-28.

385. Braza MS, van Leent MMT, Lameijer M, Sanchez-Gaytan BL, Arts RJW, Perez-Medina C, et al. Inhibiting Inflammation with Myeloid Cell-Specific Nanobiologics Promotes Organ Transplant Acceptance. *Immunity.* 2018;49(5):819-28 e6.

386. Huang SC, Everts B, Ivanova Y, O'Sullivan D, Nascimento M, Smith AM, et al. Cell-intrinsic lysosomal lipolysis is essential for alternative activation of macrophages. *Nat Immunol.* 2014;15(9):846-55.

387. Li T, Zhang Z, Bartolacci JG, Dwyer GK, Liu Q, Mathews LR, et al. Graft IL-33 regulates infiltrating macrophages to protect against chronic rejection. *J Clin Invest.* 2020.

388. Brown RA, and Byersdorfer CA. Metabolic Pathways in Alloreactive T Cells. *Front Immunol.* 2020;11:1517.

389. Linke M, Fritsch SD, Sukhbaatar N, Hengstschlager M, and Weichhart T. mTORC1 and mTORC2 as regulators of cell metabolism in immunity. *FEBS Lett.* 2017;591(19):3089-103.

390. Sun IH, Oh MH, Zhao L, Patel CH, Arwood ML, Xu W, et al. mTOR Complex 1 Signaling Regulates the Generation and Function of Central and Effector Foxp3(+) Regulatory T Cells. *J Immunol.* 2018;201(2):481-92.

391. Chinthrajah S, Cao S, Liu C, Lyu SC, Sindher SB, Long A, et al. Phase 2a randomized, placebo-controlled study of anti-IL-33 in peanut allergy. *JCI Insight.* 2019;4(22).

392. Kelsen SG, Agache IO, Soong W, Israel E, Chupp GL, Cheung DS, et al. Astegolimab (anti-ST2) efficacy and safety in adults with severe asthma: A randomized clinical trial. *J Allergy Clin Immunol.* 2021.

393. Zeiser R, Leveson-Gower DB, Zambricki EA, Kambham N, Beilhack A, Loh J, et al. Differential impact of mammalian target of rapamycin inhibition on CD4+CD25+Foxp3+ regulatory T cells compared with conventional CD4+ T cells. *Blood.* 2008;111(1):453-62.

394. Battaglia M, Stabilini A, and Roncarolo MG. Rapamycin selectively expands CD4+CD25+FoxP3+ regulatory T cells. *Blood.* 2005;105(12):4743-8.

395. Yoshizaki A, Yanaba K, Yoshizaki A, Iwata Y, Komura K, Ogawa F, et al. Treatment with rapamycin prevents fibrosis in tight-skin and bleomycin-induced mouse models of systemic sclerosis. *Arthritis Rheum.* 2010;62(8):2476-87.

396. Salmond RJ, Mirchandani AS, Besnard AG, Bain CC, Thomson NC, and Liew FY. IL-33 induces innate lymphoid cell-mediated airway inflammation by activating mammalian target of rapamycin. *J Allergy Clin Immunol.* 2012;130(5):1159-66 e6.